

**PREPARATION OF DUAL-DRUG LOADED POLYMER-
LIPID HYBRID NANOPARTICLES TOWARDS THE
TREATMENT OF BREAST CANCER**

**MEME KANSERİ TEDAVİSİNE YÖNELİK İKİLİ İLAÇ
YÜKLÜ POLİMER-LİPİT HİBRİT
NANOPARTİKÜLLERİN HAZIRLANMASI**

GÜŞTA İREM SAKIZ

PROF. DR. NİHAL AYDOĞAN

Supervisor

Submitted to
Graduate School of Science and Engineering of Hacettepe University
as a Partial Fulfillment to the Requirements
for the Award of the Degree of Master of Science
in Chemical Engineering

2023

ABSTRACT

PREPARATION OF DUAL-DRUG LOADED POLYMER-LIPID HYBRID NANOPARTICLES TOWARDS THE TREATMENT OF BREAST CANCER

GüŖta İrem SAKIZ

Master of Science, Department of Chemical Engineering

Supervisor: Prof. Dr. Nihal AYDOĐAN

Co-Supervisor: Prof. Dr. Wim DE MALSCHE

June 2023, 112 pages

Breast cancer is a major health concern worldwide, and the development of effective diagnosis and treatment methods is crucial. The incidence rates for breast cancer have increased by approximately 0.5% annually since 2004, contributing to nearly one-third of all recent malignancy diagnoses. A cancer diagnosis is an important step that affects the course and treatment of the disease. However, current imaging techniques are expensive and may cause adverse effects [1]. Preparing advanced materials with unique properties for cancer diagnosis and treatment is essential for survival rate. This thesis aims to prepare drug-loaded polymer-lipid hybrid particles for breast cancer treatment via microfluidic technologies and to investigate in vitro uptake/release studies. The first part of the study aims to prepare polymer-lipid hybrid microparticles (PLHMPs) with different

morphologies using a one-nozzle microfluidic system. The size, size distribution, morphology and optical properties of the prepared PLHMPs were investigated by Optical Microscope (OM), Scanning Electron Microscope (SEM) and Polarized Light Microscope (POM). Particles with different Janus morphologies were prepared with bi-compartmental, dumbbell and snowman morphologies by varying the polymer-lipid ratio, lipid type, surfactant type and concentration used to prepare PLHMPs. In addition to the prepared Janus PLHMPs, birefringent PLHMPs capable of rotational and translational movements were prepared by using different lipids in the particles. These particles were loaded with magnetic nanoparticles and made responsive to a magnetic field. PLHMPs prepared by microfluidic technology with different polymer-lipid compositions were functionalized for different biomedical applications as stimuli responsive. Polymer-lipid hybrid nanoparticles (PLHNPs) were prepared from different stimuli-responsive PLHMPs under selected conditions with an aluminium-glass (Al-Gl) microfluidic system designed by examining particle compositions and conditions with suitable morphology as a drug delivery system. PLHNPs with a size of 100-200 nm were prepared via microfluidic technology. Resveratrol (RES) and rhodamine-B (Rh-B) were used as model drug molecules to evaluate the drug uptake/release capacity of polymer-lipid hybrid particles prepared with desired properties for breast cancer treatment. Drug uptake/release capacities for the particles used were analyzed using UV-vis spectroscopy. Then the polymer-lipid hybrid particles were prepared for the first time in the literature with a one-nozzle microfluidic system with different stimuli. In addition, the magnetic nanoparticles added to the PLHMP structure have resulted in a new generation of hybrid structures that can be used for diagnostic and therapeutic purposes. Smart PLHMPs with different compositions and magnetic and optical stimuli were prepared with the same microfluidic system for the first time in the literature. At the same time, as an alternative to polymer-based microfluidic systems for nanoparticle synthesis for the first time in the literature, PLHNPs of 100 nm in size were prepared with high monodispersity ($PDI > 0.1$) with a microfluidic system prepared from cheap and chemically inert Al-Gl material.

Keywords: polymer-lipid hybrid particles, microfluidics, drug-loading, birefringence, stimuli-responsive

ÖZET

MEME KANSERİ TEDAVİSİNE YÖNELİK İKİLİ İLAÇ YÜKLÜ POLİMER-LİPİT HİBRİT NANOPARTİKÜLLERİN HAZIRLANMASI

GüŖta İrem SAKIZ

Yüksek Lisans, Kimya Mühendisliđi Bölümü

Tez Danışmanı: Prof. Dr. Nihal AYDOĞAN

EŖ Danışman: Prof. Dr. Wim DE MALSCHE

Haziran 2023, 112 sayfa

Meme kanseri dünya çapında önemli bir sađlık sorunudur ve etkili tanı ve tedavi yöntemlerinin geliştirilmesi hayati önem taşımaktadır. Meme kanseri insidans oranları 2004 yılından bu yana her yıl yaklaşık %0,5 oranında artarak, son zamanlarda konulan tüm malignite tanılarının yaklaşık üçte birine katkıda bulunmuştur. Kanserin erken teşhisi, hastalığın seyrini ve tedavisini etkileyen önemli bir adımdır, ancak hastalığın teşhisinde kullanılan mevcut görüntüleme teknikleri pahalıdır ve yan etkilere neden olabilmektedir [1]. Gelişmiş özelliklere sahip akıllı malzemelerin kanser teşhisi ve tedavisi için için kullanılması, hastaların hayatta kalma oranını azaltmak için büyük önem taşımaktadır. Bu tez çalışmasının amacı, meme kanseri tedavisine yönelik ilaç yüklü polimer-lipit hibrit partiküllerin mikroakışkan sistemlerle hazırlanması ve in vitro alım/salım çalışmalarını incelemektir. Bu amaçla ilk bölümde, tek nozüllü mikroakışkan sistem ile farklı morfolojilere sahip polimer-lipit hibrit mikroapartiküllerin (PLHMPLer) hazırlanması hedeflenmiştir. Hazırlanan PLHMPLer in Optik Mikroskop (OM), Taramalı Elektron Mikroskobu (SEM) ve Polarize Işık Mikroskobu (POM) ile boyut, boyut dağılımı, morfoloji ve optik özellikleri hakkında bilgi edinilmiştir. PLHMPLer

hazırlanırken kullanılan polimer-lipit oranı, lipit türü, yüzey aktif madde türü ve konsantrasyonu değiştirilerek iki-kompartmanlı, dambıl ve kardan adam morfolojilerine sahip farklı Janus morfolojilerine sahip partiküller hazırlanmıştır. Hazırlanan Janus PLHMPLerin yanında, partiküllerde farklı lipitler kullanılarak dönme ve öteleme hareketi yapabilen çift kırılma (birefringent) özelliğine sahip PLHMPLer hazırlanmıştır. Hazırlanan bu partiküllere manyetik nanopartikül yüklenerek manyetik alana duyarlı hale getirilmiştir. Farklı polimer-lipit kompozisyonları ile mikroakışkan teknolojisi ile hazırlanan PLHMPLer uyarana duyarlı olarak farklı biyomedikal uygulamalarda kullanılmak üzere fonksiyonelleştirilmiştir. Farklı uyarana duyarlı Hazırlanan PLHMPLerden ilaç taşıyıcı sistem olarak uygun morfolojiye sahip partikül kompozisyonları ve koşulları incelenerek tasarlanan alüminyum-cam (Al-GI) mikroakışkan sistem ile seçilen koşullarda polimer lipit hibrit nanopartiküller (PLHNPs) hazırlanmıştır. Mikroakışkan teknolojisi ile 100-200 nm boyutlarında PLHNPLer hazırlanmıştır. Meme kanseri tedavisine yönelik istenen özelliklerde hazırlanan polimer-lipit hibrit partiküllerin ilaç alım/salım kapasitelerinin değerlendirilmesi için model ilaç molekülleri olarak resveratrol (RES) ve rodamin-B (Rh-B) kullanılmıştır. Kullanılan partiküller için ilaç alım/ salım kapasiteleri UV-vis spektroskopisi kullanılarak analizlenmiştir. Yapılan çalışmalar doğrultusunda, literatürde ilk defa tek-nozüllü mikroakışkan sistem ile farklı uyaranlara polimer-lipit hibrit partiküller hazırlanmıştır. Ayrıca PLHMP yapısına eklenen manyetik nanopartiküller sayesinde hem teşhis hem de terapi amaçlı kullanılacak yeni nesil hibrit yapılar elde edilmiştir. Farklı kompozisyonlar ile manyetik ve optik uyaranlara sahip akıllı PLHMPLer ile literatürde ilk defa aynı mikroakışkan sistem ile hazırlanmıştır. Aynı zamanda literatürde nanopartikül sentezi için ilk defa polimer tabanlı mikroakışkan sistemlere alternatif olarak, ucuz ve kimyasal olarak inert Al-GI malzemedan hazırlanan mikroakışkan sistem ile 100 nm boyutlarında PLHNPLer yüksek monodispersite ($PDI > 0.1$) ile hazırlanmıştır.

Anahtar Kelimeler: polymer-lipid hybrid particles, microfluidics, drug-loading, birefringence, stimuli-responsive

ACKNOWLEDGMENTS

I would like to express my heartfelt gratitude to my advisor, Prof. Dr. Nihal Aydođan, for her unwavering support and guidance throughout my research journey. Her expertise, dedication, and insightful feedback have been invaluable in shaping the outcome of this study. Her mentorship helped me navigate the challenges and complexities of my research and encouraged me to explore new perspectives and push the boundaries of my knowledge. I am truly grateful for her unwavering belief in my abilities and her encouragement, which have played a pivotal role in my academic growth.

I would also like to extend my sincere appreciation to my co-advisor, Prof. Dr. Wim De Malsche, for his instrumental role in helping me discover and pursue my academic passion. His extensive knowledge, unwavering support, and provision of countless opportunities have been instrumental in shaping my academic trajectory. I am grateful for his mentorship, which has broadened my horizons and enriched my understanding of my chosen field. His guidance and encouragement have been crucial in fostering my intellectual curiosity and nurturing my research skills.

I am deeply grateful to Asst. Prof. Gökçe Dicle Kalaycıođlu for her exceptional support and guidance throughout my academic journey. Her unwavering belief in my abilities, dedication, and patience have been instrumental in my achievements. She has been more than a mentor; she has been a source of inspiration, celebrating my successes and supporting me in various aspects of my life. I am immensely thankful for her invaluable guidance, which has nurtured both my knowledge and personal growth.

I'm incredibly grateful to my mentor, Dr. Ilyesse Bihi, for his unwavering support and guidance. His assistance, encouragement, and belief in my abilities have been vital to my growth and success. His wisdom, expertise, and dedication have been truly inspiring. I can't thank him enough for his invaluable support. Working with him has been a privilege, and I'm immensely thankful for his exceptional mentorship.

I would also like to express my gratitude to Assoc. Prof. Emre Büküşođlu for his invaluable contribution in helping me understand the potential of my work. His insightful knowledge and guidance have had a significant impact on shaping the study. I am truly thankful for his support and the valuable insights he shared, which have been instrumental in the development of my research.

I would also like to thank Prof. Dr. Hülya Yavuz Ersan and Prof. Dr. Zeynep Çulfaz Emecen for serving on my thesis committee and providing helpful feedback and suggestions.

I am deeply indebted to thank TÜBİTAK, Scientific and Technological Research Council of Türkiye, for the financial support within the scope of 2210-C and 1001 Project-119M377.

I would be neglectful if I didn't acknowledge my cherished labmates, Burcu, Emin, Büşra, Emine, Gülce, Güliz, and Cansu. I want to express my deepest appreciation for their wonderful camaraderie, infectious energy, and invaluable assistance. It brings me immense joy to have the privilege of knowing individuals who consistently inspire and wholeheartedly support me. Their unwavering presence has been a source of motivation and comfort, and I am incredibly grateful for their friendship.

I am immensely grateful to my dear friends Karin and Can for their unwavering support and companionship throughout my journey. Despite the distance, Karin's presence, akin to a little sister, fills me with warmth and camaraderie. Can has been a steadfast pillar of support, standing by me through every high and low. Their friendship has profoundly impacted my life, bringing joy, laughter, and a sense of belonging. I express my deepest appreciation to Karin and Can for their unwavering support and positive influence.

I am immensely grateful to Toprakcık, whose warm-heartedness knows no bounds. She has consistently been there for me whenever I needed her, offering steadfast and unwavering support. Her presence in my life is truly remarkable, and I cannot thank her enough for her extraordinary kindness and unwavering dedication.

I'm incredibly grateful to my spiritual sister Neda Erbaşar and brother Can Erbaşar. Although we're not related by blood, their presence in my life feels incredibly genuine and special. Neda has been an extraordinary role model, always there to offer steadfast guidance. Her support and comforting presence during difficult times mean the world to me. I am forever grateful for the profound impact she has had on my journey. Their love and support have made me feel like we are a true family, and I am eternally thankful.

I would like to express my heartfelt gratitude to my mother, Nevin Sakız, my father, Halil Sakız, and my brother, Duha Batuhan Sakız, for their unwavering support. Their encouragement and presence have been instrumental in my journey. I am truly thankful for their love and assistance, which have played a significant role in my personal and academic achievements. Their support has meant the world to me, and I am forever grateful for their unwavering belief in my abilities.

In conclusion, I am deeply indebted to each of these remarkable individuals whose contributions have made this thesis and my academic journey possible. Their unwavering support, guidance, and belief in my potential have been pivotal in shaping the outcome of this study. I am humbled by their presence in my life, and I wholeheartedly express my deepest appreciation and thanks to each and every one of them.

Güştá İrem SAKIZ

June, 2023

TABLE OF CONTENTS

| | |
|--|------|
| ABSTRACT | i |
| ACKNOWLEDGMENTS | v |
| TABLE OF CONTENTS | vi |
| LIST OF TABLES | ix |
| LIST OF FIGURES | x |
| LIST OF ABBREVIATIONS | xiii |
| 1. INTRODUCTION | 1 |
| 2. GENERAL INFORMATION | 5 |
| 2.1. Micro- and nanoparticles | 5 |
| 2.2. Hybrid particles | 6 |
| 2.2.1. Preparation Methods of Hybrid Particles | 8 |
| 2.2.1.1. Emulsion-Solvent Evaporation | 8 |
| 2.2.1.2. Spray Drying | 9 |
| 2.2.1.3. Microfluidics | 10 |
| 2.3. Microfluidic Preparation of Hybrid Particles | 11 |
| 2.3.1. Microfluidic Preparation of Hybrid Microparticles | 13 |
| 2.3.2. Microfluidic Preparation of Hybrid Nanoparticles | 14 |
| 2.3.3. Effect of parameters on particle morphology | 16 |
| 2.4. Biomedical Applications of Micro- and Nanoparticles | 20 |
| 2.4.1. Drug-delivery | 20 |
| 2.4.2. Micromotor, Bioimaging and Biosensing | 22 |
| 3. EXPERIMENTAL | 25 |
| 3.1. Materials | 25 |
| 3.2. Preparation of Polymer-Lipid Hybrid Microparticles | 25 |
| 3.3. Microfluidic Preparation of Polymer-Lipid Hybrid Nanoparticles | 28 |
| 3.4. Characterization of Polymer-Lipid Hybrid Micro- and Nanoparticles | 30 |

| | |
|--|----|
| 3.4.1. Optical Microscope (OM) | 30 |
| 3.4.2. Fluorescence Microscope (FM) | 31 |
| 3.4.3. Polarized Optical Microscope (POM)..... | 31 |
| 3.4.4. Scanning Electron Microscope (SEM) | 32 |
| 3.4.5. Light Scattering (LS) | 33 |
| 3.4.6. Atomic Force Microscope (AFM) | 34 |
| 3.5. Investigation of Drug Encapsulation and Drug Release Properties of Polymer-Lipid Hybrid Microparticles | 35 |
| 3.5.1. Ultraviolet- Visible Spectrophotometer (UV-Vis) | 35 |
| 3.5.2. Rhodamine-B Encapsulation and Release Studies with PLHMP | 36 |
| 3.5.3. Resveratrol Encapsulation and Release Studies with PLHMP | 36 |
| 3.6. Investigation of Magnetic Nanoparticle Encapsulation into Polymer-Lipid Hybrid Microparticles and Characterization | 37 |
| 3.6.1. Preparation of Oleic-Acid Coated Magnetic Nanoparticles | 37 |
| 3.6.2. Characterization of Oleic Acid Coated Magnetic Nanoparticle loaded Polymer-Lipid Hybrid Microparticles | 38 |
| 4. RESULTS AND DISCUSSION..... | 39 |
| 4.1. Preparation and Characterization of Polymer Microparticles by One- Nozzle Microfluidic System..... | 39 |
| 4.2. Preparation and Characterization of Lipid Microparticles by One-Nozzle Microfluidic System..... | 41 |
| 4.3. Preparation and Characterization Of Polymer-Lipid Hybrid Microparticles by One-Nozzle Microfluidic System | 42 |
| 4.3.1. The Effect of Surfactant Type and Concentration on Polymer-Lipid Hybrid Microparticles | 43 |
| 4.3.2. Examination of Solvent Evaporation Conditions for the Morphology of Polymer-Lipid Hybrid Microparticles | 51 |
| 4.3.3. Examining The Hybrid Morphology of Polymer-Lipid Hybrid Microparticles | 53 |
| 4.3.4. The Effect of Flow Rate Ratio on the Aspect Ratio of Polymer-Lipid Hybrid Microparticles | 55 |

| | |
|--|----|
| 4.3.5. The Effect of Polymer-Lipid Ratio on the Area of Polymer and Lipid Components of Polymer-Lipid Hybrid Microparticles | 56 |
| 4.3.6. The Short Term Stability Test of PCL-Precirol ATO 5 Hybrid Microparticles | 58 |
| 4.4. Preparation of Polymer-Lipid Hybrid Microparticles with Different Lipids | 58 |
| 4.5. Preparation of Polymer-Lipid Hybrid Microparticles with Three Components..... | 61 |
| 4.5.1. The Effect of Surfactant Type and Concentration on Polymer-Lipid Hybrid Microparticles with Three Components..... | 64 |
| 4.5.2. The Effect of Exchanging the Concentrations of Lipid And Fluorinated Component on the Morphology of Polymer-Lipid Hybrid Microparticles with Three Components | 66 |
| 4.5.3. Examining The Hybrid Morphology of Polymer-Lipid Hybrid Microparticles with Three Components | 67 |
| 4.6. The Preparation of Magnetic Nanoparticle Loaded Polymer-Lipid Hybrid Microparticles | 68 |
| 4.7. The Optical Properties Examination of Polymer-Lipid Hybrid Microparticles | 73 |
| 4.8. The Microfluidic Preparation of Polymer-Lipid Hybrid Nanoparticles | 77 |
| 4.9. Investigation of Drug Encapsulation and Drug Release Properties of Different Drugs Loaded PLHMPs | 80 |
| 4.9.1. Investigation of Rhodamine-B Release from PLHMPs at Different Polymer-Lipid Ratios | 81 |
| 4.9.2. Investigation of Resveratrol Release from PLHMPs with Different Polymer-Lipid Ratio..... | 83 |
| 5. CONCLUSION AND FUTURE RECOMMENDATIONS..... | 86 |
| 6. REFERENCES | 91 |
| CURRICULUM VITAE | 98 |

LIST OF TABLES

| | |
|--|----|
| Table 4.1. The surface tensions of different co-surfactant types and concentrations | 44 |
| Table 4.2. The particle morphology and schematics of PCL- ATO 5 MP's with different co-surfactant types and concentration..... | 60 |
| Table 4.3. Particle morphologies of multi-componental PCL-Stearic Acid MPs | 65 |
| Table 4.4. Particle morphologies of multi-componental PCL-Stearic Acid-Fluo MPs.. | 66 |
| Table 4.5. Particle morphologies of multi-component PCL-Stearic Acid MPs, A) PCL-SA (1:1), B) PCL-SA-FLUO (1:0.7:0.3), C) Oleic acid coated MNP loaded PCL-SA-FLUO (1:0.7:0.3). OM-1 images are taken with a polarized optical microscope without polarizing filters, while OM-2 images are taken with an inverted light microscope..... | 70 |
| Table 4.6. Particle morphologies of multi-component PCL-Stearic Acid-Fluo MPs..... | 72 |
| Table 4.7. The nanoparticle sizes with an increasing flow rate..... | 79 |
| Table 4.8. The comparison of drug release profiles of PCL-Precirol ATO 5 microparticles with different polymer-lipit ratio | 84 |

LIST OF FIGURES

| | |
|---|----|
| Figure.2.1. Schematics of different micro/nanoparticle morphologies [21] | 5 |
| Figure 2.2. Schematic diagram of the emulsion solvent evaporation method. | 8 |
| Figure.2.3. The schematic representation of spray drying [25] | 9 |
| Figure 2.4. Functional particle production by microfluidics [37] | 10 |
| Figure 2.5. Classification of microparticles prepared by droplet microfluidics: Three main aspects of shape, compartment, and microstructure can be independently or simultaneously incorporated into microparticles [37]..... | 11 |
| Figure 3.1. A schematics of one-nozzle microfluidic system | 26 |
| Figure 3.2. The experimental setup of microfluidic preparation of microparticles A) The schematic, B) An image of experimental setup..... | 27 |
| Figure 3.3. An image Al-Gl microfluidic system for nanoparticle production..... | 29 |
| Figure 3.4. A schematic of the dynamic light scattering (DLS) setup [100] | 34 |
| Figure 4.1. A) OM image of PCL microdroplets B) OM image of PCL microparticles | 40 |
| Figure 4.2. Characterization of Precirol ATO 5 microparticles: A) OM images, B) SEM images, C) FM images of Rhodamine-B Loaded ATO 5 MPs | 41 |
| Figure 4.3. The morphology distribution of PCL- Precirol ATO 5 MPs with PVA and SDBS as surfactants. The images (A-C) are zoomed-in images of the left image. | 42 |
| Figure 4.4. The particle morphology and schematics of PCL- ATO 5 MP's with different co-surfactant types and concentration | 45 |
| Figure 4.5. The particle morphology and schematics of PCL- ATO 5 MP's with different co-surfactant types and concentration | 46 |
| Figure 4.6. The particle morphology of different microparticles by microfluidics, A) PCL microparticles [34], B) Precirol ATO 5 microparticles, C) PCL-Precirol ATO 5 hybrid microparticles, D) PCL-Precirol ATO 5 hybrid microparticles. The particles from A-C were prepared with surfactants PVA and SDBS; in part D, SDS was used instead of SDBS. | 48 |
| Figure 4.7. The particle morphology and schematics of PCL- ATO 5 MP's with different co-surfactant types and concentration | 49 |
| Figure 4.8. Morphology distribution of PCL- Prericol ATO 5 MP's with PVA and SDS as a surfactant | 50 |

| | |
|--|----|
| Figure 4.9. Particle morphologies at different solvent evaporation rates of PCL-ATO 5 MPs | 52 |
| Figure 4.10. Shrinkage rate of hybrid MPs in rapid solvent evaporation | 53 |
| Figure 4.11. OM images of PCL-ATO 5 hybrid microparticles treated with acetone for 30 s, A) before the treatment, B) after the treatment | 53 |
| Figure 4.12. DSC profiles of Precirol ATO 5 (Samples were prepared 10 mg in weight. Measurements were carried out between 0-150 °C with a heating rate of 10 °C /min). | 54 |
| Figure 4.13. The effect of increase in temperature on rate PCL-ATO 5 (1:1) hybrid MPs | 55 |
| Figure 4.14. The effect of flow rate ratio on the aspect ratio of PLHMPs, A) The Q_{in} is 0.06 ml/h, and Q_{out} is 1.6 ml, B) The Q_{in} is 0.06 ml/h, and Q_{out} is 0.8 ml/h, C) The Q_{in} is 0.18 ml/h, and Q_{out} is 2.4 ml/h, D) The Q_{in} is 0.18 ml/h, and Q_{out} is 0.8 ml/h.(The Q_{in} and Q_{out} represent the flow rate of inlet and outlet phases, respectively.). | 56 |
| Figure 4.15. The effect of polymer-lipit ratio on the area of polymer-lipid hybrid microparticles. All particles were prepared at the same flow rates for the dispersed and continuous phases. The white color shows the polymer and the lipid part is shown in blue color in the schematic representation. | 57 |
| Figure 4.16. The Particle Morphology and schematics of PCL- ATO 5 MP's with different co-surfactant types and concentration..... | 58 |
| Figure 4.17. The particle morphology Rhodamine-B labelled PLHMPs prepared using different type of lipid | 61 |
| Figure 4.18. The morphologies of PLHMPs with stearic acid, A) The OM image of PCL- Stearic Acid (1:1) PLHMPs, B) The SEM image of PCL-Stearic Acid (1:1) PLHMPs, C) The OM image of PCL-Stearic Acid-Fluo (1:0.7:0.3) PLHMPs, D) The SEM image of PCL-Stearic Acid-Fluo(1:0.7:0.3) PLHMPs..... | 63 |
| Figure 4.19. SEM-EDX analysis of PCL-SA-FLUO hybrid microparticles | 63 |
| Figure 4.20. The particle morphology and shematics of PCL- ATO 5 MP's with different co-surfactant types and concentration, A) PCL-SA-Fluo hybrid MPs, B) SA-Fluo hybrid MPs, C)PCL-ATO 5-Fluo hybrid MPs and D)PCL-SA hybrid MPs..... | 68 |
| Figure 4.21. The DLS analysis of oleic acid coated MNPs..... | 69 |
| Figure 4.22. The translational speed of oleic acid coated MNP's loaded PLHMPs in 50s, A) t=0, B) t=25 s, C) t=50 s (The scale bar=50 μ m) | 73 |

Figure 4.23. POM images of multi-component PCL-Stearic Acid MPs, A) PCL-SA (1:1), B) PCL-SA-FLUO (1:0.7:0.3), C) MNP loaded PCL-SA-FLUO (1:0.7:0.3). The white insert arrows shows the position of the analyzer and polarizer.....75

Figure 4.24. The rotational movement of MNP loaded PLHMPs, A)The magnet rotates counter clockwise under continuous rotating magnetic field, B) No magnetic field is applied at t=0, C) The magnet rotates clockwise under continuous rotating magnetic field, D-F) The schematics of the particles in A-C respectively. The POM images were taken 20 seconds after the magnetic field was applied in the A and C.The white insert arrows shows the position of the analyzer and polarizer.....76

Figure 4.25. A) AFM images of PLHNPs at a total flow rate of 110 $\mu\text{L}/\text{min}$, B) Particle size distribution of PLHNPs at a total flow rate of 110 $\mu\text{L}/\text{min}$ determined by DLS, C) AFM images of PLHNPs at a total flow rate of 1100 $\mu\text{L}/\text{min}$, D) Particle size distribution of PLHNPs at a total flow rate of 1100 $\mu\text{L}/\text{min}$ determined by DLS, E) AFM images of PLHNPs at a total flow rate of 2200 $\mu\text{L}/\text{min}$, F) Particle size distribution of PLHNPs at a total flow rate of 2200 $\mu\text{L}/\text{min}$ determined by DLS (Topography mode was used for the AFM images).....79

Figure 4.26. In vitro release profiles of Rhodamine-B from both PCL-ATO 5 MPs with different polymer-lipid ratio in PBS solution at 37 °C during 6 hours. Release medium: pH = 7.4. Inset shows Rhodamine-B release in 1 hour). [n=3]82

Figure 4.27. In vitro release profiles of Resveratrol from both PCL-ATO 5 MPs with different polymer-lipid ratio in PBS solution at 37 °C during 48 hours. Release medium: pH = 7.4, 0.1% Tween 20. Inset shows Resveratrol release in 1 hour). [n=3].83

LIST OF ABBREVIATIONS

Abbreviations

| | |
|-------|-------------------------------------|
| AFM | Atomic Light Microscopy |
| DCM | Dichloromethane |
| DLS | Dynamic Light Scattering |
| EE | Encapsulation Efficiency |
| FEP | Fluorinated Ethylene Propylene |
| FM | Fluorescence Microscope |
| ID | Inner Diameter |
| IM | Inverted Microscope |
| MNP | Magnetic Nanoparticles |
| OD | Outer Diameter |
| ATO 5 | Precirol ATO 5 |
| PCL | Polydimethylsiloxane |
| PDMS | Polydimethylsiloxane |
| PLHMP | Polymer-Lipid Hybrid Microparticles |
| PLHNP | Polymer-Lipid Hybrid Nanoparticles |
| PLM | Polarized Light Microscope |
| PVA | Polyvinylalcohol |
| RES | Resveratrol |
| RH-B | Rhodamine-B |
| SA | Stearic Acid |
| SEM | Scanning Electron Microscope |
| SDBS | Sodium Dodecyl Benzenesulfonate |

SDS

Sodium Dodecyl Sulfate

UV-Vis

Ultraviolet-Visible Spectrophotometer

1. INTRODUCTION

In recent years, there has been increasing interest in particle-based carrier systems, which frequently appear in nano/micro sizes owing to technological advancements. These systems are found in food, biotechnology, and healthcare and can contain organic or inorganic materials. These systems can be used as drug carriers of desired sizes or in applications such as water purification. The particle morphology and size properties can be optimized according to the application area. Particles with different and complex morphologies have diverse applications. This study focuses on the microfluidic preparation of polymer-lipid hybrid microparticles (PLHMP) and nanoparticles (PLHNP) for different biomedical applications. The targeted hybrid particles are anisotropic structures with two or more compartments, allowing different adjustable properties to exist simultaneously in a single particle, thus providing the desired pharmacokinetic properties, preventing drug-drug interactions, and enabling the independent control of release kinetics for drug delivery.

There is a growing interest in preparing functional micro- and nanoparticles by microfluidic technology [2, 3]. The preparation of multifunctional hybrid particles has been rapidly developed with droplet-based microfluidic systems [4]. Microfluidic technology offers a precise control which enables the formation of particles with controlled size, shape, and composition [5, 6]. Microfluidic technology also has some disadvantages, such as expensive facilities [7], low throughput [8-10] and leakage [11]. However, it is possible to overcome some problems encountered with system design, materials used and chemicals selected. In recent years, multi-nozzle microfluidic system studies have become popular, especially for high throughput, expressed as one of the bottlenecks of microfluidics [12]. In the literature, it is seen that polymer-based microfluidic systems are on the rise for the synthesis of PLHMP and PLHNP [13]. This is mainly because these systems are inexpensive, disposable and simple [14]. However, the solvents used in systems where complex structures are prepared may damage polymer-based microfluidic systems. Therefore, the material used in microfluidic chip design must also be chemically resistant. Silicon and glass are traditionally used chemically-inert materials and have been used in microfluidic system in many years [15]. PLHMPs and PLHNPs, owing to their combination of multi-components, have several advantages over other drug carrier nanomaterials, such as multifunctional application

potential, increased hydrophobic drug loading capacities, and prevention of leakage of hydrophilic drugs from nanoparticles. The polymer chosen for the hybrid particles was polycaprolactone (PCL), which has high biocompatibility and stability, whereas the lipid chosen was the lipophilic matrix Precirol ATO 5 (ATO 5). Thus, it is planned to take advantage of the benefits of both materials in the particle design in the most effective way.

This study aims to prepare drug-loaded PLHNPs for breast cancer treatment. However, preparing these particles is also aimed at preparing PLHMPs for different biomedical applications. While hybrid structures prepared with microfluidic technology are mostly target-oriented designs, studies in which structures with multiple functionalities are prepared are in the minority. In this study, different PLHMPs will be prepared with different lipids to be used in the hybrid structure, and their preparation as stimuli-responsive will be focused. These particles, thought to be prepared as magnetic, light and temperature responsive, are aimed to be used in biomedical applications such as biosensing, micromotor and bioimaging. It also aims to prepare all the functional PLHMPs with the same microfluidic system. One-nozzle microfluidic system is a compact system that can be easily prepared by assembling two capillaries with different diameters to form a co-flow geometry and is a fast and easily accessible system due to the lack of a time-consuming fabrication process compared to other microfluidic systems. In case of problems such as leakage and fouling mentioned before, it is possible to replace the components of the system in a short time or to coat the outer walls of the capillaries. In this study, we plan to prepare stimuli-responsive PLHMPs with a one-nozzle microfluidic system.

This project proposes the synthesis of PLHNPs with a size of approximately 200 nm via microfluidics. The emulsion-solvent evaporation method, a traditional method for particle synthesis, allows for the simple and fast production of particles. However, particles are obtained as uniform and monodisperse in the microfluidic method than in the emulsion-solvent evaporation method with a low polydispersity index (PDI) [16]. However, a microfluidic chip design specifically for PLHNP synthesis with a desired size and morphology is necessary. Therefore, an AI-GI microfluidic chip was designed specifically for PLHNP synthesis in this study. A nanoprecipitation based microfluidic system is being prepared for the preparation of PLHNPs. It is planned to optimize particle sizes by selecting different flow rates, and it is estimated that PLHNPs around 200 nm can be

prepared with the designed Al-Gl microfluidic chip. In this way, drug delivery systems that can be used for breast cancer treatment will be prepared with microfluidic technology. In the scope of the intended thesis study, model hydrophilic and hydrophobic drug-loaded polymer-lipid hybrid particles were prepared and characterized for use in the treatment of breast cancer. The combination of different properties in hybrid systems can provide several advantages over non-hybrid platforms, such as improvements in bloodstream circulation time, low encapsulation rate and non-specific release kinetics[17]. To overcome the limitations of lipids in hybrid structures such as low solubility, high dose toxicity and non-specific distribution to the unwanted site, and to utilize the properties of polymeric nanoparticles are used to achieve a more efficient drug delivery system.. The development of microfluidic systems could be promising for the preparation of functional nanoparticles for future biomedical applications[18]. Microfluidic technology offers a high control on size, rigidity, morphology and surface modification control in the preparation of nanomaterials [10]. One of the first studies on PLHNPs by microfluidics with low PDI was published in 2010 [19]. Since then, PLHNPs with different formulations have been prepared by microfluidics and with the development of microfluidic technology, there is a growing interest in the preparation of these structures.

In this study, it is planned to produce uniform drug-loaded polymer-lipid hybrid particles with different morphologies using microfluidic devices and the size, structure, polydispersity, drug loading capacity and drug release efficiency of the particles will be compared. The studies in the literature show that particles produced by conventional methods are more polydispersed and have lower drug loading efficiencies than particles produced with the same properties by microfluidic devices. The use of microfluidics, which will be used as a method in the study, is becoming popular for nanoparticle synthesis, especially in the field of Biotechnology. In the study, different morphologies, if any, of the obtained particles will also be examined. This will also provide information about the potential applications of hybrid structures.

Within the scope of this thesis, the advantages of the geometry of hybrid Janus micro- and nanoparticles and the use of both polymer and lipid materials as components have been evaluated and studies have been initiated by predicting that Janus high aspect ratio structures will be superior to spherical structures. In addition, the advantages offered by microfluidic technology will enable the preparation of uniform and monodisperse

particles and, thus an effective result in the targeted application. The size and other physicochemical properties of the micro- and nanoparticles planned to be produced are planned to be designed for the purpose of changing the parameters in the synthesis process or by making changes to the materials used in their composition. Thus, it is aimed to prepare ideal, stable and biocompatible PLHMPs and PLHNPs with properties for different biomedical applications.

2. GENERAL INFORMATION

2.1. Micro- and nanoparticles

Microparticles are solid particles with a size in the range of 1 to 1000 μm , while nanoparticles are solid particles with a size in the range of 1 to 1000 nm. Most microparticles and nanoparticles are smaller than 100 μm and 200 nm, respectively [20].

Micro- and nanoparticles may be composed of different materials, including polymers, lipids and inorganic materials, and also they can be designed to have multiple components, known as hybrid particles.

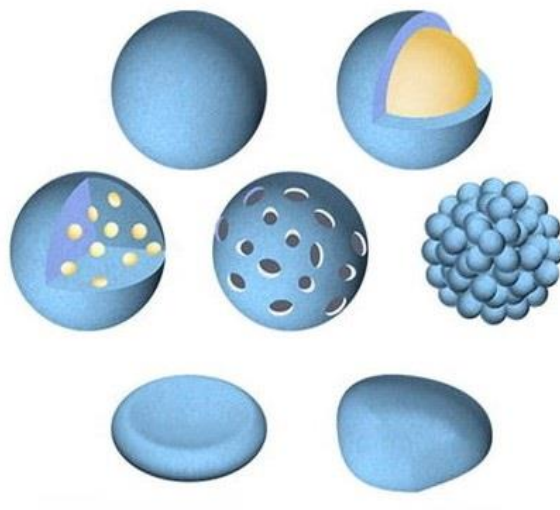


Figure.2.1. Schematics of different micro/nanoparticle morphologies [21]

Particles can generally be divided into solid, core-shell, and multicompartmental particles. Spherical, non-spherical, homogeneous, or heterogeneous microparticles can be classified as solid particles, whereas core-shell particles exhibit development characteristics with their double-compartment structure compared to solid particles. These different particle types have unique properties, applications, and advantages/disadvantages. Micro- and nanoparticles can comprise polymeric, lipid, inorganic materials or asymmetric particles with different compositions. These particles may be composed of single or multiple components. Multicompartmental particles can

have a variety of morphologies and can be integrated into complex systems with versatile functionalities.

2.2. Hybrid particles

A hybrid particle is composed of multiple components, such as polymers, lipids, and inorganic materials, in a single particle. Their unique properties are not present in the individual components, making them advantageous in drug delivery and sensing applications.

Hybrid particles are typically designed to take advantage of the properties of two or more materials, such as their different solubility, stability, or reactivity. The properties of hybrid particles can be modified by varying the size, composition, and morphology. These particles can have a more complex structure than single-component particles, with different layers or compartments that serve different functions. For example, a multicomponent particle might have a lipid layer to protect the drug payload, a polymeric layer to control release, and a targeting ligand on the surface to improve specificity for a specific application.

Polymers such as PLGA and PLA are frequently used in the literature, while studies involving PCL are more limited. However, the advantages of using PCL include a moderate drug release rate, lower in vivo adsorption time, and the creation of a minimum acidic environment during degradation, unlike other biodegradable polymers [22, 23]. It does not resemble PLA or PLGA, which exhibit prolonged drug release, longer degradation time, and an acidic environment after degradation [24]. Therefore PCL, which has high biocompatibility, was selected as the polymer component of the hybrid particle for this study. Precirol ATO 5 is a lipophilic matrix composed of mono-, di-, and triglyceride mixtures increasingly used in lipid carrier systems in recent years to prepare sustained-release products. This lipid is planned to be used as the lipid component.

Hybrid particles can be classified according to their morphologies; core-shell, hollow, patchy, and Janus. In core-shell morphology, the core material is surrounded by another material, and these morphologies are widely used in drug-delivery applications since the core could contain a drug, and the shell provides protection and can control the drug release of particles.

Janus particles have garnered significant attention due to their unique ability to present two compartments with distinct surface properties, structures, and compositions within a single particle. Their anisotropic structures enable them to contain different or completely opposing physical and chemical properties in one particle, making them easily modifiable and capable of acquiring many functional properties. By compartmentalizing different properties within a single particle and providing adjustable properties, Janus particles can offer desired pharmacokinetic properties, prevent drug-drug interactions, and enable independent control of release kinetics. The physical, chemical, and optical properties of each compartment within a Janus particle are contained within the particle despite the presence of two autonomous compartments. This results in a synergistic effect that has garnered considerable interest in biomedical research because of the ability of Janus particles to combine different structures and surface chemistries to achieve high performance. The generation of Janus particles via the phase separation technique relies on the spreading coefficient theory, which elucidates the impact of interfacial tension between phases on particle morphology. In the design of hybrid structures using phase separation-based methods, interfacial tensions of the constituent phases constitute critical parameters.

Various methods can produce Janus particles, including self-assembly, surface modification, self-clustering, and microfluidic methods. The self-clustering method, the oldest method for producing polymeric Janus particles, involves the self-assembly of double and triblock copolymers. In the surface modification method, homogeneous particles are synthesized first, and then a masking method is used to modify a specific part of the particle through chemical modifications. The emulsion method is another approach to preparing Janus particles, in which a solvent dissolves the particles to create a two-phase system. Also, the microfluidic method involves the manipulation of fluids in microchannels, resulting in the production of particles in microscale droplets. This method has advantages over other preparation techniques since the particles have high monodispersity and uniformity.

Janus particles have shown promise as potential drug carrier systems due to their anisotropic surface structures, which can encapsulate hydrophilic and hydrophobic drugs in a single particle. The emulsion phase separation method is economically feasible for synthesizing Janus particles, enabling large-scale production. However, controlling the phase separation of different materials that form the hybrid structure in a dynamic system

poses a challenge. Additionally, the structure of Janus particles can change after the drug loading, as reported in previous studies.

2.2.1. Preparation Methods of Hybrid Particles

Several methods exist to prepare hybrid micro and nanoparticles from organic and inorganic materials. Emulsion-solvent evaporation, spray drying, and microfluidics are the most widely used methods for preparing hybrid particles depending on the desired size, composition and morphology.

2.2.1.1. Emulsion-Solvent Evaporation

This method is a conventional method to produce micro and nanoparticles. The method also enables the production of hybrid particles with an optimization of the production process. Emulsion-solvent evaporation method is a simple, versatile and high-yield method for particle production. This method can be modified to produce particles with different morphologies, such as core-shell, Janus, or hollow structures, by adjusting the emulsion conditions and the materials used. However, the method leads to polydispersity, difficult particle morphology control, and potential material instabilities.

In this method, polymer and lipid dissolve in an organic solvent, emulsified in an aqueous phase with surfactants. Different emulsification techniques may be applied for particles of different sizes. After the emulsion preparation, solvent evaporation forms particles from droplets by extracting the organic solvent. The schematic diagram of the emulsion-solvent evaporation steps is shown in Figure 2.2.

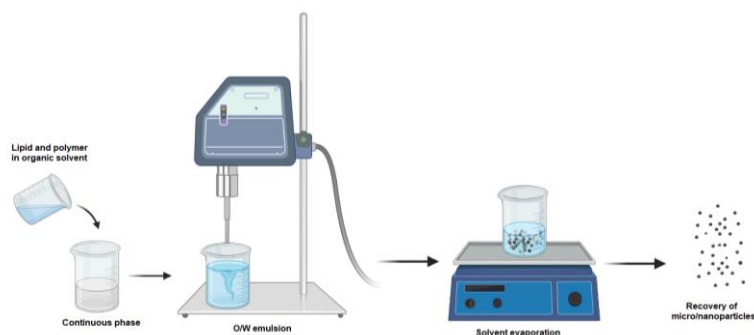


Figure 2.2. Schematic diagram of the emulsion solvent evaporation method.

2.2.1.2.Spray Drying

Spray drying is a widely used method for producing micron and sub-micron particles from liquid materials in the pharmaceutical, food and chemical industries. The method is rapid, single-step, and continuous, and the production is high-throughput which are the advantages of this method for industrial applications. The schematic diagram of spray drying is shown in Figure 2.3.

The process starts with the preparation of the feedstock. Feedstock is a liquid feed material composed of materials with the desired concentration and composition for particle production. The liquid feed was atomized using an atomizer. In the drying process, the atomized droplets come into contact with hot air or gas, which causes the droplets to evaporate and become particles. After particle formation, the cyclone separated the particles, and the collected particles were obtained.

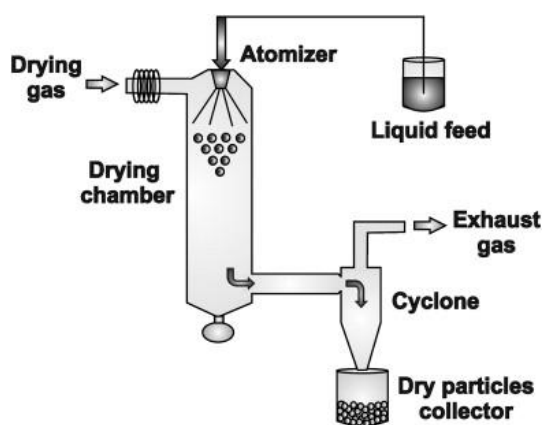


Figure.2.3. The schematic representation of spray drying [25]

An example of this is the study by Joyce et al., in which they produce PLGA-lipid hybrid microparticles about 5 μm in size by the spray drying method [26]. The studies presented so far support the idea that spray drying is a method to produce hybrid microparticles. Recent studies show that new devices enable the production of drug-loaded nanoparticles by spray drying [25]. Wang et al. [27] reported the production of 420 ± 30 nm hybrid nanoparticles as a nanocarrier using the spray drying method. However, the limitations of this technique are the difficulty in controlling the size of particles, leading to polydispersity and irregular particle morphologies, loss of products resulting in lower yields (20-70%), and the difficulty of equipment cleaning and fouling problems [28].

2.2.1.3. Microfluidics

Microfluidic technology controls and manipulates fluids in a micron-scale channel that is etched or moulded into a plastic or glass material. Microfluidic devices can be used in cell encapsulation, culture studies, particle synthesis, biosensors, agricultural applications, and healthcare [29]. Furthermore, due to the precise control of fluids in micron-scale channels, particles with the desired structure and size can be produced, and drug-encapsulated particles can be prepared [30, 31]. Figure 2.4. shows the schematics of particles with different morphologies by microfluidics. Microfluidic technology offers precise control of particle size and morphology [32].

The particle geometry have an important role in drug delivery.

Microfluidic devices also enable the continuous production of hybrid microparticles and nanoparticles. While much more uniform particle production can be achieved in these devices compared to conventional methods, the design and manufacturing processes of the devices can be challenging, and the high throughput is another limiting factor [33]. However, microfluidic technology offers enhanced control over particle size compared to conventional methods [34]. In order to achieve the desired particle size and morphology, the unique design of microfluidic devices is crucial. The most important advantage of microfluidic devices is that they allow more uniform, controllable and small particles to be obtained compared to conventional methods such as emulsion [35, 36].

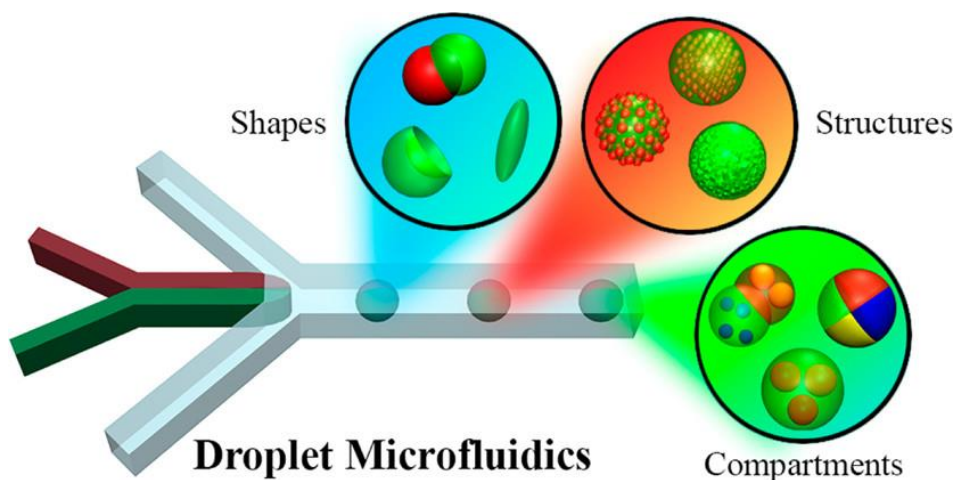


Figure 2.4. Functional particle production by microfluidics [37]

Microfluidic technologies with precise fluid control have systems that provide uniform structures and higher drug encapsulation efficiency will be used to prepare polymer-lipid hybrid particles. Traditional methods have limitations, such as low drug loading efficiency and high polydispersity; therefore, microfluidic technology allow the production of drug-loaded particles with higher monodispersity, drug encapsulation efficiency and an improved control over size and morphology [38, 39].

2.3. Microfluidic Preparation of Hybrid Particles

In order to prepare particles by droplet-based microfluidic systems, the regimes that will enable the flows to form droplets are of great importance. In order to form droplets in microfluidic systems, fluids are fed into the microfluidic system at specific flow rates with the help of microfluidic pumps. Uniform droplet production is achieved in microchannels through continuous, uniformly formed droplets at the intersection of the dispersed and continuous phases. Different particle morphologies can be achieved by droplet microfluidics (Figure 2.5)

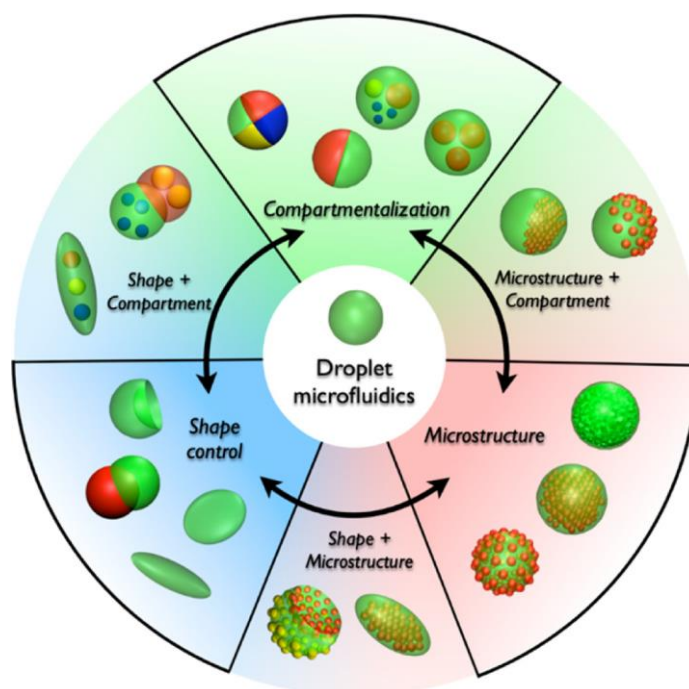


Figure 2.5. Classification of microparticles prepared by droplet microfluidics: Three main aspects of shape, compartment, and microstructure can be independently or simultaneously incorporated into microparticles [37].

The preparation of particles in microfluidic systems are prepared with forming the drops one by one in the system. The phase that will form the droplet is selected as the dispersed phase, while the continuous phase compresses and interrupts the dispersed phase to form droplets. The dripping regime is the ideal flow regime to generate droplets. However, in the regime where jet flow is observed, assuming a constant "continuous phase" flow rate, droplet formation cannot be achieved uniformly since the dispersed phase flow rate is much higher than in the dripping regime. In this case, no monodisperse droplet formation is observed, resulting in polydisperse particles. In the stable co-flow regime, the dispersed phase creates continuous droplets in the continuous phase, allowing the formation of uniform droplets. However, this is not a desirable regime for droplet formation as it does not provide an opportunity for droplet formation. Therefore, in a microfluidic device where uniform particle formation is aimed, the flow rates of the phases to be used should be operated in a flow rate range that will create a dripping regime.

The channel width and depth in the microfluidic chip design and the channel's position are the parameters that directly affect the droplet size. Therefore, the geometry of the microfluidic device directly affects the particle size [40]. In addition, physicochemical properties of the phases, such as concentration and viscosity, are other parameters that affect the size and structure properties of the particles. In addition to other conditions that affect phase separation during solvent evaporation, important parameters also determine particle morphology.

In order to achieve the targeted particle morphology and size, selecting the material for the microfluidic system is essential. Physical properties of the material, such as light transmittance, durability, chemical resistance, and electrical conductivity, should be evaluated, as well as production processes suitable for the selected material and the associated limitations [41]. The materials used for manufacturing microfluidic devices can be analyzed in three primary groups: inorganic, polymer and paper. While silicon and glass are frequently used as inorganic materials, ceramic materials baked at low temperatures have also been used recently. As polymer materials, elastomers (PDMS, TPE, etc.) and thermoplastics (PMMA, COC, etc.) are frequently used. Paper materials are entirely different from polymer and inorganic materials and are emerging materials used in microfluidic technology [41].

2.3.1. Microfluidic Preparation of Hybrid Microparticles

Droplet-based microfluidic systems use at least two different fluids for particle production. In these systems, the dispersed phase is compressed by the continuous phase with different geometries to form droplets. For this purpose, three basic geometries are frequently used in microfluidic systems. These geometries are co-flow, flow-orientated, and T-junction geometries (Figure 2.6).

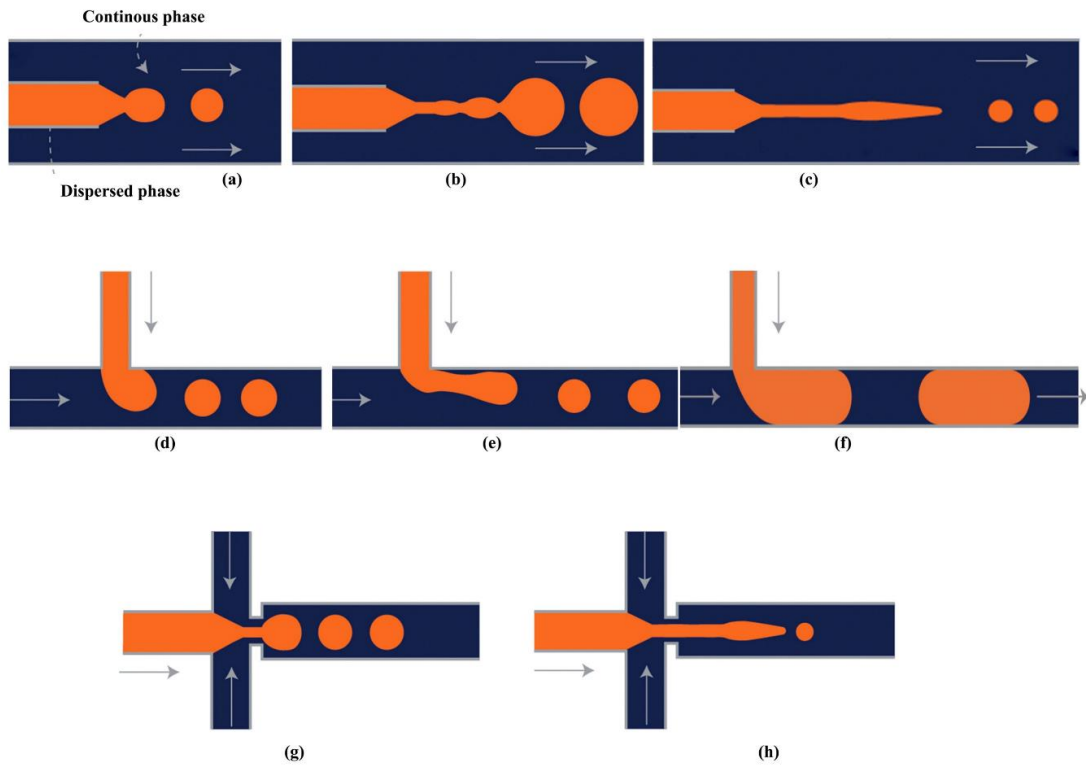


Figure 2.6. A droplet breakup in each of the three primary microfluidic geometries used for droplet formation; (a–c) show dripping, widening jetting and narrowing jetting, respectively, in co-flow drop-makers; (d–f) show dripping, jetting and squeezing in T-junction; (g,h) show dripping and jetting in flow-focusing drop maker. Orange and dark blue represent the dispersed phase and continuous phase, respectively [42]

Recent studies indicate that polymer-lipid Janus MPs are prepared using a microfluidic device with a flow-focusing geometry made of polydimethylsiloxane (PDMS) and used as a drug carrier system[43]. Particles are designed based on different Janus structures

with various lipids-polymer ratios and morphologies ranging from 33 μm to 121 μm in size. In the study, polylactic-glycolic acid (PLGA), widely used in the pharmaceutical industry, is used as a polymer, while Softisan 100 is chosen as the lipid. Although polymers such as PLGA and PLA are frequently used in the literature, studies involving PCL polymers are limited. However, the use of PCL has advantages such as a moderate drug release rate, a lower in vivo adsorption time, and a minimal acidic environment during degradation as opposed to other biologically degradable polymers. It is not comparable to PLA or PLGA, which exhibit prolonged drug release, longer degradation times, and a highly acidic environment after degradation [44].

Therefore, this study chose biocompatible PCL as the polymer for the hybrid particle component. As a lipid component, Precirol ATO 5, a lipophilic matrix composed of mono, di, and triglycerides that have been increasingly used in lipid carrier systems and for the preparation of sustained release products, will be used. Microfluidic systems that offer the advantages of uniform structure and higher drug encapsulation capacity will be utilized. Traditional methods have limitations regarding drug loading efficiency and high polydispersity. Therefore, this study aimed to produce uniform drug-loaded polymer-lipid hybrid Janus particles using microfluidic devices. The fused silica capillary-based one-nozzle microfluidic system with higher chemical resistance will be used to design the microfluidic device. A co-flow geometry will be selected for the device flow geometry. Therefore, in this study, biocompatible PCL was chosen as the polymer for the hybrid particle. As a lipid component, ATO 5, will be used. The microfluidic systems that offer the advantages of uniform structure and higher drug encapsulation capacity will be used for preparing PLHMP's.

2.3.2. Microfluidic Preparation of Hybrid Nanoparticles

Microfluidic nanoparticle production is being developed with the nucleation and growth of nanoparticles by nanoprecipitation. Microfluidic technology enables the production of uniform nanoparticles and consists of several steps. First of all, the mixing of the phases takes place by diffusion. The channel geometry of the microfluidic system is used to control the mixing and reaction precisely. Precise control over the microfluidic system during mixing enables the production of monodisperse nanoparticles. For particle production, organic and aqueous solutions containing nanoparticle precursor components

are introduced into the microfluidic device at a predetermined flow rate and flow rate ratio between aqueous and organic solvents. Mixing the organic solution with the 'anti-solvent' (mostly aqueous solution) causes the precipitation of the precursor components as nanoparticles. The anti-solvent can be an organic solvent other than aqueous solution. The ability to control the mixing of fluids makes it suitable for solvent/antisolvent precipitation of nanoparticles.

Active and passive methods can be used for nanoparticle production via microfluidic technology. Creating micro vortices in microchannels under normal conditions can be challenging. Therefore, active methods achieve effective particle formation by controlling the mixing with different manipulations applied on the system. In passive methods, on the other hand, a herringbone geometry is created on the system without any external manipulation, providing a chaotic mixing on the system and passively creating mixing in the system. Different microfluidic systems used for nanoparticle production are given in Figure 2.7.

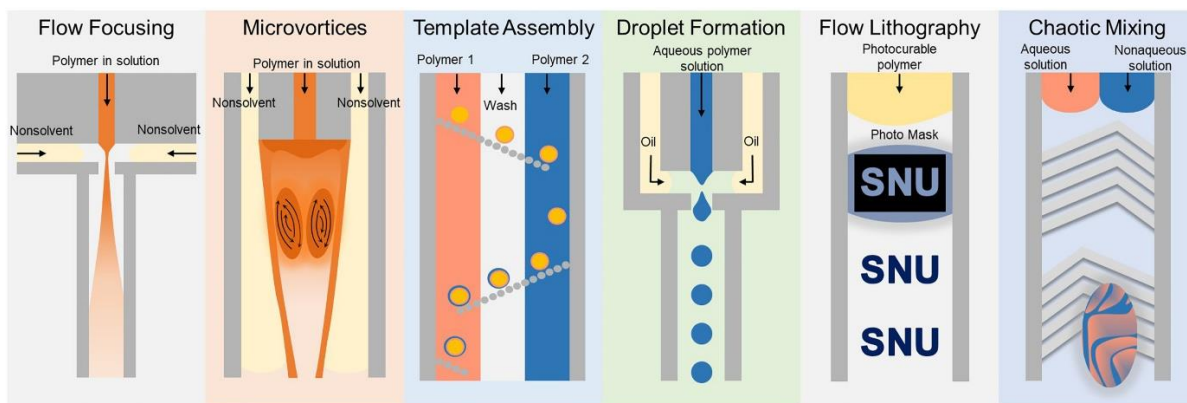


Figure 2.7. Various microfluidic-based particle fabrication methods which offer controllable particle production [45]

Current research on producing hybrid nanoparticles using microfluidic devices is limited, with most studies focussing on particle sizes greater than 200 μm and lacking anisotropic structures. However, Xie et al. reported the successful synthesis of Janus polymeric nanoparticles capable of carrying hydrophobic and hydrophilic drugs within a single nanoparticle using a fluidic nanoprecipitation system (FNPS) [46]. The FNPS device used

two stainless steel capillaries with an i.d. of 0.127 mm as the sample inlet channels for two polymer injections. One inlet delivered a PLA/PGA 50:50 solution in DMF, while the other contained PLGA in acetone. The dispersing stream was composed of 1% PVA in water. Inlets were set at a flow rate of 100 μ L/h, while the dispersing channel flowed at 75 ml/min, resulting in Janus nanoparticles with sizes of 305 ± 8 nm. Similarly, Mieszawska et al. synthesized high-throughput polymer-lipid nanoparticles using a flow-focusing microfluidic chip for cancer therapy [47]. The microfluidic chip was designed with three inlets, and nanoparticles were synthesized at the intersection of these inlets. Varying the flow rates in the inner and external channels allowed for the production of nanoparticles with sizes ranging from 30-170 nm, high productivity (~ 3 g/hour), and low polydispersity (~ 0.1). Although the synthesized particles lacked anisotropic structures, they were multifunctional nanoparticles with dual drug loading and diagnostic properties. These studies demonstrate the potential of microfluidic devices in fabricating hybrid nanoparticles with varying chemical composition, morphology, and multi-functionality. However, producing uniform, multifunctional, and multicompartmental sub-micron particles using microfluidic devices is promising. This study aims to overcome that limitation by fabricating these particles via microfluidic devices.

2.3.3. Effect of parameters on particle morphology

Particle morphology have a crucial role in biomedical applications [48]. While most drug delivery systems are designed in spherical geometry, there has been an increasing interest in non-spherical particles in recent years. One of the reasons for this is the increasing studies showing that the efficiency of drug delivery depends not only on particle size but also on morphology [49]. Especially in the last 20 years, it is known that there has been an increasing amount of interest in the production of non-spherical particles and their interaction with cells in the literature [50]. However, in recent years, studies have been published proving that non-spherical particles have many advantages for cancer immunology and vaccination [51-53]. Particles with a high aspect ratio also have a greater impact on different aspects of cellular function, including cell proliferation, apoptosis and migration [54]. Janus particles, which also have functional asymmetry with independent compartments within a single particle, have high potential for many potential biomedical applications not offered by homogeneous particles.

It is also possible to obtain particles with different morphology by using different ratios of components while forming hybrid structures. Since changing the type of polymer and lipid will also change the thermodynamic equilibrium, different morphologies can be achieved by using different polymers and lipids. In the literature, it has been shown that Janus microparticles prepared by microfluidic method result in Janus and core-shell structures when lipids with different melting temperatures are employed [55]. Fan et al.[56] reported that PLGA-PCL microparticles with different morphologies were obtained by using different polymer ratios. Their study showed that a core-shell structure was obtained when PLGA-PCL was used in a ratio of 20:10, however, changing the polymer-to-polymer ratio to 19:11 transformed the structure into a Janus structure. In addition, in their morphology studies with different drug-loaded particles in the study, it was stated that the load of the drug had an effect on the particle morphology. Puspita et al.[57] also synthesized hybrid nanoparticles with different polymers and lipids at ratios of 1:7, 1:3 and 3:5 and stated that changing polymer-lipid ratios resulted in significant changes in particle sizes. Since it is known that non-spherical and high aspect ratio particles are advantageous in biomedical applications[58, 59], the effect of different polymer-lipid ratios on particle morphology will be examined in this study.

In this study, the effect of the parameters affecting the particle morphology is evaluated and microfluidic preparation of particles with the potential to be used in biomedical applications is aimed. The morphology of hybrid particles is thermodynamically a function of the interfacial tensions between the phases forming the hybrid particle. The morphology of a hybrid structure composed of polymer and lipid depends on the interfacial tensions between the polymer phase and water, between the lipid phase and water phase and finally between the polymer and lipid phases. The relationship between interfacial tensions and particle morphology can be explained by Spreading Coefficient Theory (SCT) [60]. This theory states that the relationship between the oil, water and polymer phases determines the final particle morphology. The relation between interfacial tensions based on SCT can be expressed by Equation 2.1.

$$S_i = \gamma_{jk} - (\gamma_{ij} + \gamma_{ik}) \quad \text{Equation 2.1}$$

The change in the interfacial tensions of the phases for different hybrid structure morphologies can also be determined by changing the types and concentrations of surfactants present in the water phase. According to the SCT equation, for a polymer-lipid hybrid structure, i, j and k are the lipid, water and polymer phases, respectively. According to this theorem, morphologies that can be expressed as acorn shape or Janus structure can only be achieved if the S values calculated for all three phases are negative. This is also directly related to the interfacial tensions between each phase. If one of the S values is greater than zero, according to the theory, either core-shell structures are formed or droplet separation is observed. Therefore, optimization of interfacial tensions to form a Janus structure is of great importance to form the desired particle morphology. There are both theoretical and practical studies on SCT in the literature. In a study, SCT was used to predict the morphology of polymer-polymer hybrid particles [56]. Different polymer ratios were studied in the study, and it was observed that the morphologies obtained as a result of SCT and experimental studies were compatible with each other. In another study, experimental and theoretical studies were performed using SCT to predict the morphology of Janus droplets [61]. In the study using different organic solvents, SCT was used to describe the morphologies in more detail. In the literature, it is seen that SCT is used to explain particle morphologies in detail by using interfacial tensions. In the scope of the present study, it was aimed to produce different morphologies by utilizing different interfacial tensions by changing the surfactant type and concentration.

Surfactants are an important parameter for the stability of emulsions. It is known that increasing the surfactant concentration in the water phase allows the particle size to be reduced [62]. However, this does not happen when working at a concentration above the CMC of the surfactants. Increasing the concentration at a concentration above the CMC has no effect on particle size reduction. In pharmaceutical applications, FDA-approved nonionic surfactants such as PVA, Tweens and nonionic surfactants with low toxicity are frequently used. In addition to non-ionic surfactants, ionic surfactants such as SDS, SDBS allow the formation of smaller-sized particles compared to nonionic surfactants, however, they are used relatively less in pharmaceutical products than nonionic surfactants due to their negative side effects. The literature reports that nonionic and ionic surfactants are used separately or in combination to form hybrid structures. In a study, it was observed that different surfactants used in the preparation of PS-PMMA composite particles had different effects on particle morphology [63]. In the study, it was found that nonionic

surfactants caused size change, but ionic surfactants also affected morphology. This also supports previous studies [64, 65]. Based on this, surfactants with different properties will be used to prepare particles and their effect on particle morphology will be investigated.

Another crucial aspect in the preparation of hybrid particles is the selection of the solvent. It is known that solvent significantly affects particle size and shape [66]. Since the solubility of the components will be different in the organic solvent used in the preparation of a hybrid particle, it is possible to obtain different morphologies with different solvents. Cao et al. [67] used dimethyl carbonate (DMC) and dichloromethane (DCM) solvents both singly and in 1:5 and 2:1 ratios to prepare polymeric hybrid particles and obtained four different particle morphologies as core-shell, patchy, patchy Janus and Janus. In another study, PLGA-ATO 5 microparticles were prepared with different organic solvents by emulsification solvent evaporation, and it was reported that the particles were Janus structured in the presence of ethyl acetate and when DCM and methanol were used, the particles were not Janus but needle-like. It was also stated in the study that the particles using ethyl acetate were obtained in smaller size when DCM and methanol were used.

The particle morphology is also affected by the duration of the solvent removal process during the preparation of hybrid structures. After the droplets are collected, the concentration in the environment where the droplets are located is of great importance until the solvent is completely removed. Winkler et al. [68] performed solvent removal at three different rates in the presence of different temperature and volume conditions during the preparation of PLGA-PCL hybrid microparticles. While 24 hours of solvent evaporation at room temperature showed Janus structure, they stated that the particles were spherical and some of them had Janus morphology in conditions with less volume at room temperature. In another study [69], it was stated that the evaporation of solvent at different rates caused the formation of different particle morphologies such as cup-like, shell-like and wrinkled particles. This study, it is planned to investigate different conditions during the solvent removal stage.

2.4. Biomedical Applications of Micro- and Nanoparticles

Microparticles have several advantages over other drug delivery systems, including protecting drugs from degradation, improving drug solubility, and controlling drug release kinetics. They can also be designed to target specific cells or tissues, reducing systemic toxicity and improving drug efficacy. Microparticles have been used to treat various diseases, including cancer, diabetes, and cardiovascular diseases. In breast cancer therapy, microparticles have been used to deliver chemotherapeutic agents directly to the tumor site, reducing systemic toxicity and improving drug efficacy. Microparticles can also target specific cells or tissues, such as cancer cells, by functionalizing their surface with ligands that bind to specific receptors on the cell surface. This targeted drug delivery approach can improve the efficacy of breast cancer therapy by reducing side effects. Since microparticles are small particles that can be used as drug delivery systems due to their ability to encapsulate drugs, protect them from degradation, and control drug release kinetics [70]. They have several advantages over other drug delivery systems and have been used to treat various diseases, including breast cancer. Microparticles provide several advantages over conventional drug delivery systems, including preventing drug degradation, increasing drug solubility, and regulating drug release kinetics. They can also target specific tissues or cells, lowering systemic toxicity and boosting therapeutic effectiveness. Microparticles have been used in the treatment of a variety of diseases.

2.4.1. Drug-delivery

Particles encapsulate drugs, protect them from degradation, increase drug solubility, and control drug release kinetics, which makes them useful in drug delivery systems.

Drug-loaded particles are used for the targeted delivery of active pharmaceutical agents to a specific region as controlled release systems to release the agents at a particular time. The desired chemical modifications, different molecule sizes, and high drug-loading capacities can be achieved by selecting an appropriate particle synthesis method. The advantageous properties of drug carrier systems are due to modifications in the pharmacokinetic profiles of loaded therapeutics [71]. These systems offer controlled drug release profiles, a protective effect against the degradation of therapeutic agents, and the

ability to transport drug molecules to the target site. Drug-loaded particles can be micro- or nano-sized depending on the treatment in which they will be used.

Polymeric drug delivery systems guarantee continuous drug delivery due to their higher stability compared to lipid particles while at the same time providing greater control over the intracellular release of the active pharmaceutical molecule [72]. However, the lower biocompatibility and low affinity of polymer particles for the cell membrane offer a low cell interaction, resulting in lower drug delivery efficiency [73].

Lipid particles are preferred due to their biocompatibility, which allows rapid uptake of active therapeutic substances into the cell and is higher than polymeric particles. Lipid particles generally have lower drug-loading capacities than polymers due to disadvantages such as the solubility of the drug in lipids, rapid drug loss due to the structure of the lipid matrix, and a tendency to aggregate [74]. Therefore, by designing a hybrid drug delivery system, more unique treatments can be achieved by utilizing the advantages of two different materials. In addition, the studies on lipid-polymer hybrid systems show that the interest in these hybrid systems has increased rapidly in recent years [75]. In treating breast cancer, a dynamic disease, the use of functionalized hybrid systems is gaining significant importance as it increases the effectiveness of treatment.

In conventional methods, drug loading efficiency and high polydispersity lead to some limitations. Besides the fact that hybrid particles are frequently observed in biomedical applications, they can encapsulate unique combinations of materials from colloids to cells. The literature shows that magnetic colloids and cells are encapsulated in hybrid particles with 91% viability [76]. Compared to the encapsulation of a hydrophobic drug into a polymeric structure or a hydrophilic drug into a lipid, in the hybrid particles being prepared, the drug release of the hydrophobic drug in the polymer can proceed in a more controlled way. In contrast, the lipid part can help to achieve controlled or slowed release in addition to the polymer part. It was planned to develop a system in which hydrophilic and hydrophobic model drugs can be loaded as hydrophilic model drugs to release the drug active ingredient commonly used in breast cancer treatment. Thus, a multifunctional material design will be implemented, and the structure-function interaction will be presented with the systematic approach to be carried out during this thesis. In the section where the parameters which affect the particle morphology will be studied, which is the major part of the study, it is planned to prepare particles with different morphology or compartments that can be used as a drug delivery system. Within the scope of this study,

Rhodamine-B, a hydrophilic model drug, will be loaded into hybrid particles, and release studies will be carried out. Resveratrol, widely used in breast cancer treatment, will be encapsulated as a hydrophobic drug, and drug release studies will be carried out.

2.4.2. Micromotor, Bioimaging and Biosensing

In cancer treatment, chemotherapy and radiotherapy resistance often occurs in cancer cells for various reasons, such as mutations in drug targets, drug inactivation or removal of the drug from the cell, thus creating a challenge in cancer treatment management. Cancer stem cells (CSCs) are responsible for metastasis, and conventional treatment approaches cannot destroy drug-resistant CSCs. Thus, developing smart, unconventional therapies targeting these CSCs in metastatic cancers is needed. Considering conventional drug delivery systems, localization to non-tumorous sites results in systemic toxic side effects, which makes cancer treatment quite challenging. However, it is important to provide effective treatment, especially for metastatic cancer. In recent years, with the development of new advanced materials, cancer diagnostic techniques have gained a different perspective. Janus particles are remarkable for their anisotropic structure, allowing multiple drugs to be localized in different compartments and releasing drugs independently. It provides high mobility by directing movement thanks to its asymmetric structure for active drug transport [77]. In a study, Feng et al. designed a magnetic nanoparticle and paclitaxel-loaded Janus microparticles and then used the anti-cancer drug to kill cancer cells, magnetic nanoparticles for target location, and Rhodamine B for fluorescence tracing in this structure [78].

Drug delivery applications can also be enabled with micro/nanomotors. Micro/nanomotors are small vehicles that can move through the fluids and be loaded with cargo, such as drugs, for targeted delivery. Researchers have turned to nature, especially microorganisms, for inspiration, resulting in the emergence of artificial micro/nano-size swimmers that mimic these natural swimmers, molecular biomotors [79]. Due to their non-biodegradability, most existing nano/micro-motors are unsuitable for in vivo biomedical applications. Therefore, it is crucial to prepare biodegradable micro/nanomotors with multiple-functionality that can be used in cancer diagnostics and treatment. Zhang et al. have designed functionalized self-propelled SiO₂-Pt Janus micromotor, which is light-induced and can be used for drug delivery applications [80].

Janus structures provide directional self-propulsion thanks to their geometrical asymmetry [81]. In another study, Janus nanomotors were designed for 'active photoacoustic imaging and synergistic photothermal/chemodynamic therapy' [82]. Studies show the great necessity of smart and multifunctional micromotors, which can be 'self-propelled' or 'externally powered', especially for diagnosing and treating metastatic cancer. Janus structures have the potential to load many different 'cargoes' with their asymmetric and compartmentalized structures that can be used as micro/nanomotors.

Micromotors can be driven by external stimuli such as light. Light-responsive materials can be used for the fabrication of hybrid micro and nanoparticles. The structures must show birefringent properties so that they can be light-responsive. Birefringence is the double refraction of incident light as it passes through an anisotropic sample which is caused by the the light has different refractive indices as it passes through the sample. Materials with birefringent properties can be characterized by polarized light microscopy. Birefringence properties can be in crystals, polymers and biological tissues. Birefringent materials have potential applications in biosensing and bioimaging applications [83]. Tissue birefringence is an intrinsic marker that can be used for cancer diagnosis [84]. Studies have reported that tissue birefringence is associated with collagen fiber density. Lack of tissue birefringence has been observed in cancerous areas due to low collagen fiber density [85]. Loss of tissue birefringence in cancerous areas can be used as a 'diagnostic marker'. Birefringence particles can be used as The particles with birefringence properties can be used tissue scattering [86]. At the same time, structures with these properties can benefit bioimaging by acting as contrast agents through their high sensitivity and fast response. Birefringent particles are thought to exhibit the potential to be used for bioimaging and biosensing with their optical and structural properties.

In addition to optical properties, magnetic-responsive particles can be designed to functionalize the targeted structures. Deep tumor tissue penetration can be achieved in cancer diagnosis with magnetic targeting [87]. Magnetic nanoparticles are commonly used in various biomedical applications for their extensive benefits, such as high surface area, precise tunability, size-dependent superparamagnetic properties and ease of surface modification over the past two decades [88]. Microfluidic technology provides uniform particle production, which enables magnetically responsive particles to have a more efficient sensitivity [89]. In order to improve magnetic particles' biocompatibility and

reduce the possible side effects of particles, magnetic nanoparticles can be coated [90]. In biomedical applications, it is well known that magnetic-responsive particles have recently been used clinically in targeting cells and tissues, cell repair and magnetic resonance imaging [91]. Current imaging techniques such as computed tomography and magnetic resonance imaging are used to find out where and under what condition the tumor is located [92]. These methods are expensive and may also cause adverse effects on the patient [1].

The literature has reported that micro and nanomotors can be used for 'on-the-fly' sensing and biosensing by improving mass transfer through their mobile structures [93]. The hybrid structures can be used to mark cells and tissues, determine the structure and size characteristics of cells, detect and characterize tissue damage and monitor drug release via their optical properties. The literature has also reported that a biosensor containing hybrid nanoparticles can detect breast cancer cells with metastatic potential [94]. In the study of Yu et al., micromotors were designed to detect cancer biomarkers [95]. Janus particles also have an advantage for biosensing since the Janus structure has two different faces with different components [96]. Wu et al. reported 'Janus particles for targeting and sensing' of breast cancer tumor cells, and their Janus nanoparticles showed promising results on 'selectively attaching to the breast cancer cells [97]. Another study on the preparation of multifunctional Janus nanomotors was reported by Hsieh et al. The study shows the three different functions of Janus nanoparticles for 'sequentially recognizing tumor cells, real-time monitoring of biological responses and drug delivery [98]. These studies shows the great potential of Janus micro-nanoparticles for biosensing applications.

This study will investigate the potential biomedical applications of Janus micro/nanoparticles as a drug delivery system for cancer treatment and diagnostics. In this study, the microfluidic preparation of Janus micro/nanomotors, which can be loaded with drugs with different characteristics for cancer diagnosis and treatment, is also planned.

3. EXPERIMENTAL

3.1. Materials

Polycaprolactone (Mn 45,000) (PCL), dichloromethane (DCM), poly(vinyl alcohol) (MW 13,000-23,000) (PVA), sodium dodecylbenzene sulfonate (SDBS), dimethylformamide (DMF), acetonitrile, Iron (II) sulfate heptahydrate, iron (III) chloride hexahydrate, sodium hydroxide, sodium chloride, acetone, rhodamine-B (Rh-B), resveratrol (RES), sodium phosphate monobasic monohydrate and sodium phosphate dibasic dodecahydrate were purchased from Sigma Aldrich (St. Louis, MO, USA). Stearic acid (SA) and tween-20 were purchased from Merck (Darmstadt, Germany). Oleic acid (OA) was obtained from Fisher Chemicals (Loughborough, UK). Nitric acid and 1,4-Dioxane were obtained from Carlo Erba (Milano, Italy). Sodium dodecyl sulfate (SDS) was purchased from Fluka (Buchs, Switzerland). Ultrapure water was used for the synthesis and dilution (Millipore Direct-Q3 UV). All materials were used without further purification.

3.2. Preparation of Polymer-Lipid Hybrid Microparticles

In this study, a one-nozzle microfluidic system is assembled for the preparation of PLHMPs. The system is assembled using various components, which were carefully chosen based on their compatibility with the experimental setup. The polyamide-coated fused silica inner capillary and the outer capillary were purchased from CM Scientific (Silsden, UK). The outer capillary (TSP200350) had an inner diameter of 200 μ m \pm 6 μ m, an outer diameter of 360 μ m \pm 10 μ m, and a coating thickness of \sim 18 μ m per side. The inner capillary (TSP040105) had an inner diameter of 40 μ m \pm 3 μ m, an outer diameter of 105 μ m \pm 6 μ m, and a coating thickness of \sim 12 μ m per side. The natural FEP tubing (JR-T-6803), with a specific inner diameter of 0.75 mm and an outer diameter of 1/16", was purchased from Achrom (Machelen, Belgium). Two tubing sleeves were used in the assembly of the mentioned capillaries into the connectors, namely a green sleeve (F-2423) with an outer diameter of 1/16" and an inner diameter of 0.0155 inches and a red sleeve (F-2374) with an outer diameter of 1/16" and an inner diameter of 0.005 inches, both of which were sourced from IDEX (Northbrook, USA). Stainless steel materials, including the

tees, ferrules, unions, nuts, and plug for 1/16" tubing, were purchased from VICI® (Texas, USA). The tee with a bore of 0.75 mm is used to create a co-flow geometry of dispersed and continuous phases. These materials were selected based on their mechanical and chemical properties, which ensured the required durability, resistance to pressure, and compatibility with the solvents being used. The ceramic cutter is used to cut the fused capillaries. The capillary lay along the length of a finger, and the ceramic cutter was perpendicular to the length of the capillary. Then, using the smooth edge to place a small score on the outside capillary, the capillary is successfully cut. The polymer tubing cutter purchased from IDEX (Northbrook, USA) was used to cut the FEP tubing. The chosen materials successfully assembled the microfluidic system for the experimental setup, shown in Figure 3.1.

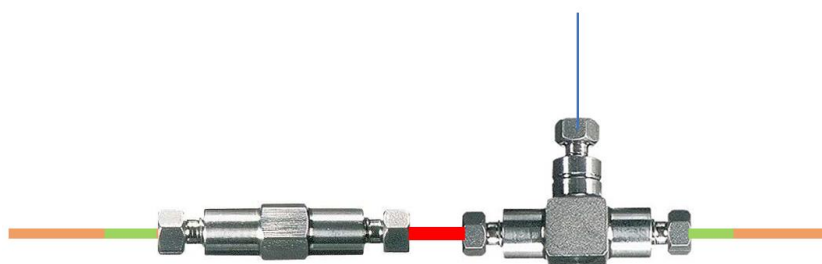


Figure 3.1. A schematic of one-nozzle microfluidic system

To assemble a microfluidic device with co-flow geometry, firstly, the nuts are placed on both ends of red sleeves. Nuts should be hand-tight. The red sleeve is inserted into tees after inserting the inner capillary into the red sleeve. After inserting the capillary, it should remain outside the sleeve by about 2 mm. That part is placed on a union connected from the syringe of the dispersed phase to the microfluidic system. Otherwise, the tip may break when it is inserted into the union. The FEP tubing is also inserted into the tees with nuts on both ends. After this assembly, the system is connected to two syringes. A glass syringe (500 μ L) and a 20 ml disposable syringe were used for the dispersed and continuous phases, respectively. After the one-nozzle microfluidic system is assembled, the systems are connected to syringe pumps. The syringe pumps (NE-300) were purchased from New Era Pump Systems (New York, USA).

After the one-nozzle microfluidic system is assembled, the microfluidic system can be operated for microparticle production.. The experimental setup of microfluidic preparation of microparticles is shown in Figure 3.2. First, the dispersed and continuous phase is prepared for microparticle synthesis.

The polymer (PCL) is selected due to its FDA-approved biodegradable nature. First, 25 ml of aqueous phase containing surfactants (0.30% PVA and 0.10% SDBS) was mixed at 700 RPM for 3 hours at 60C. In preparation for the dispersed phase, PCL (0.0625 g) and ATO 5 (0.0625 g) were dissolved in DCM for 30 minutes at 200 RPM for 30 minutes at room temperature.

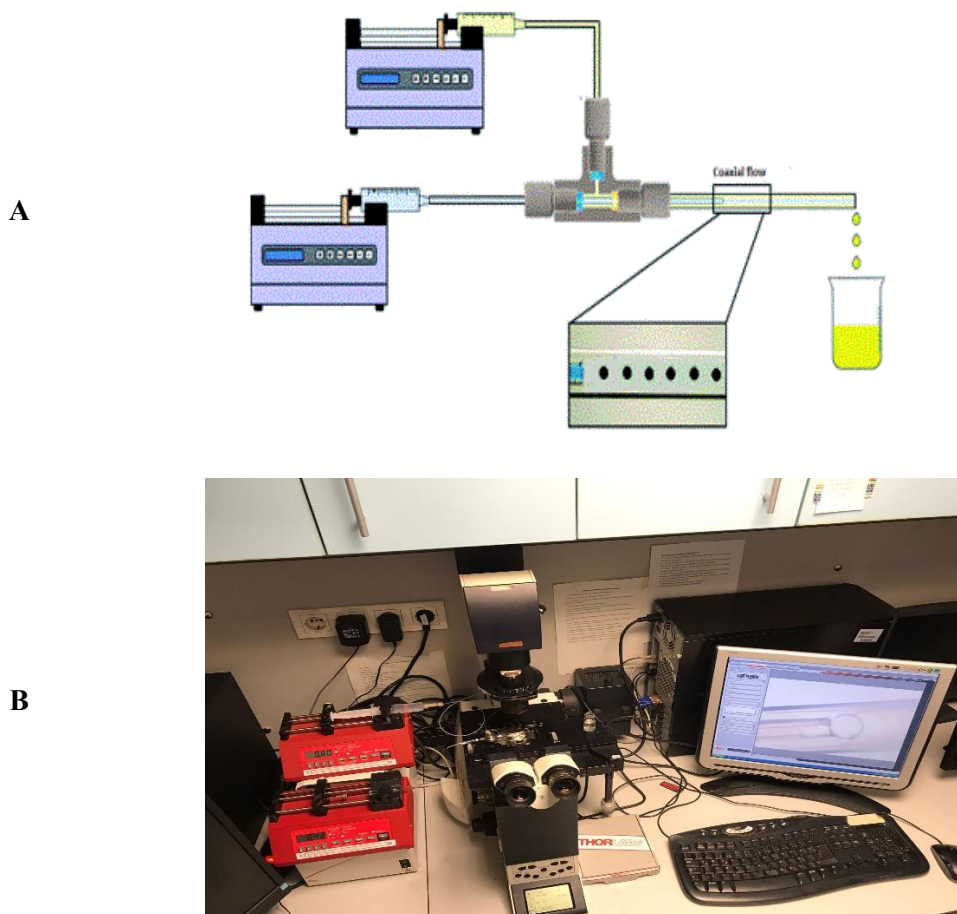


Figure 3.2. The experimental setup of microfluidic preparation of microparticles A) The schematic, B)An image of experimental setup

Once the dispersed and continuous phases are prepared, the syringes are filled with them. The glass syringe is used for dispersed phase since DCM is the solvent of dispersed phase. In order to maintain a continuous droplet formation, it is necessary to ensure that no air bubbles remain in the syringes. The filled syringes are fixed to the syringe pumps and can be used to flush the one-nozzle system at selected flow rates. The system is flushed with the continuous phase through the one-nozzle microfluidic system at a constant flow rate of 1 ml/h before starting the microparticle production. After flushing the system, the aqueous phase flow rate is reduced to 0.8 ml/h, and the dispersed phase flow rate is adjusted to 0.06 ml/h. After the flow rates are set, the system is allowed to establish a 'dripping regime' that will continuously form the droplets in the one-nozzle system. If the system is clogged or there is a leaking in the system, droplet formation may not be observed as it is expected. In this case, the system must be carefully controlled, and the related problem must be eliminated.

The droplets were collected during the synthesis from the exit of outer capillary. The outer capillary was submerged in a beaker containing 25 ml of aqueous surfactant (0.30% w/v PVA and 0.1% w/v SDBS). The surfactant concentrations mentioned here were changed in the parameter studies carried out in the later sections of this study and different surfactant types and concentrations were used for different hybrid particle preparations. The droplets were collected from the one-nozzle system were kept at room temperature for 24 hours for solvent evaporation. No centrifugation process was applied to the hybrid microparticles since the particles settled over time. In SEM sample preparation, however, the particles were centrifuged at 3000 RPM for 5 minutes. After phase separation process was completed, the hybrid MPs were ready for characterization.

3.3. Microfluidic Preparation of Polymer-Lipid Hybrid Nanoparticles

Aluminium (Al) and glass (Gl) were chosen as microfluidic system materials for producing hybrid nanoparticles. Silicon and glass materials are most widely used as microfluidic devices; however, aluminium has recently been employed due to its low cost [99]. The design and fabrication process of aluminium-glass chips was made by Dr. Ilyesse Bihi at μ Flow group in Vrije Universiteit Brussel. The fabrication begins with the microfluidic chip's CAD design using AutoCAD software. The microfluidic chip was designed with three inlet channels connected to a larger channel with rectangular cross

sections 200 μm wide, 400 μm high, and 10 mm long. The CAD design was fed to the computer connected to a CNC machine. Aluminium substrates were milled with a CNC machine. After milling, a liquid UV-curable adhesive is used for the spin coating of a glass lid, and the system is placed under UV after clamping. The designed Al-GI microfluidic chip is shown in Figure 3.3.

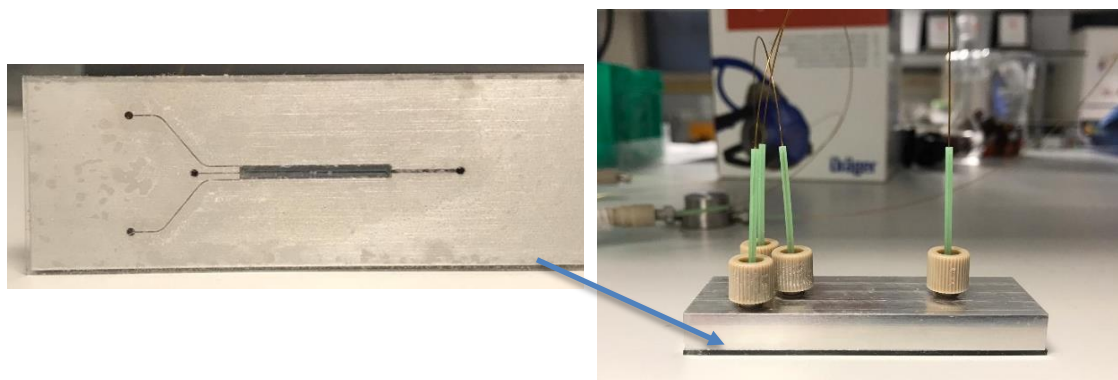


Figure 3.3. An image Al-GI microfluidic system for nanoparticle production

The microfluidic preparation of hybrid nanoparticles is different from that of hybrid microparticles. In nanoparticle production by microfluidics, higher flow rates are used to create micro vortices. This study used an Al-GI microfluidic chip to prepare polymer-lipid hybrid nanoparticles. The phases are called internal and external phases. The internal phase that contains the polymer in DMF is surrounded by the external phase of PATO 5 in 1,4-dioxane. The solvents should be miscible in the preparation of particles by microvortices-based 3D-HFF microfluidic device. First, 50 ml of polymer phase containing the polymer (0.83% PCL) in DMF was mixed at 400 RPM for 30 min at 50 C. Since the melting temperature of PCL is 60 C, the temperature should be controlled during the preparation of the polymer phase. In preparation for the lipid phase, PATO 5 was dissolved in 1,4-dioxane for 24 hours at 200 RPM at 37 C.

After preparation of polymer and lipid phase, syringes were placed in syringe pumps. Flow rates of 100 $\mu\text{L}/\text{min}$ for the polymer phase and 1000 $\mu\text{L}/\text{min}$ for the lipid phase were initially set. The particles to be collected from the system were collected in a beaker containing water phase containing PVA (0.15%) and SDS (0.05%). The particles were

then centrifuged at 3000 RPM for 5 minutes. After the phase centrifuge, the PLHNPs were ready for characterization with DLS and AFM.

3.4. Characterization of Polymer-Lipid Hybrid Micro- and Nanoparticles

The size and morphologies of polymer-lipid hybrid micro and nanoparticles in this study were characterized by different techniques. An inverted microscope (IM) and Scanning Electron Microscope (SEM) were used for the size and morphological properties of hybrid microparticles. Rhodamine-B labelled hybrid microparticles analyzed with Fluorescence Microscope (FM). The optical characteristics of birefringent hybrid microparticles were analyzed using a Polarized Optical Microscope (POM). Dynamic Light Scattering (DLS) and Atomic Light Microscope (AFM) were used for the characterization of hybrid nanoparticles. The hybrid particles were dried for analysis with AFM and SEM. The particles were dispersed in water before the characterization for the other methods, except AFM and SEM. Each technique provides insightful details about the morphology and particle sizes.

3.4.1. Optical Microscope (OM)

An optical microscope is a device which is powered by visible light used for imaging and analysing micro- and macro structures. The optical microscopes are composed of mechanical, optical and illumination parts. The mechanical part is the part carrying the optical section elements and forming the main body of the microscope. This section includes macro and micro screw assembly, microscope leg, body, carriage and object table. In some microscopes the stage is fixed, in other microscopes it can go up and down. The image is obtained by the optical section and consists of the optical section and light source, objective, ocular and condenser. It is the most important part of the microscope. The condenser distributes the light from the light source homogeneously. The most important place in the optical section of the microscope is the objective. Objectives create the intermediate image by magnifying the sample to be analyzed at its own magnification ratio and the quality of the image obtained is determined by the actual objective. The compartment that magnifies the intermediate image created by the objective according to

its own magnification ratio and delivers it to the eye is the ocular. The ocular should be selected in accordance with the characteristics of the objective in the microscope. The ocular part is the part of the optical part that is viewed by the eye and placed on the upper part of the tube. Its task is to magnify the object image formed by the objective and to correct some errors of the objective.

Microparticles characterization by optical microscopy was performed on a Leica DMI 4000B inverted light microscope with a 20X objective. The particles prepared by microfluidic method were dispersed in water and the particle morphologies were examined by dropping the sample on a glass slide.

3.4.2. Fluorescence Microscope (FM)

Compartments or surfaces that cannot be clearly characterized with an optical microscope can be observed with a fluorescence microscope after the particles are labelled with fluorescent dye. In fluorescence microscopes, the light from the light source passes through the filter and excites the sample and emits the light of a certain wavelength/range. The particle characterization by Optical Fluorescence Microscopy was carried out with the Leica DMI 4000B, which allows both OM and FM analysis. The solution or dry particles placed in the sample chamber can be illuminated by light with a narrow wavelength range. Therefore, the wavelength range of the fluorescent dye to be analyzed must be compatible with the filters used in the FM device. In order to obtain fluorescent images in the study, the fluorescent dye Rhodamine B was dissolved in ethanol and the solution was added to the dispersed phase during the microfluidic preparation of microparticles. During particle formation, the particles were kept in a dark environment and microparticle characterization were made after the particles were formed.

3.4.3. Polarized Optical Microscope (POM)

POM is used to determine the optical properties of materials with birefringence properties by refracting the light passing through the sample in different directions. In order to analyze the material with POM, the material must exhibit birefringence properties. In

POM, light passes through a polarizing filter that only allows specific wavelengths. This light is then directed at the sample being analyzed, and the resulting image is passed through a second polarizing filter (called an analyzer) which can be rotated to control the plane of polarization of the light. After the analysis, the positions of the analyzer and polarizer are switched then the sample's optical properties can be determined by analyzing changes in the intensity of the light.

In the materials analysis, dark and light areas are formed by the refraction of light passing through the material with a birefringence property. This is due to the fact that light is refracted in materials with anisotropic structures and travels at different speeds. In isotropic materials, bright regions are not formed, and these materials cannot be analyzed with POM; dark regions are seen. When polarised light passes through anisotropic and birefringence materials, the light is refracted or bent in different directions depending on the direction of the optical axes of the material. Constructive interference leads to bright fields, while destructive interference leads to dark fields. In this respect, the structure and optical properties of a material with birefringence can be determined with the help of light that undergoes different refractions from the material's surface.

3.4.4. Scanning Electron Microscope (SEM)

The SEM analysis was performed using a HITACHI SU5000 field emission scanning electron microscope (FE-SEM) in order to examine the morphology of the prepared PLHMPs in further detail. The samples in solution were dropped onto the silicon substrate, dried at room temperature, and prepared for SEM analysis. The SEM analysis was conducted after the sputtering process was performed for 12 seconds at 0.02 mbar pressure using a Leica EM ACE 200 device to make the surface conductive.

The SEM consists of three main parts; electron gun, magnetic lenses, and detectors. Electrons from the electron gun, focused through magnetic lenses, are sent to the sample. The scattered electrons resulting from the electron-sample interaction are analyzed by different detectors.

SEM analysis is a topographic examination method in which a beam of electrons is scanned across a sample and the scattered electrons are detected and images are formed by detectors. The SEM uses secondary electrons emitted by sample atoms excited by the

electron beam to create images. The variation in the number of secondary electrons emitted from different regions of the sample depends primarily on the angle at which the beam meets the surface, i.e. the topography of the surface. In addition to secondary electrons, the backscattered electrons, characteristic X-rays, cathode ray and transferred electrons are also used to obtain various signals from the sample and to analyze the topography and composition of the sample.

3.4.5. Light Scattering (LS)

The dimensional analyzes of the PLHNPs prepared as part of this study were carried out with the Light Scattering (LS) device of the Malvern CGS-3 series with a laser wavelength of 632.8 nm. The data obtained from this device is converted using the ALV-correlator.

There are four different interactions that can take place between light and material. These interactions can be classified as transmission of light through the material, reflection of light off a material, absorption of light into the material and the scattering of light on a material. In the case of light scattering off the material, the amount and intensity of the scattered light can provide information about the size and shape properties of the material. The light scattering method can be divided into two "Dynamic Light Scattering (DLS)" and "Static Light Scattering (SLS)" methods. The DLS method is often preferred for particle size determination. In this study, DLS is used for the size analysis of PLHNP. Information about the size of a particle can be obtained by changing the wavelength of monochromatic (monochromatic) light sent on particles making a Brownian motion in a solution when it hits the particle. The diffusion coefficient value can be obtained by measuring the intensity of the scattered light, and the radius value can be obtained using various correlations. A schematic of the dynamic light scattering (DLS) setup is shown in Figure 3.4.

The device turns on 20 minutes before DLS measurements are made, and the light intensity is expected to reach the desired level. The container where the samples will be placed is filled with filtered toluene with a filter with a pore size of 0.02 μm . The newly filled toluene pool is kept for at least one day so that the particles to be analyzed are not

affected by impurities and fractures. Reference measurements are taken before the sample is placed on the LS. analysis

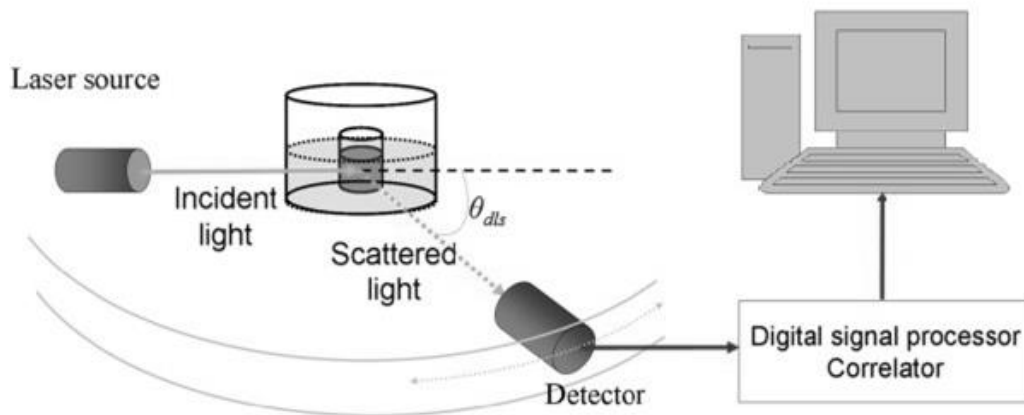


Figure 3.4. A schematic of the dynamic light scattering (DLS) setup [100]

3.4.6. Atomic Force Microscope (AFM)

Examining nanoparticle morphology and size distribution involves using Atomic Force Microscopy (AFM) within this thesis. AFM is a technique used to scan the surface topography and is more suitable for the analysis of nanometre-scale structures. Specialized probes called cantilevers are used to scan the surfaces of dry samples. At the ends of the cantilevers, tips are positioned in order to obtain the surface topography. In order to analyze the sample, the tip is brought close to the sample surface and then the surface is scanned at a suitable area and speed. At the end of the AFM analysis, three-dimensional images of the sample surface are obtained. The AFM device, which can operate in different modes such as static mode and dynamic mode, stands at a certain distance from the sample surface and follows the surface during the measurement. When it is required to work in dynamic mode, the type approaches the surface. Working in static mode is generally considered for highly crystalline materials and non-smooth samples, while working in dynamic mode is suitable for analyzing softer materials.

The measurements within the scope of the study were carried out in non-contact mode using ACTA 10M type Cr-Au cantilever and PSIA Corporation, XE-100E instrument with a scan rate of 0.3 Hz. In order to prepare the samples, AFM analyzes were performed

after the samples in solution were dropped on a glass strip and dried at room temperature overnight.

3.5. Investigation of Drug Encapsulation and Drug Release Properties of Polymer-Lipid Hybrid Microparticles

3.5.1. Ultraviolet- Visible Spectrophotometer (UV-Vis)

The drug encapsulation and drug release studies was performed with UV-VIS spectrophotometer (Thermo Scientific™ GENESYS™ 10). Samples of drug active ingredients with hydrophilic and hydrophobic properties encapsulated in particles were taken from the release medium with a volume of 300 μ L then poured into quartz cuvettes. The samples were then analyzed with a UV-VIS spectrophotometer which can perform measurements between 190 and 1100 nm wavelengths.

In order to investigate the release profiles and encapsulation efficiencies of the model drugs from PLHMPs, calibration curves of the model drugs were first established. For this purpose, standard samples were prepared at various concentrations and absorbance values were obtained at the relevant wavelengths for the model drugs. By utilizing the equations of the calibration curves generated with the absorbance data obtained at wavelengths specific to the active pharmaceutical ingredients, the active pharmaceutical ingredients not incorporated into the structure of the particles and the changes in the concentrations of the active pharmaceutical ingredients released from the particles under appropriate conditions were determined. Equation 3.1 was used for encapsulation efficiency. For this, the particles prepared after synthesis were centrifuged and the supernatant value was read and the amount of unencapsulated drug was calculated and the encapsulation efficiency of the particles was found since the amount initially loaded was also known..

$$EE\% = \frac{W_{initial\ drug} - W_{free\ drug}}{W_{initial\ drug}} \times 100 \quad \text{Equation 3.1}$$

3.5.2. Rhodamine-B Encapsulation and Release Studies with PLHMP

Rhodamine-B (Rho-B), a hydrophilic model drug, was encapsulated into PLHMP's in this thesis study. Rho-B was added to the oil phase in PLHMP's. In order to observe the Rho-B release behavior of the particles, 1.5 mL of the drug-containing particle dispersion was taken, centrifuged at 3000 rpm for 5 minutes, and the supernatant was analyzed. This analysis was performed at 554 nm in a UV-vis spectrophotometer.

The amount of free drug was determined from the supernatant analyzed with the prepared calibration curve and the encapsulation efficiency was calculated with the help of equation 3.3. Drug release studies were performed with 1.5 ml of particle dispersion placed on a dialysis membrane in pH 7.4 PBS. Samples were taken from the release medium at regular intervals and analyzed by UV-vis and the sample was returned to the release medium.

3.5.3. Resveratrol Encapsulation and Release Studies with PLHMP

RES is a polyphenolic compound found in nuts, pine trees and fruits such as grapes, mulberries and raspberries. Resveratrol, which has prominent antioxidant properties, is also known to prevent lipid peroxidation and related cell death. Studies have shown that RES reduces apoptotic death of cancer cells and inhibits vascularization and tumor growth [101]. As a result of recent studies, it has been proven to have multifunctional and pleiotropic effects thanks to its anti-cancer, anti-inflammatory, cardioprotective and neuroprotective properties. RES shows low bioavailability and its biological and pharmacological advantages cannot be fully utilized due to its limitations such as low chemical stability, being affected by pH change and UV light, degrading at high temperatures, low solubility in water (0.05 mg/ml). For these reasons, it is very important to administer RES in a suitable carrier rather than administering it alone [102, 103].

Resveratrol (RES), a hydrophobic model drug, was encapsulated into PLHMP's in this thesis study. To encapsulate RES, it was added to the oil phase in the preparation of PLHMP's. In order to observe the RES release behavior of the particles, 1.5 mL of the drug-containing particle dispersion was taken, centrifuged at 3000 rpm for 5 minutes, and the supernatant was analyzed. This analysis was performed at 304 nm in a UV-vis

spectrophotometer. In order to examine the drug release profile, unlike Rh-B, 3.0% Tween 20 was added to the PBS release medium and the release profile was performed as done for Rh-B in the previous section.

3.6. Investigation of Magnetic Nanoparticle Encapsulation into Polymer-Lipid Hybrid Microparticles and Characterization

3.6.1. Preparation of Oleic-Acid Coated Magnetic Nanoparticles

The following steps were carried out to produce oleic acid-coated magnetic nanoparticles. First, Oleic acid-coated magnetic nanoparticles were synthesized using the co-precipitation method. Specifically, 0.18 g of Iron (II) sulfate heptahydrate ($\text{FeSO}_4 \cdot 7\text{H}_2\text{O}$) and 0.34 g of Iron (II) chlorate ($\text{FeCl}_3 \cdot 6\text{H}_2\text{O}$) were dissolved separately in 1.75 mL and 2 mL of DI water. The two solutions were then combined to obtain a single solution. A 0.2 M Sodium hydroxide (NaOH) solution was prepared by dissolving 0.8 g of NaOH in 20 mL of water, and this solution was added to the mixture containing iron salts until the pH reached 10, while stirring with a magnetic stirrer.

Next, 80 μL of oleic acid was added to the solution and stirred for 1 hour at room temperature. The temperature gradually increased to 95 °C at 2 °C per minute, within half an hour to convert the iron hydroxides to magnetite. The solution containing the magnetic particles was cooled to room temperature. Nitric acid (HNO_3) was added until the pH of the solution reached 5, allowing the oleic acids to coat the surface of the magnetites. This caused the oleate layer and the magnetic particles to precipitate due to the increased hydrophobicity.

Finally, the precipitated particles were washed four times with acetone to separate them from unreacted salt residues. Then, an additional wash was performed to eliminate any remaining impurities.

3.6.2. Characterization of Oleic Acid Coated Magnetic Nanoparticle loaded Polymer-Lipid Hybrid Microparticles

The size properties of magnetic nanoparticles were investigated by light scattering. The size measurements of MNPs were carried out on DLS using acetone as a solvent. For the DLS analysis, the MNPs were diluted with a ratio of 1:20 dilution.

The rotational and translational movement of particles were characterized by different procedures. A magnet with a magnetic field strength of 0.48 Tesla applied an external magnetic field for the translational speed analysis of PLHMPs. OM was used to monitor the movement of the particles under a magnetic field. A magnet was positioned 0.5 cm away from the sample dropped on the glass slide, and the movement of the particles was observed over a certain period, depending on the sample. The video taken during the analysis calculated the speed of PLHMPs under the magnetic field applied with a magnet. The speed of ten particles selected from the video was calculated, and the average was given as the average particle velocity. The same magnet was used to analyze the rotational movement of PLHMPs. For this, a 90-degree moving magnetic field was created around the sample in clockwise and counterclockwise directions. First, the magnet was rotated clockwise in the same direction and then back in the same direction to move the magnet over the sample. The magnet was moved back and forth in a field that would create a 90-degree angle for a few minutes, and video was taken in the meantime. The same procedure was repeated in the counterclockwise direction. Based on the image at time $t=0$, the number of degrees the focused particle moved in the clockwise and counterclockwise magnetic field was determined from the images cut from the video and the average of the calculated angular speeds was calculated.

4. RESULTS AND DISCUSSION

This study aimed to prepare polymer-lipid hybrid nanoparticles as drug-delivery systems by microfluidic technology. PLHNP and PLHMP were prepared for biomedical applications, including drug delivery, biosensor and micromotor. FDA-approved PCL and Precirol ATO 5 were selected as the materials of these hybrid nanoparticles. The effect of parameters on particle morphology was studied, and different morphologies showed potential for different applications. In other words, this thesis discusses the potential of polymer-lipid hybrid micro and nanoparticles prepared by microfluidics for different applications.

PCL - ATO 5 hybrid microparticles were successfully prepared by microfluidics. The type of lipid, the surfactant type, surfactant concentration, the ratio of polymer to lipid, and the concentration of polymer/lipid were selected as parameters, and the effect of these parameters on particle morphology was discussed in detail. After the parameter studies, two morphologies were selected as potential drug delivery systems. Furthermore, hydrophobic and hydrophobic drugs were loaded separately in PLHMPs, and release kinetics were compared. Hybrid microparticles with more than two components were also studied. Magnetic and light-responsive PLHMPs were successfully prepared with a one-nozzle microfluidic system. The potential biomedical applications of those multi-component microparticles were discussed.

The effect of parameters on particle morphology was discussed in the first part of this study. Then the microfluidic preparation of PLHNPs was studied. Microvortices-based Al-Gl microfluidic chip was designed for nanoparticle preparation. The second part discussed the Finally, release studies of hydrophilic and hydrophobic drug-loaded PLHMPs with different polymer-to-lipid ratios were performed.

4.1. Preparation and Characterization of Polymer Microparticles by One-Nozzle Microfluidic System

The microparticles were first formed with polymer and lipid materials separately with the assembled one-nozzle system. The microfluidic system's design impacts the production of particles with different morphologies in droplet-based microfluidic systems. It is possible to prepare particles with different morphologies according to the channel size and flow geometry.

All the microparticles mentioned in this study were produced in a single nozzle system at the same flow rate with a few exceptions.

At the beginning of the study, the PCL microparticles were prepared by a one-nozzle system. PCL is a promising polymer with high biocompatibility, slow degradation rate and low toxicity in the literature [31]. PCL is more stable than polylactides as it has fewer ester bonds per monomer, and therefore PCL chain fragments take longer to hydrolyze in the body. The slow degradation rate and mechanical properties make the PCL a good candidate for prolonged drug release. Therefore, different drug delivery systems prepared using PCL have also been developed to treat many diseases, including cancer [104-106]. Hence, PCL was selected as the polymer component of hybrid particles to be designed as a drug delivery system. DCM was used as a solvent for the dispersed phase, and PVA and SDBS were used as co-surfactant for the continuous phase for the prepared polymer MPs. 0.83% w/v PCL was dissolved in DCM for the dispersed phase, 0.30% w/v PVA and 0.1% w/v SDBS were dissolved in water. The flow rates of dispersed and continuous phases were set to 0.06 ml/h and 0.8 ml/h, respectively.

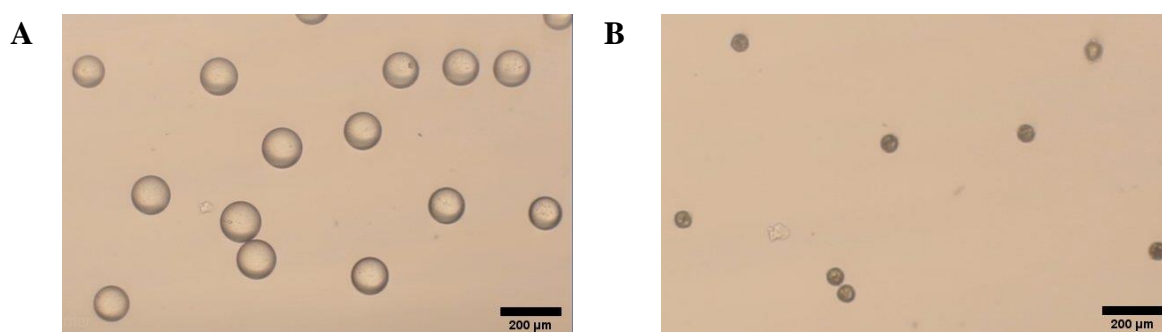


Figure 4.1. A) OM image of PCL microdroplets B) OM image of PCL microparticles

The PCL MPs formed by the one-nozzle system are shown in Figure 4.1. The droplet size was determined as $125.056 \pm 6.28 \mu\text{m}$. After the solvent evaporation, spherical particles were formed with a size of $48.021 \pm 4.23 \mu\text{m}$. This result indicates that polymeric particles can be prepared using the microfluidic set-up and conditions that we used.

4.2. Preparation and Characterization of Lipid Microparticles by One-Nozzle Microfluidic System

After preparing polymer MPs, the lipid particles with ATO 5 were synthesized by a one-nozzle system. Precirol ATO 5 is a palmitostearate glyceride mixture of palmitic and stearic acid esters. This complex structure makes it a great candidate for a hybrid particle. The variety of fatty acids such as mono-, di- and triglycerides contained in the Precirol ATO 5 molecule and also its porous structure due to its high amorphousness and deviation from crystallinity enable the active pharmaceutical ingredients to be located much better in the particle and thus exhibit higher drug retention ability [107]. ATO 5 MPs were characterized by OM and SEM, shown in Figure 4.2. Lipid MPs images show a nonhomogeneous structure. In Figure 4.2.B, a nonhomogenous morphology of ATO 5 is shown. A non-homogeneous structure in the lipid particle is observed since the ATO 5 is a complex mixture of ester structures. In order to visualize the morphology more clearly, the structure is labelled with Rhodamine-B, as shown in Figure 4.2.C. Although the morphology (Figure 4.2.B) changed with the rhodamine-B, the non-homogeneous structure became more prominent with the labelling. In order to visualize the structure more clearly, the structure is labelled with Rho-B, as shown in Figure 4.2.C.

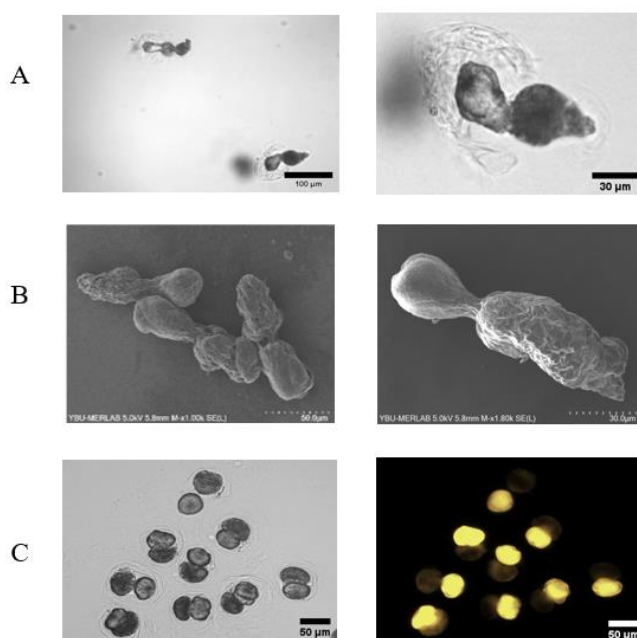


Figure 4.2. Characterization of Precirol ATO 5 microparticles: A) OM images, B) SEM images, C) FM images of Rhodamine-B Loaded ATO 5 MPs

The morphology changed with the Rhodamine loaded, yet the 2-component structure became more prominent with the labelling. These features showed that the selected lipid would be attractive for the hybrid structure to be prepared.

4.3. Preparation and Characterization Of Polymer-Lipid Hybrid Microparticles by One-Nozzle Microfluidic System

The hybrid PCL- Precirol ATO 5 MP's were prepared with the same device at the same flow rates after microfluidic preparation of polymer and lipid MPs separately. The particle morphologies of PCL- Precirol ATO 5 MP's are in Figure 4.3. As seen in the figure, the hybrid MPs were not uniform. The preparation of hybrid MPs resulted in three different morphologies; 47% of particles were with tails (Figure 4.3.A), 32% of particles were spherical-like particles (Figure 4.3.B), and 21% of particles were smaller particles (Figure 4.3.C). Since one of the objectives of this master's thesis is uniform particle production by microfluidics, a parameter study was performed to obtain particles uniformly.

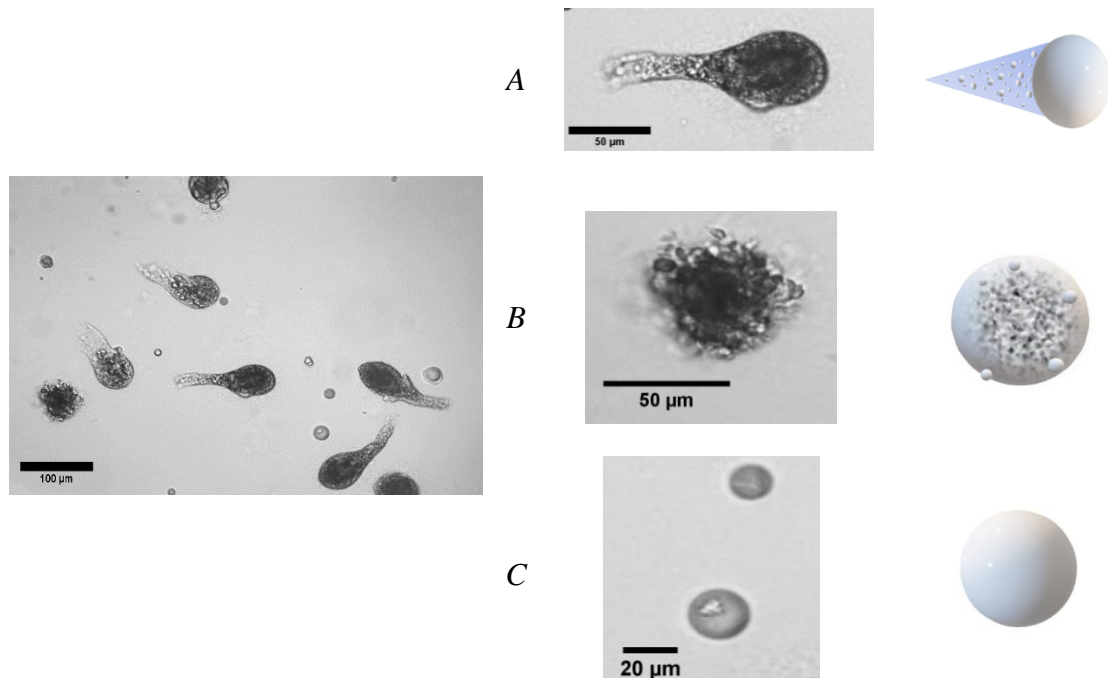


Figure 4.3. The morphology distribution of PCL- Precirol ATO 5 MPs with PVA and SDBS as surfactants. The images (A-C) are zoomed-in images of the left image.

Optimization of particle morphology; precise control over the phase separation of a droplet under various conditions can be achieved by the theory of spreading coefficient theory using interfacial tension between the polymer, lipid and water phases.

4.3.1. The Effect of Surfactant Type and Concentration on Polymer-Lipid Hybrid Microparticles

PCL - ATO 5 (1:1) PLHMPs were prepared using different concentrations of nonionic and ionic surfactant pairs. The effect of these parameters on the morphology of PLHMPs was investigated. For this purpose, three different surfactant pairs were tested at the same polymer-lipid ratio (1:1) at three different concentrations. PLHMPs were prepared with a one-nozzle microfluidic system and kept at room temperature for 24 hours for solvent evaporation. During the preparation of PLHMPs, the inner phase flow rate was set as 0.06 ml/h and the outer phase flow rate as 0.8 ml/h. The surfactant types and concentrations tested are given in Table 4.1.

Since it is known that one of the parameters affecting the morphology of hybrid particles is the interfacial tensions between the water phase and polymer/lipid phases according to the 'Spreading Coefficient Theory', PCL-ATO 5 PLHMPs were prepared with different surfactant pairs and concentrations. The surface tensions of the water phases are given in Table 4.1. The properties of groups A, B and C are given in Figure 4.4 and are detailed in Table 4.1.

When groups A, B and C are examined, it is seen that the surface tensions of group A, where PVA and SDS pairs were used, were higher than those of sample pairs B and C at all surfactant concentrations. For each group, increasing total surfactant concentration resulted in a decrease in surface tension. This is in agreement with the literature data. The morphology of group A samples will be further discussed since they raised concerns about their morphologies' multicomponent nature. In particular, sample A1 has the highest surface tension and the most uniform structure among all samples. Although the surface tensions of group B samples vary between 33-35 mN/m, the morphologies do not show the desired compartmentalization or particles with a high aspect ratio. There is a high polydispersity in size and morphology at all concentrations of the PVA-SDBS pair with the lowest surface tension values; approximately half of the structures were formed particles with tails and high aspect ratios.

Consequently, PVA-SDBS and PVA-SDS surfactant pairs were selected to form high aspect ratio hybrid structures and uniform Janus particles in the rest of the study, respectively. When

these results are considered overall, it is seen that the samples have uniform and Janus morphology-like structures under conditions where the surface tension of the water phase is higher than approximately 41 mN/m. When the surface tension drops below 30 mN/m, the particles have tails and high aspect ratio morphologies. Since the structures are polydisperse but have high aspect ratios at low surface tension conditions, these structures and conditions will be examined in more detail in the following sections of the study.

Table 4.1. The surface tensions of different co-surfactant types and concentrations

| Co-surfactant concentrations (w/v %) | The surface tensions of different co-surfactant types (mN/m) | | |
|--------------------------------------|--|-------------------|-------------------|
| | PVA-SDS | SDS-SDBS | PVA-SDBS |
| 0,150 - 0,100 | A1 - 45,67 | B1 - 35,58 | C1 - 30,21 |
| 0,250 - 0,083 | A2 - 41,74 | B2 - 33,83 | C2 - 28,21 |
| 0,300 - 0,100 | A3 - 39,34 | B3 - 33,51 | C3 - 27,24 |

The effect of co-surfactant types and concentration on particle morphology was examined. The polymer-lipid hybrid particles were prepared using PVA (0.25% w/v) and SDBS (0.08% w/v) as co-surfactants. After the preparation of hybrid MPs resulting in low uniformity, hybrid MPs were prepared at a lower total surfactant concentration of PVA (0.1% w/v) and SDBS (0.1% w/v). Then SDS was used instead of SDBS as an ionic surfactant with PVA. In preparation for hybrid MPs using the PVA-SDS in an aqueous phase, two different concentrations were tried, as in PVA-SDBS co-surfactant pair.

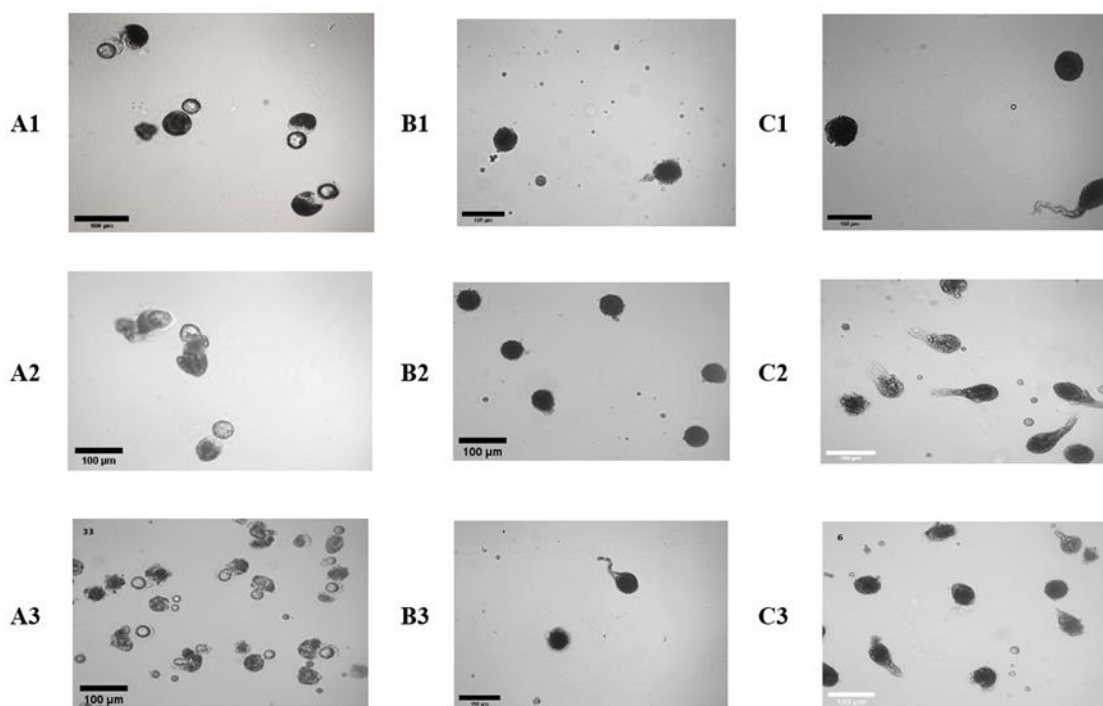


Figure 4.4. The particle morphology and schematics of PCL- ATO 5 MP's with different co-surfactant types and concentration

The morphologies of hybrid PCL-ATO 5 MPs prepared with selected water phases using different surfactant pairs are shown in Figure 4.5. The microparticles prepared by the co-surfactants of PVA-SDBS were observed to have particles with tails. However, it is also observed that there is no significant change in morphology at different concentrations of PVA-SDBS and in both concentrations, the particles are prepared with tails. However, in the presence of PVA-SDBS as co-surfactants, hybrid particles are not uniform like in PVA-SDS. In both cases, in the presence of SDBS, about half of the particles were with tails, while the remaining particles had different morphologies. Therefore, hybrid particles were prepared by choosing SDS instead of SDBS to have uniform particles.

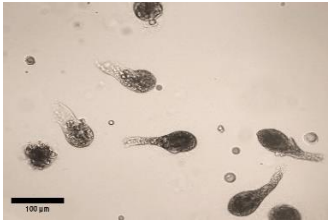
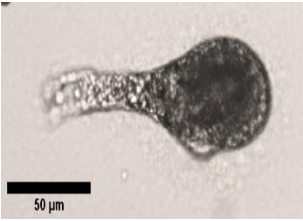
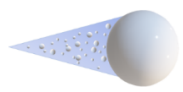
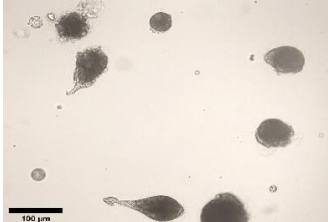
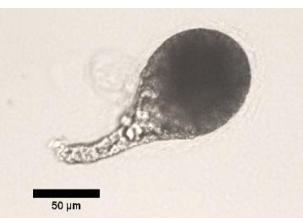
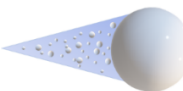
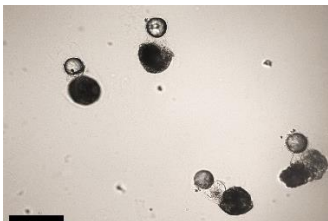

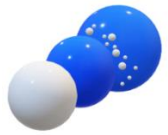
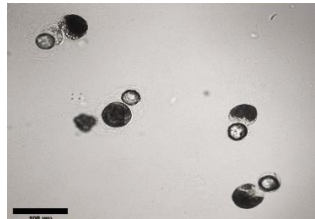
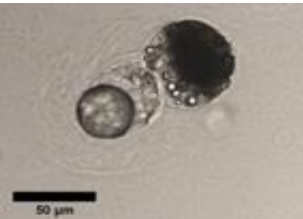

| Surfactant type and concentration | | <i>OM images</i> | | <i>Schematics</i> |
|-----------------------------------|---------------------|---|--|---|
| PVA 0,25 | SDBS 0,08 |  |  |  |
| PVA 0,10 | SDBS 0,10 |  |  |  |
| PVA 0,20 | SDS 0,06 |  |  |  |
| PVA 0,15 | SDS 0,05 |  |  |  |

Figure 4.5. The particle morphology and schematics of PCL- ATO 5 MP's with different co-surfactant types and concentration

When SDBS is used, it is clear that the particles have a tail and are less uniform, while in the presence of SDS, they are more uniform and have a different morphology. With SDS, the structure has more rigid compartmentalization at both concentrations, as seen in the schematics in the table and the OM image. The morphology with like 3-compartments seen in the particle morphology of particles prepared by PVA-SDS as surfactants are shown in white in the schematic representation and the lipid part in blue. Figure 4.6 shows that the morphologies in OM and SEM images of polymer, lipid and hybrid particles confirm that they are similar.

However, the particles in A, B and C are in Figure 4.6. were prepared in the water phase using PVA-SDBS surfactants. In Figure 4.6.D, PVA-SDS was used as a surfactant in the water phase. As seen in Figure 4.6.C, the hybrid particles prepared in the presence of SDBS have a morphology that combines the single component particles in A and B in the figure. In section D, it is also observed that the lipid compartment is not as elongated as in the presence of SDBS due to the change in the surfactant type. When PVA-SDBS and PVA-SDS are compared, it is evident that the morphologies do not change at different concentrations of both. Therefore, when Figure 4.5 is examined, it is possible to observe that the change of surfactants at specific low concentrations does not affect the morphology. However, the change of ionic surfactants from surfactants has resulted in a great morphological difference. This is because of the change in interfacial tension caused by changing the surfactant. In both hybrid structures, however, it can be analyzed that the polymer and lipid parts appear in a Janus particle structure located at two different ends of the particle.

After evaluating the type and concentration of surfactant, one of the parameters affecting the morphology of the prepared hybrid structures, the effect of higher concentrations of a non-ionic surfactant and the presence of ionic surfactant, was examined for a more in-depth investigation. Surfactants provide stabilization of the droplets formed in the microfluidic system both in the formation and also in the solvent evaporation process. While non-ionic surfactants do not affect particle morphology, different ionic surfactants are reported to change the morphology [64, 65]. Figure 4.7 indicates that when the SDS concentration increased to 5%, a different morphology was formed than 0.05%. This is due to the decreasing surface tension with increasing SDS at constant PVA concentration. At a PVA concentration of 0.15%, in the absence of SDS, the morphologies have the same multi-component structures as in the presence of low concentrations of SDS. However, in the absence of SDS, it is seen that the white part, symbolized as the polymer compartment and shown in the schematic, remains as a core in the structure and is not positioned at different poles with the lipid as in the presence of SDS.

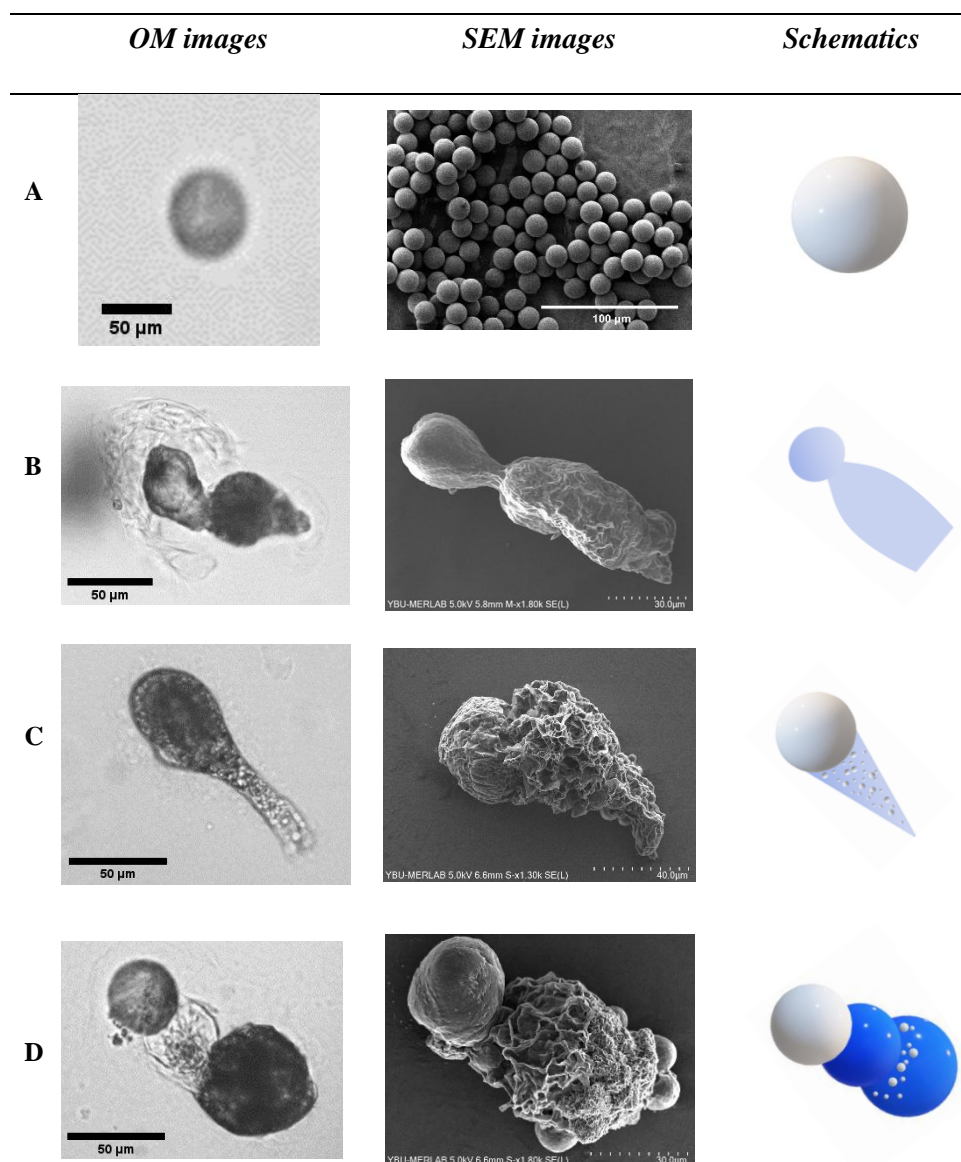


Figure 4.6. The particle morphology of different microparticles by microfluidics, A) PCL microparticles [34], B) Precirol ATO 5 microparticles, C) PCL-Precirol ATO 5 hybrid microparticles, D) PCL-Precirol ATO 5 hybrid microparticles. The particles from A-C were prepared with surfactants PVA and SDBS; in part D, SDS was used instead of SDBS.

Consequently, the remainder of the current study aims to work with two different surfactant pairs, non-ionic and ionic. This will enable the studies to be carried out under these conditions where compartmentalization is desired and undesired in particles to be engineered for different applications. The relationship between compartmentalization and surfactant type/concentration mentioned here is in the case of PCL-ATO 5 hybrid MPs. In the following sections, particle

morphologies at different surfactant types and concentrations in hybrid structures prepared with different lipids will be discussed separately. Since it was determined that the Janus structure was achieved when SDS was used as an ionic surfactant, it has also been investigated how the surfactant concentration changes the morphology at a higher value (Figure 4.7). The parameter study in Figure 4.7 aims to design the optimal morphology for the targeted drug-loaded hybrid nanoparticles. In this regard, the concentration of SDS was increased, resulting in a decreased aspect ratio.


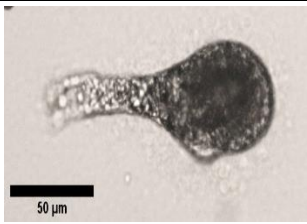
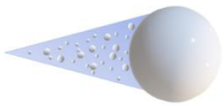

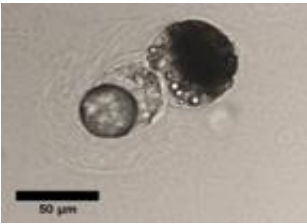
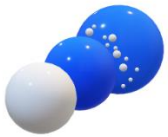
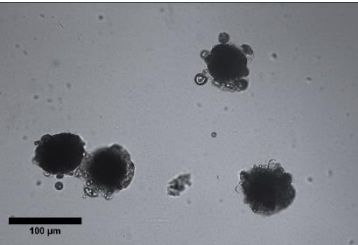
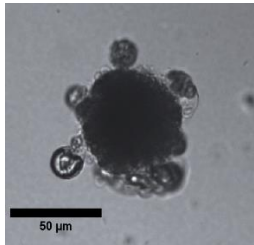

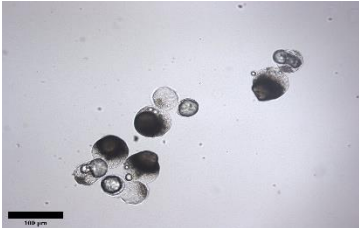
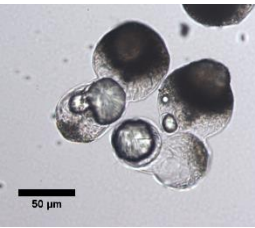

| <i>Surfactant type and concentration</i> | | <i>Particle Morphology</i> | | |
|--|-----------------------------|---|--|---|
| PVA | SDBS 0,25 0,08 |  |  |  |
| PVA | SDS 0,15 0,05 |  |  |  |
| PVA | SDS 0,15 5,00 |  |  |  |
| PVA | 0,15 |  |  |  |

Figure 4.7. The particle morphology and schematics of PCL- ATO 5 MP's with different co-surfactant types and concentration

The high aspect ratio provides a large surface area, which can reduce drug toxicity. While the high surface area provides a more controlled release, it also prevents the drug from being released in an amount that will cause toxic effects in the body. One of the objectives of the particles to be used as a drug carrier system is to provide a high aspect ratio. This allows for increased encapsulation efficiency with increased surface area and improved targeting; the particles with a high aspect ratio are preferred over spherical particles [108]. In Figure 4.3, it was previously shown that the morphology of PCL-ATO 5 MPs prepared with PVA-SDBS co-surfactants had low uniformity. Uniform microparticles were obtained when SDS was used instead of SDBS in preparing the same hybrid MPs. The morphologies of the hybrid MPs using PVA-SDS as a surfactant are shown in Figure 4.8. When the particle morphologies were carefully analyzed, it was seen that the polymer and lipid components of the particles were positioned at two different poles of the particle, forming a Janus morphology. When the morphological distribution of these particles is examined, it is possible to determine that there are very small morphological differences.

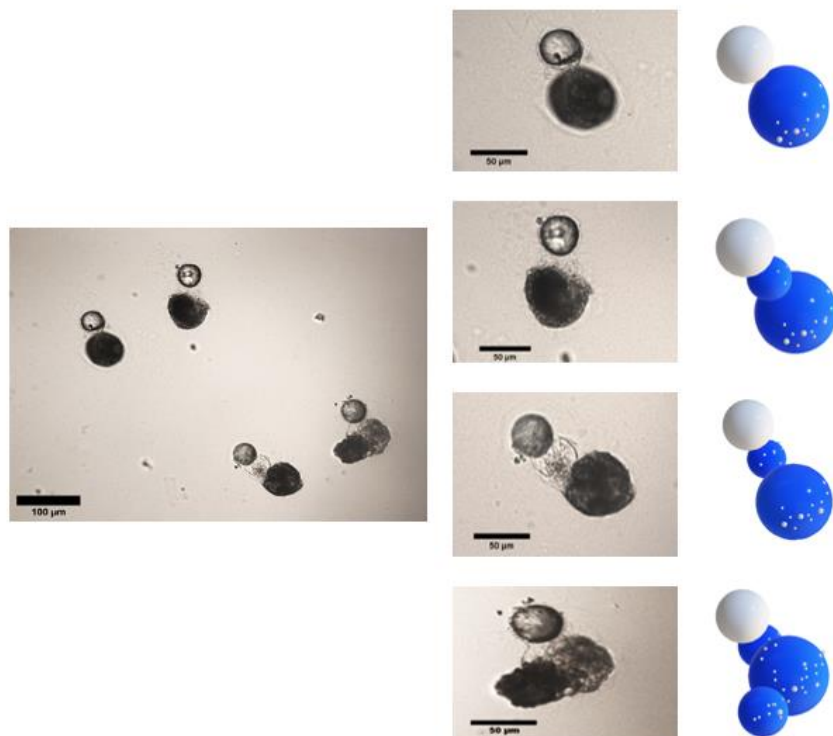


Figure 4.8. Morphology distribution of PCL- Prericol ATO 5 MP's with PVA and SDS as a surfactant

The difference here is the aspect ratio of the lipid part as shown in the schematic in blue colour. This is due to the fact that the lipid structure is more flexible than the polymer structure. However, in these particles where SDS is used as an ionic surfactant, there is no such polydispersed distribution as in SDBS. Therefore, using PVA-SDS as a surfactant in the preparation of hybrid PCL-ATO 5 MPs provided a more uniform size and morphology distribution.

4.3.2. Examination of Solvent Evaporation Conditions for the Morphology of Polymer-Lipid Hybrid Microparticles

After the PLHMPs were obtained in a uniform shape, phase separation conditions, another parameter affecting the morphology of the prepared particles, were analyzed. The purpose is to control the phase separation process and obtain the desired morphology. During phase separation, the ambient temperature, the concentration of the particles in the medium and the concentration of the surfactants in the medium are of great importance. Therefore, PLHMPs in which PVA-SDS was used as the surfactant were analyzed under three different conditions after being collected as droplets from the microfluidic device (Figure 4.9.). In the first condition, the droplets were collected for 30 min in a 25 ml water phase in the same conditions as the aqueous phase during synthesis, and the beaker was left at room temperature for 24 h for the solvent evaporation process (Figure 4.9.A). In the second case, the particles were collected for 10 min in a water phase volume of 10 ml, and the particles were stirred at 40C at 125 rpm for 6 hours (Figure 4.9.B). In conditions A and B, droplets were collected in the same beaker volume. In the second case, the particle concentration is less than in the first case, and the height of the water phase in the beaker is relatively low. Therefore, instead of 24 hours, where the particles undergo phase separation in a denser environment, particles were obtained at a higher temperature with less particle density in a much shorter time, such as 6 hours.

However, when the particles obtained quickly in this condition are examined, it is observed that they have similar morphologies; however, the aspect ratios are different. In condition C, the droplets were collected in the beaker as in condition B and a 100 μ l sample was taken from the beaker and poured onto the glass slide. While the OM was running, the droplets underwent phase separation within 8 minutes due to the heated glass slide and dilute particle concentration. During this period, the droplet size shrinkage of PLHMPs was analyzed (Figure 4.10). The

average size of the droplets was 179.37 μm when the droplets were transferred onto the glass slide. After 7 minutes and 15 seconds, the droplet volume decreased to 59.31 μm and remained at a constant volume until the 8th minute, but due to phase separation, the droplet rapidly transformed into two different compartments. Firstly, the polymer part was phase separated in an area equal to the droplet volume, and after 7 minutes and 30 seconds, the lipid part was finalized in a few seconds next to the polymer part, and the particle had a Janus shape. In all these conditions, the particles were kept at room temperature for 24 hours, and it was examined whether there was a change in particle morphology; it was observed that there was no change in morphology in the last 24 hours. Since it was observed that the particles had a higher aspect ratio at room temperature for 24 hours without any mixing, the 24-hour condition was selected as the phase separation condition after this part of the study.

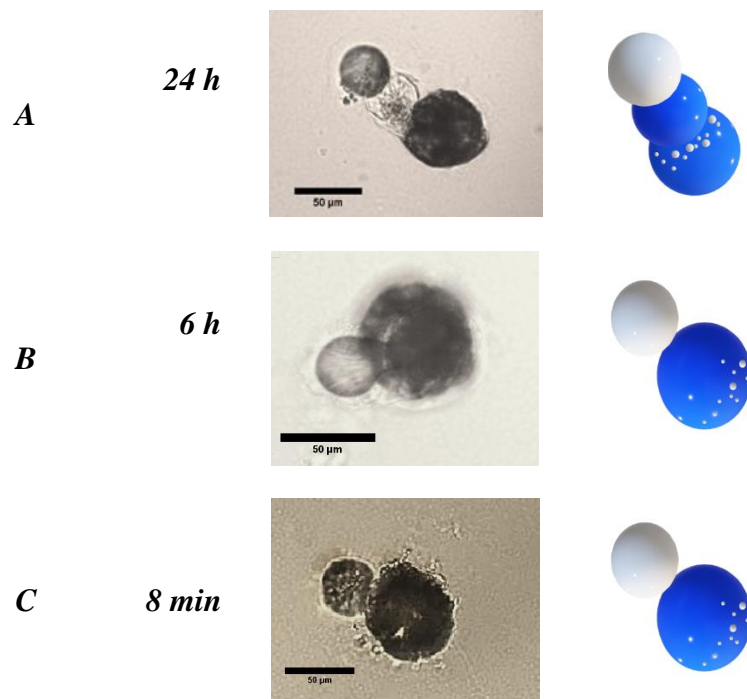


Figure 4.9. Particle morphologies at different solvent evaporation rates of PCL-ATO 5 MPs

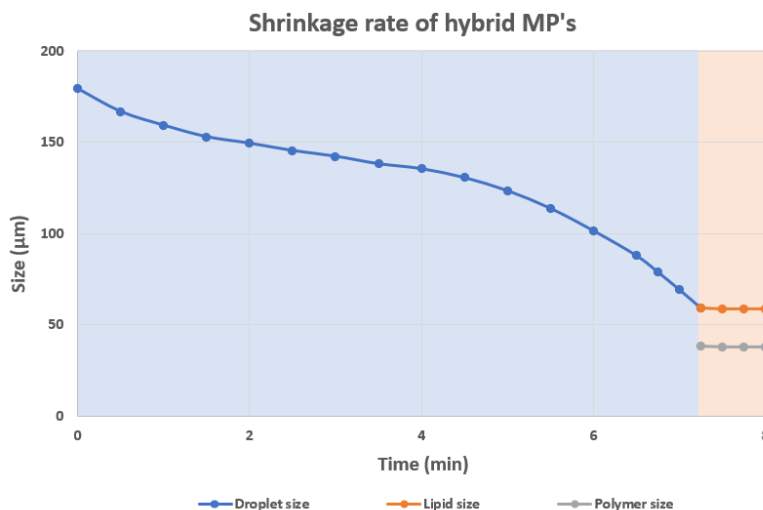


Figure 4.10. Shrinkage rate of hybrid MPs in rapid solvent evaporation

4.3.3. Examining The Hybrid Morphology of Polymer-Lipid Hybrid Microparticles

To distinguish the polymer and lipid-based compartments of PCL-ATO 5 hybrid MPs more closely, the studies of Cao et al. were taken as a reference [67]. The lipid ATO 5 used to prepare PLHMPs was evaluated to be faster and better soluble by acetone than PCL polymer, and the prepared PLHMPs were treated with acetone for 30 seconds. The images obtained from the process were analyzed by OM and shown in Figure 4.11. As can be seen from the images, it was found that PCL still maintained its spherical structure after treatment with acetone, but the surrounding and elongated lipid structure was dissolved, and only spherical particles were imaged. This indicated where ATO 5 was positioned in the particle morphology, as it surrounded the PCL in a thin layer and elongated to form a softer separate compartment.

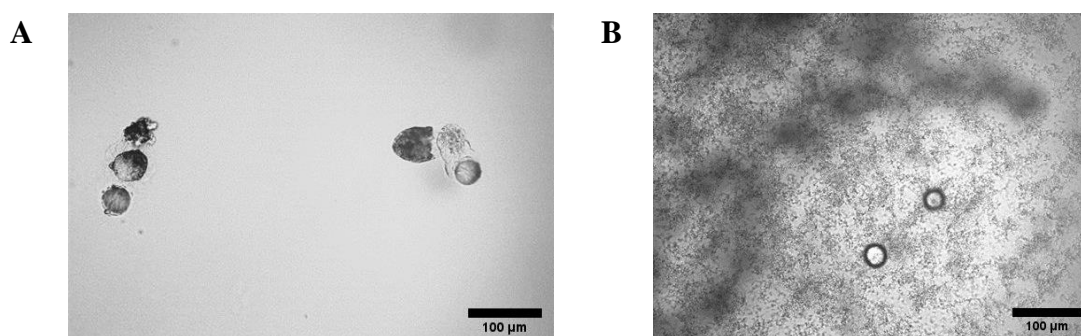


Figure 4.11. OM images of PCL-ATO 5 hybrid microparticles treated with acetone for 30 s, A) before the treatment, B) after the treatment

After this study, another study was planned to be carried out to distinguish polymer and lipid-based compartments. For this purpose, the particles were heated to different temperatures and expected that the lipid part with a lower melting temperature would start to melt before the polymer part. Precirol ATO 5 lipid has a melting temperature between 50-60 °C (Figure 4.12), while the melting temperature of PCL is 60 °C [109]. For this study, the particles were dispersed in water and heated in a beaker in an oven while still in the solution state. For each temperature increase, 30 minutes had waited after the oven reached that temperature, and after this time, the sample temperature was confirmed with a thermal imaging camera.

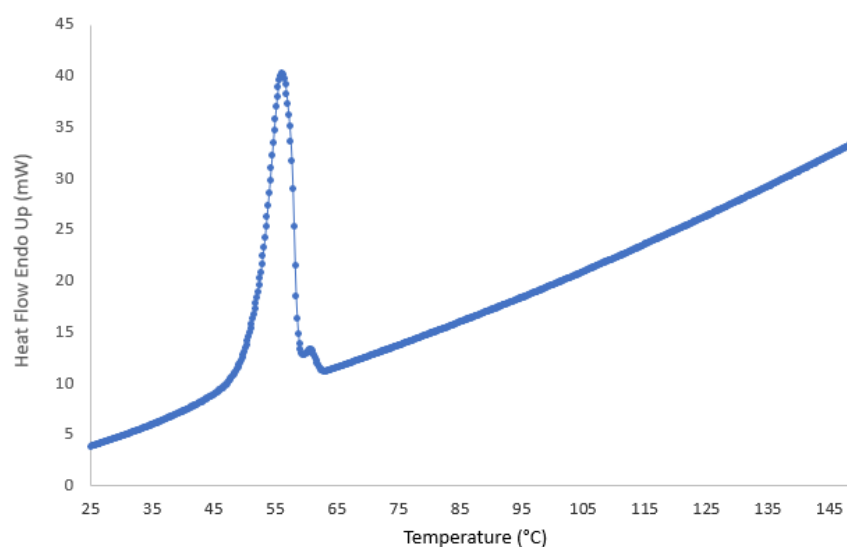


Figure 4.12. DSC profiles of Precirol ATO 5 (Samples were prepared 10 mg in weight. Measurements were carried out between 0-150 °C with a heating rate of 10 °C /min).

In this study, 5% (w/w) Rho-B was incorporated during synthesis for better analysis of the particles and the particles were analyzed by fluorescence optical microscopy (Figure 4.13). It was observed that there was no change in the morphology of the particles at room temperature and 50 °C. However, when the temperature was increased to 55 °C, there was a visible change in the morphology of the particles. At 55 °C, it is observed that at lower temperatures, the part that is characterized as spherical and thought to be the polymer part remains the same, but the morphology of the softer part changes as in the previous study (Figure 4.11). In the DSC profile of ATO 5, it can also be seen that the melting temperature range starts at 55-56 °C. This confirms that the lipid part of the hybrid particle has the lower melting temperature and the more rigid and spherical part is the polymer part. When the OM images are analyzed at 60°C, it is seen that both the polymer and lipid structures are melted and no morphology is preserved.

The study showed that polymer and lipid can be distinguished during the melting of components with close melting temperatures by precise temperature control. Temperature increase and acetone treatment confirmed PCL-ATO 5 PLHMPs to be a hybrid structure, with polymer in the spherical part and lipid in the more dispersed part.

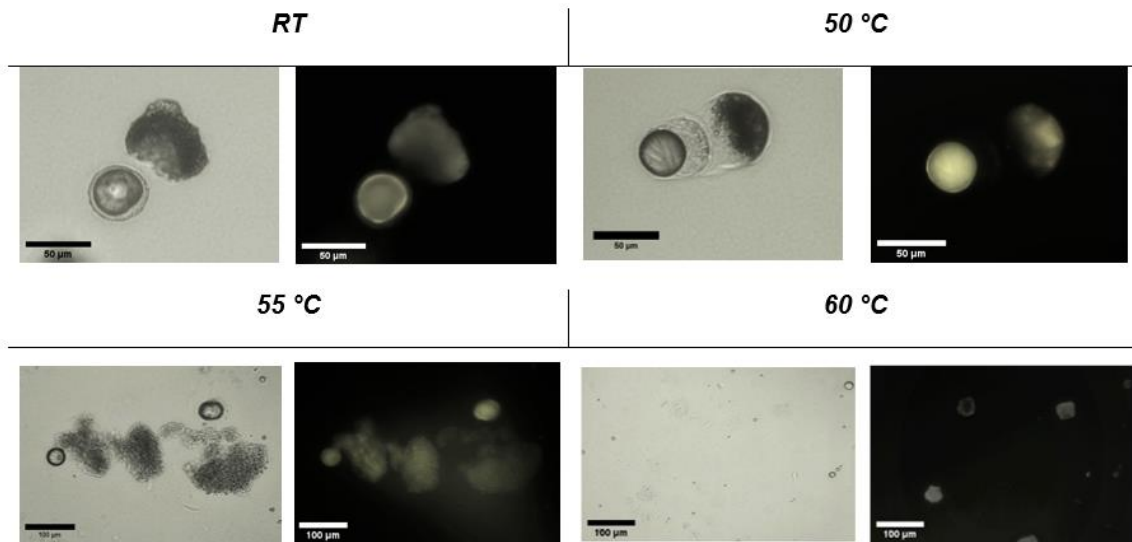


Figure 4.13. The effect of an increase in temperature on rate PCL-ATO 5 (1:1) hybrid MPs

4.3.4. The Effect of Flow Rate Ratio on the Aspect Ratio of Polymer-Lipid Hybrid Microparticles

The flow rate ratios of the inner and outer phases, which are one of the parameters affecting the morphology of particles prepared with microfluidic technology, are evaluated in this section. In microfluidic systems, internal and external phase flow rates are essential for the continuous formation of droplets. Increasing the outer phase flow rate at a constant inner phase flow rate reduces the size of the droplets and increasing the inner phase flow rate at a constant outer phase flow rate increases the droplet size [110]. When the flow rates are changed, the flow can change from a dripping regime to jetting regime [111]. Therefore, the flow rates changed in the study were carried out at flow rates where the dripping regime rate was observed. Up to this point in the study, the inner phase flow rate was kept constant at 0.06 ml/h, and the outer phase flow rate was kept constant at 0.8 ml/h. In this section of the study, the flow rates were changed by varying the flow rates at different ratios and the effect of this on the aspect ratio of the particle was analyzed (Figure 4.14). Figure 4.14 shows that as the flow

rate ratios increase, the aspect ratios decrease. This shows that there is an inverse relationship between the flow rate ratio and the aspect ratio of the particles.

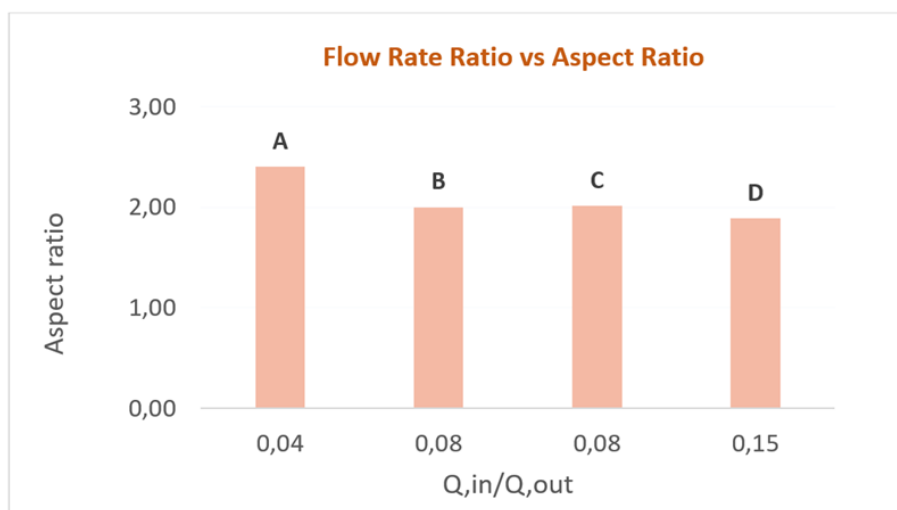


Figure 4.14. The effect of flow rate ratio on the aspect ratio of PLHMPs, A) The Q_{in} is 0.06 ml/h, and Q_{out} is 1.6 ml, B) The Q_{in} is 0.06 ml/h, and Q_{out} is 0.8 ml/h, C) The Q_{in} is 0.18 ml/h, and Q_{out} is 2.4 ml/h, D) The Q_{in} is 0.18 ml/h, and Q_{out} is 0.8 ml/h. (The Q_{in} and Q_{out} represent the flow rate of the inlet and outlet phases, respectively.)

Looking at samples B and C, it is seen that the flow rate ratios are constant. The difference between these samples is that although the flow rate ratios are the same, the total flow rate in C is three times higher than in B. This shows that the same aspect ratio can be achieved even when the particles are produced at higher production rates.

4.3.5. The Effect of Polymer-Lipid Ratio on the Area of Polymer and Lipid Components of Polymer-Lipid Hybrid Microparticles

In the previous parts of the study, the polymer and lipid ratio of PCL-ATO 5 hybrid microparticles prepared by microfluidic technology was selected as 1:1. In this section, the morphology of the hybrid particles prepared at different polymer-lipid ratios and the changes in their morphology will be analyzed. The graph and particle morphologies of PLHMPs prepared at different polymer-lipid ratios are given in Figure 4.15. For area calculations, the

polymer and lipid areas of 25 particles were calculated separately using OM images and the average values are provided in the figure.

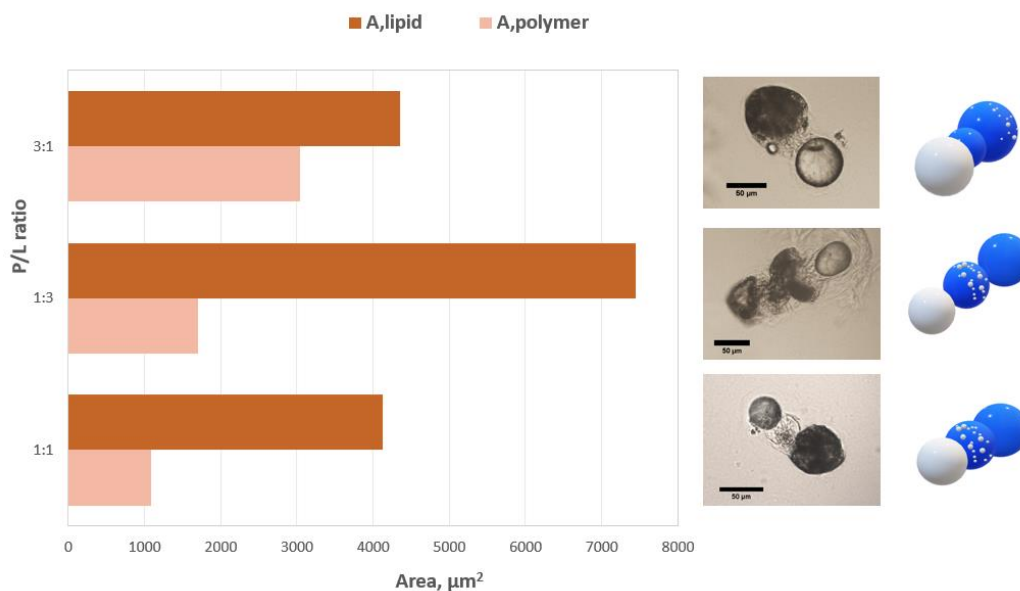


Figure 4.15. The effect of polymer-lipid ratio on the area of polymer-lipid hybrid microparticles. All particles were prepared at the same flow rates for the dispersed and continuous phases. The white color shows the polymer and the lipid part is shown in blue color in the schematic representation.

When the areas of the polymer and lipid parts of the hybrid microparticles with a polymer-lipid ratio of 1:1 prepared previously were examined, it was observed that the area of the lipid part occupied a larger area than the polymer used in the same ratio. In these particles, the average lipid area was calculated as $4120.02 \mu\text{m}^2$ and the area of the polymer part was calculated as $1085.30 \mu\text{m}^2$. In particles with 1:1 polymer-lipid ratio, the area of the lipid part was approximately 3.80 times that of the polymer part. This can be explained by the fact that the polymer with a rigid structure forms a more rigid structure in morphology, while the lipid is more dispersed due to its softer structure. When the polymer ratio was increased to 3 times, the ratio of the area of the lipid part to the polymer part was calculated as 1.43. Although the polymer concentration was increased 3 times, it is observed that the lipid part still has a larger area in the calculated areas. However, it should not be forgotten that these calculations are two-dimensional measurements. When the polymer ratio was 1, and the lipid part was increased 3 times, it was seen that the lipid part increased 4.35 times. When the concentrations were

increased 3 times, the areas did not increase according to these ratios, but it was observed that there was a significant change in the areas in the compartments and the particles maintained their multi-compartmental structure. As a result of this study, these particles were analyzed. In the following parts of the study, the efficiency of the drug carrier system will be evaluated when these particles are used as drug delivery systems.

4.3.6. The Short Term Stability Test of PCL-Precirol ATO 5 Hybrid Microparticles

In this section, the PLHMP's short-term stability test was performed to examine the stability of PCL-ATO 5 hybrid microparticles (Figure 4.16). The PLHMPs were dispersed in the water phase containing PVA and SDS and kept at room temperature for 23 days, and morphology analysis was performed with OM. SDS and PVA were used in the medium where the particles are kept since these agents were used to increase stability in some studies in the literature [63]. The slight morphology differences seen in the figure are because of the lipid's soft structure. The images belong to different PLHMPs in the same batch. In all images, the three component morphology is seen, and the test performed shows that the PLHMPs have high stability at room temperature in a short-term stability test.

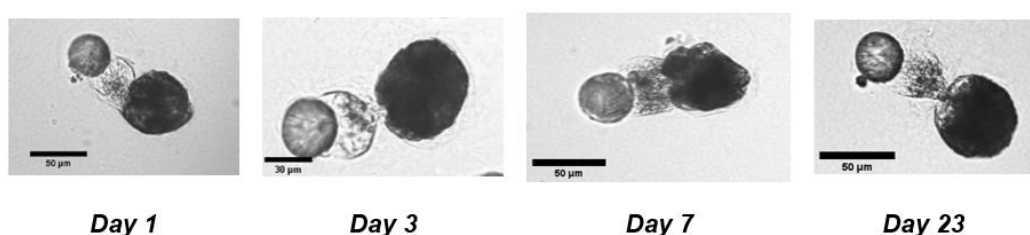


Figure 4.16. The Particle Morphology and schematics of PCL- ATO 5 MP's with different co-surfactant types and concentration

4.4. Preparation of Polymer-Lipid Hybrid Microparticles with Different Lipids

In hybrid MP studies, Janus structure and particles with high aspect ratio were obtained when ATO 5 was used. In order to evaluate the potential use of different hybrid structures in different applications, stearic acid and Softisan 100 were used as lipid components in hybrid structures

other than ATO 5. These lipids were chosen due to their difference in melting temperatures. Softisan 100, which has a melting temperature below body temperature (33.5 - 35.5 °C), was planned to be used when designing temperature-sensitive hybrid particles. Stearic acid has a higher melting temperature than the other lipids and is also the only lipid among the selected lipids with a higher melting temperature than the polymer.

Stearic acid is a naturally present saturated fatty acid of plant and animal origin. Compared to other fatty acids, it has been observed in the literature that it is used as a lipid in lipid-based drug delivery systems due to its short chain length [112]. ATO 5 exhibits high drug retention ability by providing easier adhesion and positioning of drug-active ingredients with its porous structure due to its deviation from crystallinity and high amorphousness [107].

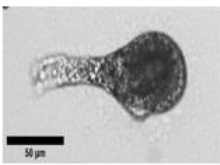

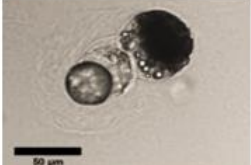



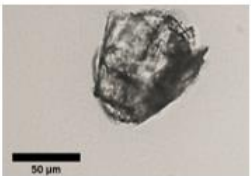

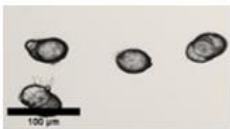

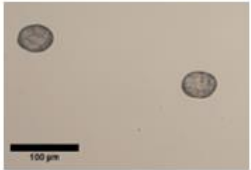

Table 4.3 shows the morphology of polymer-lipid (1:1) hybrid MPs prepared with different lipids in the presence of different co-surfactants and their schematics. In the schematics, the lipid part is marked in blue and the polymer part in white. As mentioned before, the morphologies of PLHMPs in which ATO 5 was used as a lipid in the presence of different ionic surfactants changed and how this change affected the monodispersity of the prepared particles were discussed. The change of ionic surfactant type when different lipids were used was also tested for all lipids. Table 4.2 shows that the hybrid structures using Stearic Acid as a lipid are different from the structures with ATO 5. However, with the ionic surfactant change, the hybrid structures were changed as in ATO 5. Therefore, it can be claimed that ionic surfactant alteration changes the particle morphology for both ATO 5 and SA. When PCL-SA hybrid MPs are examined, it was observed that spherical particles similar to the core-shell structure with multiple compartmentalizations within the structures were obtained in the presence of SDBS. This situation has changed when SDS was used instead of SDBS. In the presence of SDS, more rigid layers are observed around the particles.

When PCL-Softisan 100 hybrid MPs are examined, it is apparent that the structures do not form particles with high aspect ratio as in ATO 5, and are even characterized as a more Janus hybrid particle in the presence of SDS. Considering the PLHMPs prepared with different lipids in the presence of different ionic surfactants, particles with high aspect ratio, multi-compartment and uniform properties were prepared to be used for different applications.

During the characterization of PCL-SA with OM, the presence of these layers has raised a question and different characterization methods are planned to be used to confirm the presence of these layers. Since the targeted anisotropic hybrid structure is not as obvious as PCL-ATO

5 in PCL-SA hybrid MPs, different studies will be further discussed in the following sections in order for the structure to have the desired anisotropy.

Table 4.2. The particle morphology and schematics of PCL- ATO 5 MP's with different co-surfactant types and concentration

| <i>Lipid type</i> | <i>PVA-SDBS</i> | | <i>PVA-SDS</i> | |
|-----------------------|---|---|--|---|
| | OM image | Schematics | OM image | Schematics |
| <i>Precirol ATO 5</i> |  |  |  |  |
| <i>Stearic Acid</i> |  |  |  |  |
| <i>Softisan 100</i> |  |  |  |  |

In Table 4.2, in order to determine the compartments of PLHMPs prepared with different lipids, they were labelled with Rhodamine-B, a dye with fluorescent property. The labelled hybrid particles prepared with different lipids are shown in Figure 4.17.

As a result of the labelling of PCL-Precirol ATO 5 hybrid MPs labelled with Rhodamine-B, it is seen that almost the entire particle is labelled by the hydrophilic dye. Studies were carried out by predicting that the hydrophilic dye used in labelling would be positioned on the lipid part, which is the less hydrophobic part. In the labelling of hybrid MPs in which ATO 5 is used as a lipid, it is seen that the dye is not positioned in a single compartment of the particle. However, it is seen that the compartments of the three-component PCL-Precirol ATO 5 hybrid MPs expressed in previous studies encapsulate different concentrations of dye and fluoresce at different concentrations.

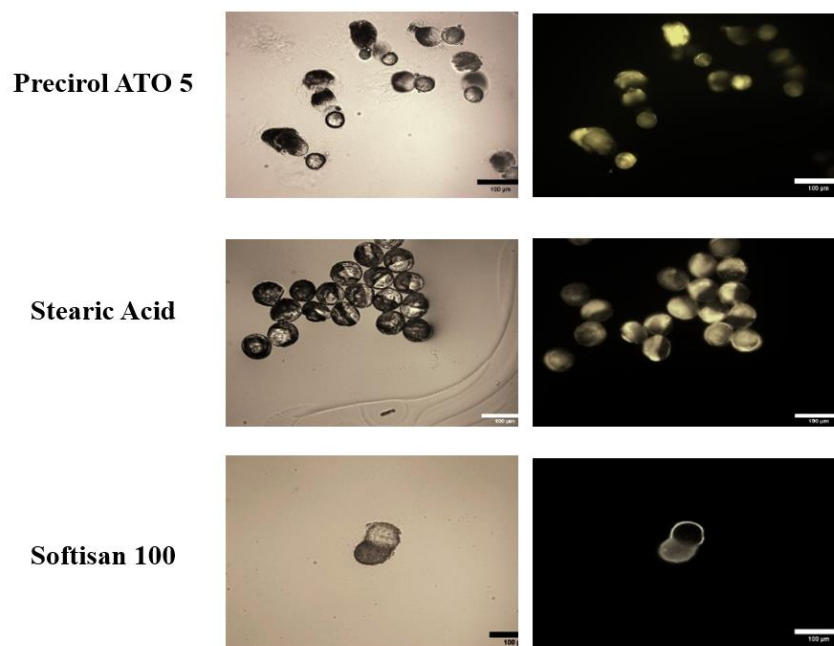


Figure 4.17. The particle morphology Rhodamine-B labelled PLHMPs prepared using different type of lipid

When the stearic acid particles are examined, it is clearly seen that the particles labelled with Rhodamine-B have a Janus structure. This morphology appeared after labelling. With the added hydrophilic dye, it is seen that the hydrophilic and hydrophobic components are more clearly positioned in the Janus morphology. PLHMPs prepared with Softisan 100 also clearly showed the Janus structure just like Stearic acid particles. In the labelling study, it was seen that Stearic Acid and Softisan 100 were successful in distinguishing polymer and lipid components. However, it should not be forgotten that Rhodamine changes the morphology of the structure, although it varies according to each particle. For this reason, other studies are planned in order to distinguish the components in the images characterized with OM.

4.5. Preparation of Polymer-Lipid Hybrid Microparticles with Three Components

During the characterization of PLHMPs using stearic acid with OM, it was observed that the surfaces of the particles consisted of layers. It was discussed in section 4.4 of the study that the hybrid particles prepared with SA had very different morphologies from the particles prepared with ATO 5. PLHMPs prepared with microfluidic technology were intended to be used for

different biomedical applications. PCL-SA hybrid particles, in which the hybrid structure was not clearly observed as a component, were noticeable due to their surface layers. In order to compartmentalise the particles prepared with stearic acid, it was decided to add a third component to the particles. For this purpose, 1H,1H,2H,2H,2H-Perfluoro-1-decanol (Fluo) was added to the particles as the third component. FLUO is a fluorinated alcohol and has high hydrophobicity and oleophobicity [113]. By adding a hydrophobic component to the hybrid structure, it was desired to examine whether the components of the structure could be distinguished.

In order to form the three-component structure, firstly, the polymer ratio was kept constant and 70% of the amount of lipid used in the same ratio was used as lipid and 30% of the third component, Fluo, was used. Figure 4.18. shows the OM and SEM images of the two and three components of the stearic acid hybrid particles. In the preparation of these particles, the inner phase flow rate was set to 0.06 ml/h and the outer phase to 0.8 ml/h. PVA (0.15% w/v) and SDS (0.05% w/v) were used in the water phase to stabilise particle formation. The droplets obtained from the one nozzle microfluidic system were kept in the water phase containing PVA and SDS for 24 hours and then analyzed by OM. SEM samples were prepared for more detailed examination of the results obtained in OM analysis. When the OM and SEM images were compared for both samples, the layers characterized by OM are very clearly identified by SEM analysis. This confirms that PLHMPs with SA have hard edges on the particle surface. Figure 4.18.C and D show the OM and SEM images of the three-component structures. In the SEM images, the structures that are not clearly visible in the OM images are clearly distinguished and it is determined that the prepared three-component structure has a structure similar to the bipolar structure. At the same time, SEM images of the three-component structure showed that the two-component structure has similar properties. Although the aim of the study was to have multi-component structures, structures that can be used for different applications have also been successfully prepared by optimising the parameters. As it was mentioned in earlier sections, Fluo was added to the PCL-SA hybrid microparticles. In the images given in Figure 4.18, it shows that after the addition of fluo, the layers in the structure are more clear and evenly ordered. The study carried out to investigate in which applications this structure can be used will be discussed in following sections.

SEM-EDX analysis was performed to determine whether the fluorine in the FLUO added microparticle structures was integrated into the structures (Figure 4.19). As a result of the

analysis, the presence of 3.4% fluorine in the structures was detected by the EDX detector and the presence of the added FLUO in the structure was proved.

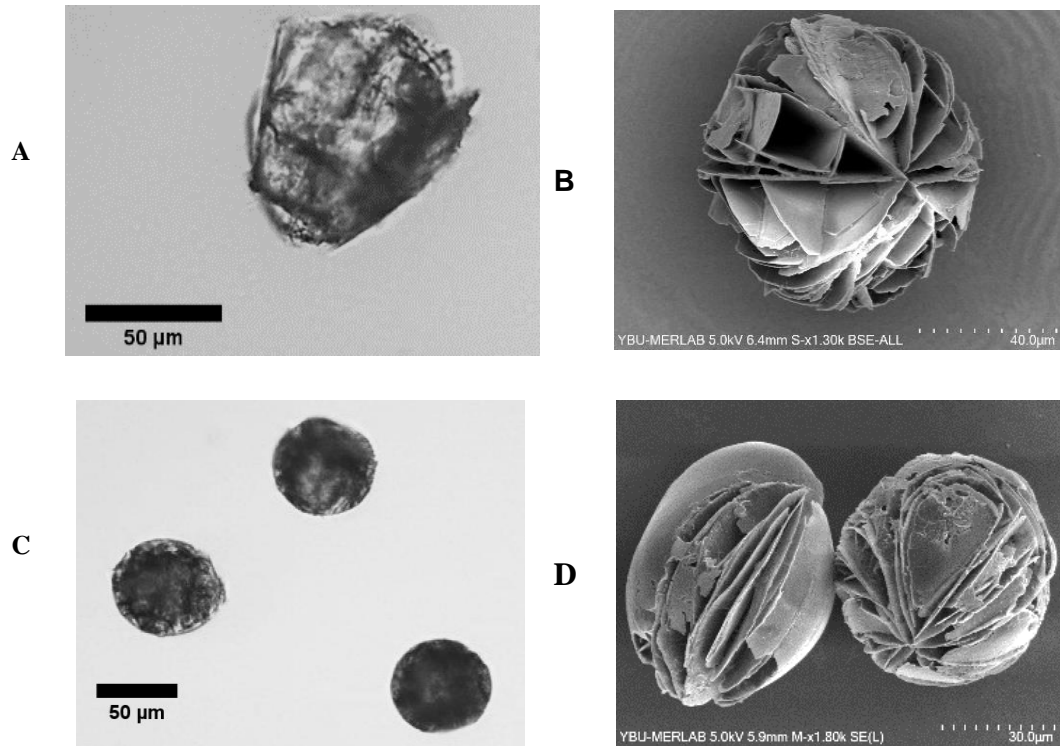


Figure 4.18. The morphologies of PLHMPs with stearic acid, A) The OM image of PCL-Stearic Acid (1:1) PLHMPs, B) The SEM image of PCL-Stearic Acid (1:1) PLHMPs, C) The OM image of PCL-Stearic Acid-Fluo (1:0.7:0.3) PLHMPs, D) The SEM image of PCL-Stearic Acid-Fluo(1:0.7:0.3) PLHMPs

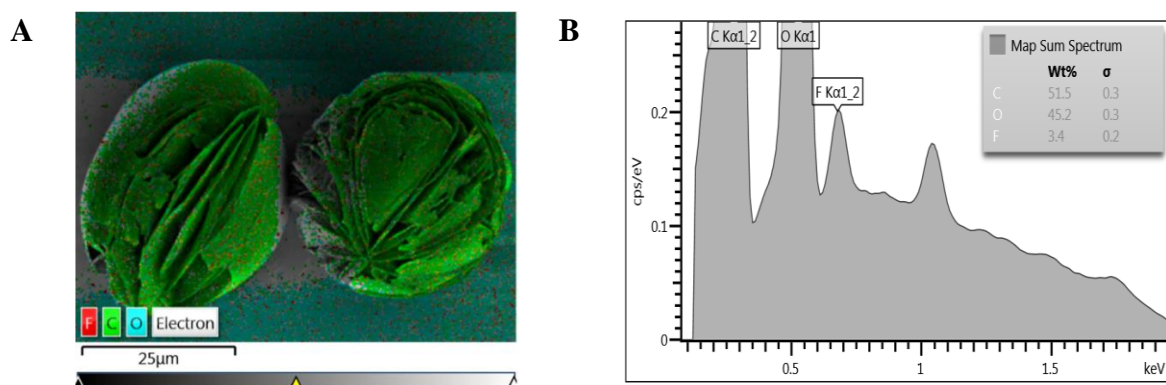


Figure 4.19. SEM-EDX analysis of PCL-SA-FLUO hybrid microparticles

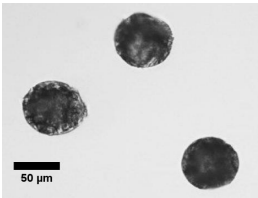

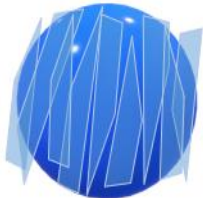
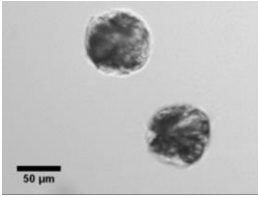
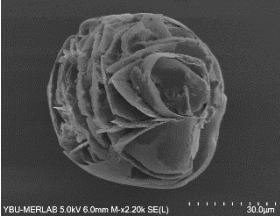

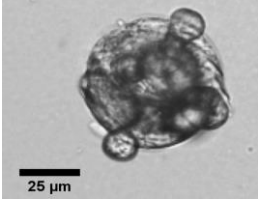
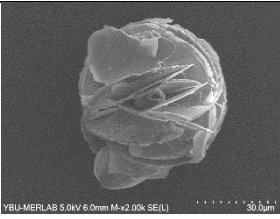
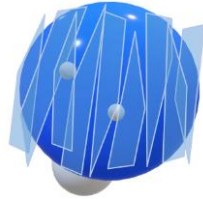
4.5.1. The Effect of Surfactant Type and Concentration on Polymer-Lipid Hybrid Microparticles with Three Components

In the previous sections of this work, the effect of solvent type and concentration in the preparation of polymer-lipid hybrid microparticles was analyzed in a detail. It was discussed how PVA, SDBS and SDS surfactants change the structure morphology and under which conditions. In this part of the study, the same study will be carried out for the three-component structures obtained and the changes in the morphology of spherical structures with layered surfaces will be evaluated.

In order to examine the effect of surfactant type and concentration on the morphology of the three-component structures, the particles were prepared in the composition prepared previously. The polymer ratio was kept constant and 70% of the amount of polymer used as lipid and 30% of the third component, Fluo, was used. The droplets obtained from the one nozzle microfluidic system were kept in a water phase containing PVA and SDS for 24 hours and then analyzed by OM. Three different surfactant types and concentration conditions were selected for the study and the structures of the three-component hybrid microparticles were characterized by OM and SEM (Table 4.3). Comparing the two samples in which PVA and SDS were used as surfactants, it is seen that both structures have layers as seen previously in the two-component structure. However, the positioning of the layers arranged on the surface of the microparticles differs from each other. In the case where the surfactant concentration was lower, the longitudinal arrangement of the particle morphology was observed and in the other case, the layers were positioned transversely cyclically. However, this slight morphological difference was not considered as a significant change. Then, SDBS was used together with PVA as surfactant and it was observed that this change caused a significant change in particle morphology. The three-component hybrid particles, which have structures positioned in different forms on the spherical surface in the presence of PVA and SDS, were found to have a different morphology on the surface in the presence of SDBS. When SDBS was used, it was observed that there were more than one compartment in a more rigid form inside the structures and OM analysis was supported by SEM analysis. Since only the surface of the structures can be determined by SEM analysis, different studies will be applied in the future parts of the study. In the previous studies carried out to separate the components of the hybrid particles, it was determined that the more spherical and rigid parts were the polymer parts. In the presence of SDBS, the structures observed inside and also outside the structure

were thought to be polymer. A similar component determination study with PCL-ATO 5 hybrid particles will be applied for three-component structures in the following sections.

Table 4.3. Particle morphologies of multi-componental PCL-Stearic Acid MPs

| <i>Components</i> | <i>OM images</i> | <i>SEM</i> | <i>Schematics</i> |
|-------------------------|---|--|---|
| PVA: 0.15% SDS:0.05% |  |  |  |
| PVA: 0.2% SDS:0.07% |  |  |  |
| PVA: 0.1% SDBS:0.1% |  |  |  |

When SDBS used instead of SDS, the OM and SEM images showed that the polymer particles which are rigid were no longer trapped in the hybrid particles. Since there are different interfacial tensions in the presence of SDS and SDBS, this change in these particles with the same composition was thought to occur during phase separation. The sizes of the three-component particles were also calculated using OM and SEM images. The sizes of the particles shown from top to bottom in the table are 60.48 μm, 67.44 μm and 64.48 μm, respectively.

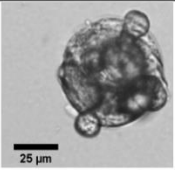

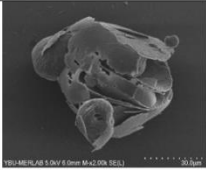

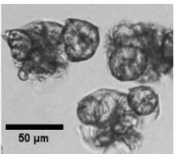
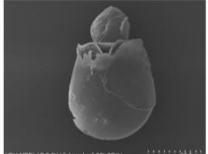
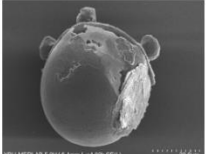

4.5.2. The Effect of Exchanging the Concentrations of Lipid And Fluorinated Component on the Morphology of Polymer-Lipid Hybrid Microparticles with Three Components

In the presence of SDBS in the three-component structures, it was observed that small particles were located on the inner and outer surfaces of the spherical structures. However, at the same time, the layers on the surface in the presence of SDS were also present in the presence of SDBS. For the determination of these structures, it was decided to change the composition of the three-component structure. For this purpose, the ratios of lipid, which was previously used as 70% of the polymer, and fluorone, which was used as 30%, were changed. The prepared multicomponent hybrid microparticles were characterized by OM and SEM.

The morphologies of PCL-SA-Fluo MPs with different compositions are given in Table 4.4. In the given table, it was observed that the layers on the surfaces of the particles disappeared when the lipid ratio was decreased. However, it was also observed that the small particles trapped inside and on the surface of the structure in the previous composition were still present.

In conclusion, it was confirmed that the small particles in the structure were related to the type of surfactant. While there are no small particles on the surface of the structure at different concentrations of different surfactants, small particles can be seen on the surface in the presence of SDBS. It was observed that the stratification on the surface of 3-component structures decreased when the amount of lipid decreased and the particle surface was smoother. This suggests that this stratification is due to stearic acid.

Table 4.4. Particle morphologies of multi-componental PCL-Stearic Acid-Fluo MPs

| <i>Components</i> | <i>OM images</i> | <i>SEM images</i> | | <i>Schematics</i> |
|--|---|---|--|---|
| PCL (1.0) Stearic Acid (0.7) Perfluoro-1-decanol (0.3) |  |  |  |  |
| PCL (1.0) Stearic Acid (0.3) Perfluoro-1-decanol (0.7) |  |  |  |  |

4.5.3. Examining The Hybrid Morphology of Polymer-Lipid Hybrid Microparticles with Three Components

In the characterization of the three-component structures, it was observed that there were some layers on their surfaces and these layers were positioned differently. When the lipid and Fluo ratios were changed, it was observed that these layers disappeared with decreasing lipid amount. In order to determine these layers and to examine the effect of the components used on the morphology, two- and three-component structures were obtained by removing some of the polymer, lipid and fluo components of the 3-component structures or replacing them with another component. The morphologies of these hybrid microparticles were characterized by OM. OM images of these particles and schematics of the particles are given in Figure 4.20.

PCL-SA-Fluo hybrid MPs had attracted attention with their layered outer surface. For this reason, the polymer component was firstly removed from the structure and particles were prepared with a one-nozzle microfluidic system keeping the component composition constant for the remaining components. Looking at the SA-Fluo particles (Figure 4.20.B), layers were observed on the surface of the structure as in the same three-component structure. Based on this, it was thought that these layers were not of polymer origin. Then the lipid used was replaced with ATO 5 (Figure 4.20.C) and PCL-ATO 5-FLUO particles were prepared in such a way that the polymer-lipid-fluo composition remained constant.

When the given figure is examined, it is seen that the layers seen on the surface in the presence of stearic acid completely disappeared and the particles had a morphology similar to two-component PCL-ATO 5 hybrid microparticles. This result showed that the layers may be caused by stearic acid. When Fluo was removed from the 3-component structure, it was confirmed that the layers on the surface of the structure were preserved as in the case where the polymer was removed.

In the study carried out for the determination of the layers of the three-component structures prepared with stearic acid, it was observed that the layers originated from the selected lipid. In the presence of ATO 5, it was observed that there was no dispersed lipid and layers, however, when stearic acid was used as a lipid, the presence of layers was observed in all cases.

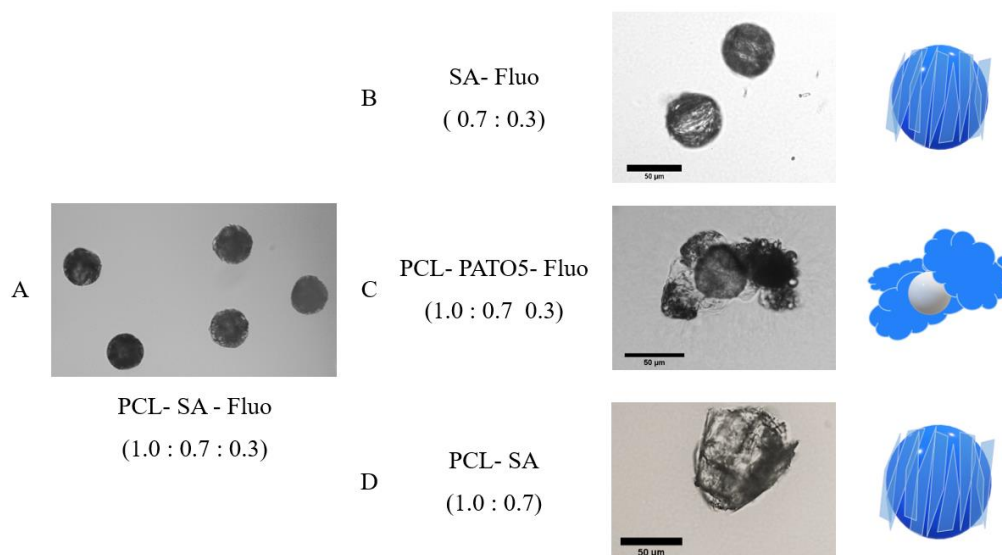


Figure 4.20. The particle morphology and schematics of PCL-ATO 5 MP's with different co-surfactant types and concentrations, A) PCL-SA-Fluo hybrid MPs, B) SA-Fluo hybrid MPs, C) PCL-ATO 5-Fluo hybrid MPs and D) PCL-SA hybrid MPs.

4.6. The Preparation of Magnetic Nanoparticle Loaded Polymer-Lipid Hybrid Microparticles

In order to functionalize the three-component structures in which stearic acid was used as a lipid, oleic acid coated magnetic nanoparticles were loaded into the structures. For this purpose, oleic acid coated magnetic nanoparticles were first synthesised by the co-precipitation method and nanoparticle sizes were analyzed by DLS (Figure 4.21). As a result of the analysis, it was observed that the size of oleic acid coated MNPs was 13.72 nm. In order to integrate the prepared MNPs into the structure, HLHMPs were prepared with one nozzle microfluidic system after making sure that the MNPs in acetone were dispersed in the dispersed phase by adding 7.84% (w/w) of the dispersed phase.

The morphology of the particles prepared by loaded oleic acid coated MNPs into stearic acid PLHMPs were characterized by OM and SEM. Oleic acid coated MNPs loaded PLHMPs are shown in Table 4.5. Oleic acid coated MNPs were examined by VSM (), the magnetic saturation of MNPs was found as 37.94 emu/g in previous study [114].

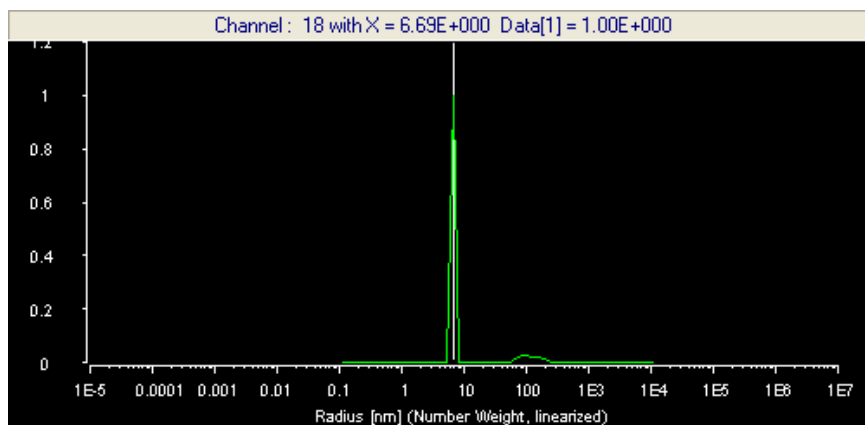


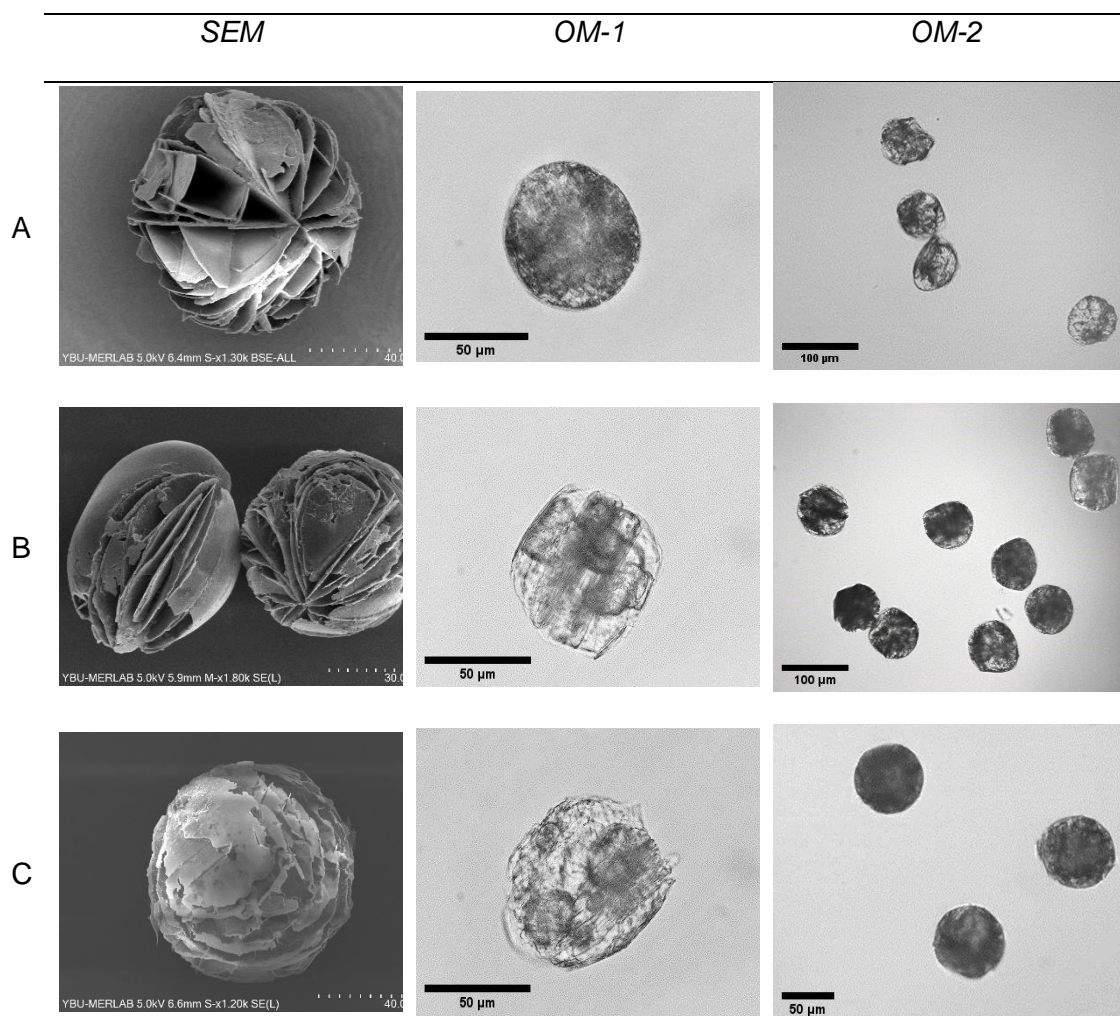
Figure 4.21. The DLS analysis of oleic acid coated MNPs

The morphologies of the prepared MNPs loaded hybrid microparticles were compared with different component samples of the same structure in Table 4.5. Table 4.5.C shows the MNP-loaded hybrid structure without MNP loading and Table 4.5.B shows the MNP-loaded hybrid structure. When these two structures are examined, it is seen that the layers on the surfaces of the MNP loaded structures are not as hard and organized than the PLHMPs without MNP loading. However, the structure maintained its spherical morphology after MNP loading. For the characterization of the hybrid structures, Inverted Optical Microscope (OM-2) and Polarised Light Microscope (OM-1) were used to characterize the particle morphology without the use of polarising filters. Looking at the OM-1 and OM-2 images of MNP-loaded structures, it can be said that OM-2 provides a different perspective in terms of examining the morphology. While the surfaces of the MNP-loaded PLHMPs could be clearly characterized with OM-1 and SEM images, it was seen that there were different compartments located inside these structures with the help of OM-1. When the morphology of three-component PLHMPs with stearic acid was analyzed previously (Table.4.5.B-OM-2), the compartments inside the structures were not noticed. However, Polarised Light Microscope revealed that there were different compartments inside the structures. However, this was not observed in the same way for two-component structures.

In the OM-1 images of PCL-SA-containing PLHMPs, it is clear that the structures are different from PCL-SA-Fluo-containing PLHMPs. One of the major differences between these two structures is the hydrophobic component Fluo added to the structure in the three-component structure. In the first characterizations of PCL-SA PLHMPs, it was observed that the structure was not compartmentalized like PCL-ATO 5 and it was

thought that the structure could be compartmentalized by adding a hydrophobic component to the structure. However, this compartmentalization was not evident in the characterization of OM-2. However, with the characterization of OM-1, it was seen that the structure of the hydrophobic component added to the structure was in a core-shell structure containing more than one core. Looking at both the MNP loaded (Table 4.5.C) and unloaded (Table 4.5.B) structures, it is clear that the Fluo used causes particle nucleation in both structures. This confirms that the Fluo added to the structure is beneficial for the compartmentalization of the structure and fulfills its purpose.

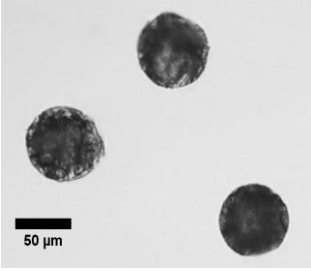
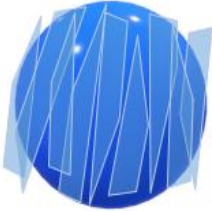
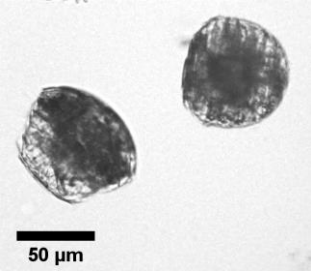
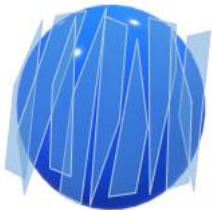
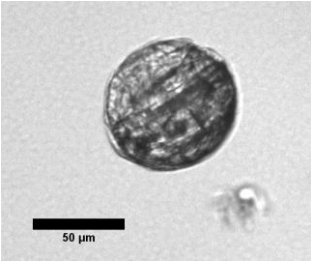
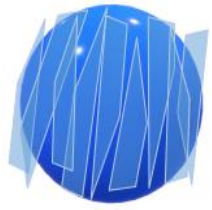
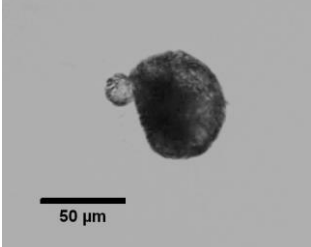
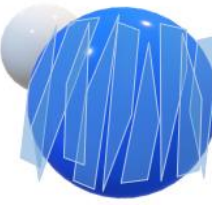
Table 4.5. Particle morphologies of multi-component PCL-Stearic Acid MPs, A) PCL-SA (1:1), B) PCL-SA-FLUO (1:0.7:0.3), C) Oleic acid coated MNP loaded PCL-SA-FLUO (1:0.7:0.3). OM-1 images are taken with a polarized optical microscope without polarizing filters, while OM-2 images are taken with an inverted light microscope.



MNPs loaded into three-component structures were prepared with particles with polymer, lipid and fluo ratios of 1.0, 0.7 and 0.3, respectively. In previous studies, it was observed that changing this composition changed the morphology of PLHMPs. Therefore, PLHMPs were prepared by changing the polymer, lipid and fluo concentrations of the prepared structures as 0.3, 0.7 and 1.3, respectively. The prepared structures were also loaded with oleic acid coated MNPs (7.8% w/w). The prepared particle morphologies were characterized by OM and given in Table 4.6.

Hybrid MPs prepared by changing the polymer and fluo ratios of PCL-SA-Fluo PLHMPs are shown in Table 4.6.C. When the structures characterized by OM are examined, layers like the previous structures are clearly seen on the surface of the structures. When compared with the PLHMPs (Table 4.6.A) before the polymer and fluo ratio was changed, it was observed that there was no major change in the morphology of the hybrid structures. When oleic acid coated MNPs were loaded on PLHMPs prepared with decreasing polymer concentration, there was a major change in morphology. The layer and more homogeneous spherical-like structures on the surface before MNP loading turned into Janus structure with the addition of MNP to the structure. The reason for this can be expressed as the hydrophobic oleic acid coated MNPs increase the concentration of hydrophobic components in the structure and thus the structure is positioned at two different poles. When MNP-loaded PLHMPs with different polymer concentrations were compared, it was observed that the hybrid particles with high polymer ratio were spherical and had nuclei inside the structures (Table 4.6.B). Although this nucleation could not be seen during the characterization with Inverted Optical Microscope, it was thought that with the changing polymer ratio, addition of MNPs to the structure and increasing hydrophobic component concentration, the hydrophobic components previously trapped in the structure came out of the structure and formed the Janus structure.

Table 4.6. Particle morphologies of multi-component PCL-Stearic Acid-Fluo MPs

| | Components | OM | Schematics |
|---|--|---|---|
| A | PCL- SA- Fluo (1.0 : 0.7 : 0.3) |  |  |
| B | PCL- SA- Fluo (1.0 : 0.7 : 0.3) + 7.84% (w/w) MNP |  |  |
| C | PCL- SA- Fluo (0.3:0.7:1.0) |  |  |
| D | PCL- SA- Fluo (0.3:0.7:1.0) + 7.84% (w/w) MNP |  |  |

In order to investigate the sensitivity of MNP-loaded PLHMPs (Table 4.6.A) with high polymer ratio to the magnetic field and to analyze whether they move with the applied magnetic field, the magnet with a magnetic field strength of 0.48 Tesla was kept 2 cm away from the particles while being analyzed with an optical microscope and the translational movement of the particles was examined. The images of the movement of PLHMPs under magnetic field are given in Figure 4.22.

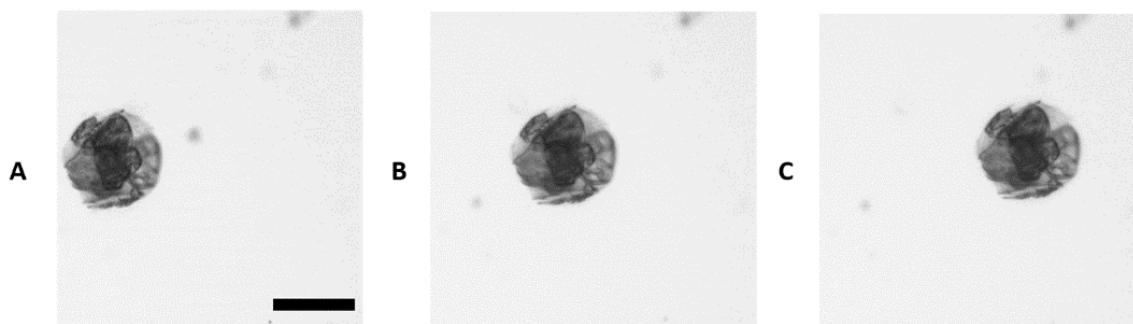


Figure 4.22. The translational speed of oleic acid coated MNP's loaded PLHMPs in 50s, A) t=0, B) t=25 s, C) t=50 s (The scale bar=50 μm)

The translational motion of MNP-loaded PLHMPs was successfully observed in the given graph. However, during the experiment under an optical microscope, the magnet could not be brought closer than 2 cm to the particles due to the positioning of the microscope lenses. For this reason, the same experiment was repeated with an inverted optical microscope and it was found that all particles were sensitive to the magnetic field and their translational velocities were calculated as $81.11 \pm 38.86 \mu\text{m/s}$ when the same magnet was brought closer to 0.5 cm of the particles and left fixed in that position. When MNP loaded PLHMPs with lower polymer ratio (Table 4.6.D) were analyzed under the same conditions, the translational velocities of the particles were calculated as $42.53 \pm 32.49 \mu\text{m/s}$. When these two particles were compared, it was observed that the particles with higher polymer ratio moved about 2 times faster than the particles with lower polymer concentration than the particles with the same lipid and MNP concentration.

Magnetic field sensitive MNP loaded three-component PLHMPs were successfully prepared. It was proved that both MNP loaded PLHMPs were magnetic field sensitive, although the morphologies were also changed by changing the polymer and fluo ratio in studies with different polymer concentrations.

4.7. The Optical Properties Examination of Polymer-Lipid Hybrid Microparticles

In the previous parts of the study, two- and three-component structures were successfully prepared with different lipids and PLHMPs with stearic acid were functionalized and responsive to magnetic field. Especially the layers on the surface of the particles prepared with stearic acid attracted attention and the reason for this was thought to be SA. It was

aimed to investigate whether the three components containing PCL-SA-Fluo are optic responsive particles in their particles due to the more regular positioning of the layers in the structures. For this purpose, SA-containing two-component, three-component and MNP-loaded three-component structures were analyzed by polarised optical microscopy (POM).

It was considered that PCL-SA-Fluo hybrid particles may exhibit birefringence due to the orientation of the layers seen in the morphology. The images of POM analysis with three different particles containing SA are given in Figure 4.23. In Figure 4.23, the first image for each sample is the bright field and the second and third images are the images where polarized light was used. In the table, it is seen that all particles have some bright and dark fields in the images. This proves that the prepared hybrid particles have birefringence properties.

In the bright field image of B and C, it is seen that there is compartmentalization within the structures. This does not appear in the two-component hybrid structure. In the images where the polarizer and analyzer are positioned at 45° , it is seen that each structure has different light and dark fields in different regions. This is due to the different refractive indices of the prepared hybrid structures.

In the previous part of this study, oleic acid-coated MNPs were loaded to functionalize the particles and their translational motions and related angular speeds under magnetic field were evaluated. However, some materials with birefringence properties can also move rotationally under a certain magnetic field. For this, it is necessary to change the position of the magnetic field in a certain area. Within the scope of this study, a rotating magnetic field was manually created with POM by continuously displacing the magnet with a magnetic field strength of 0.48 Tesla clockwise and counter-clockwise. Meanwhile, images of the particles were taken under polarized light. The images obtained are given in Figure 4.24.

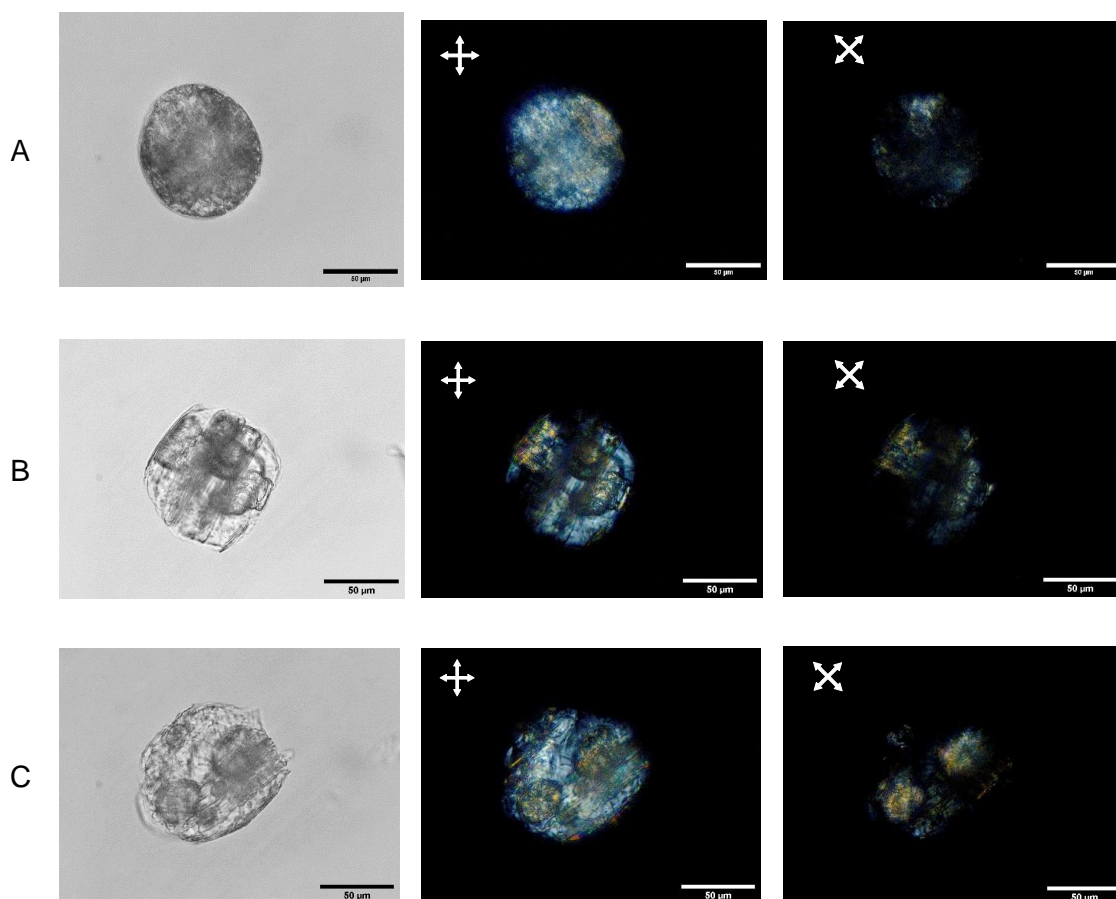


Figure 4.23. POM images of multi-component PCL-Stearic Acid MPs, A) PCL-SA (1:1), B) PCL-SA-FLUO (1:0.7:0.3), C) MNP loaded PCL-SA-FLUO (1:0.7:0.3). The white insert arrows shows the position of the analyzer and polarizer.

Due to the limited mobility of the magnet due to the position of the microscope and the sample and the magnetic field strength of the magnet used was insufficient except for MNP-loaded PLHMPs, images could only be taken for MNP-loaded particles. Since the two- and three-component structures without MNPs rotated very slowly and at a very narrow angle, they were not included in the results section of the study. It is considered that a higher magnetic field strength is needed to analyze the rotational motion of non-MNP-loaded particles.

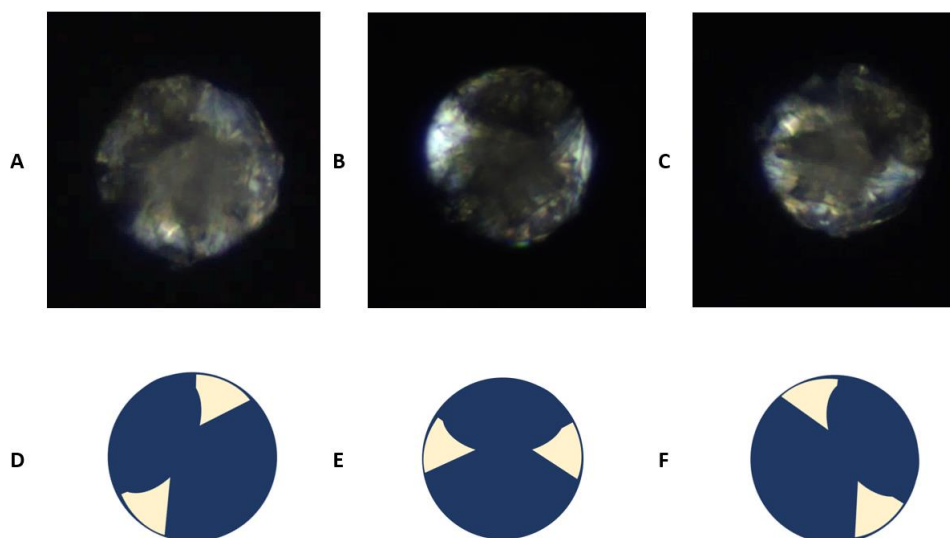


Figure 4.24. The rotational movement of MNP loaded PLHMPs, A) The magnet rotates counter clockwise under continuous rotating magnetic field, B) No magnetic field is applied at $t=0$, C) The magnet rotates clockwise under continuous rotating magnetic field, D-F) The schematics of the particles in A-C respectively. The POM images were taken 20 seconds after the magnetic field was applied in the A and C. The white insert arrows shows the position of the analyzer and polarizer.

When the rotational motions of the MNP-loaded particles under rotational magnetic field were observed, it was observed that they had an angular velocity of 0.05 rad/s under the applied magnetic field. In the calculations of these velocities, the image B in the figure was taken as a reference and based on the particle position given in the schematic, the number of angular movements of the final image of the particles, which received the magnetic field applied for 20 s, from the reference image was calculated. It is estimated that the values given are different from the data that can be obtained by using a different system due to the fact that the rotational magnetic field applied with a magnet cannot be done properly and is applied manually. However, in the rotational magnetic field applied manually, it was observed that the MNP-loaded PLHMPs moved partially (maximum 60°) rotationally, although not 360° clockwise and counter-clockwise. As a result of the POM analyzes performed with MNP-loaded PLHMPs, the potential of the particles to be used as magnetically responsive, rotationally and translationally moving micro-motors was highlighted.

4.8. The Microfluidic Preparation of Polymer-Lipid Hybrid Nanoparticles

For the preparation of hybrid NPs, which is the main objective of the thesis, two and three component multifunctional PLHMPs were prepared with different lipids with different surfactant types and concentrations. The ultimate aim of the studies with MPs was to design the most favourable morphology as a drug delivery system. In the studies, aspect ratios, surface properties and morphologies of particles were evaluated in MPs in which ATO 5 and SA lipids were used. In the information obtained from the different PLHMPs prepared, it was determined to prepare PLHMPs that can be used as drug carrier systems using ATO 5. When compared with SA, particle morphologies with high aspect ratio were obtained with ATO 5 at the same composition and conditions. At the same time, PLHNPs were prepared with PCL and ATO 5 since the palmitic and stearic acid components of ATO 5 can provide advantages in the particles formed.

A previously designed and fabricated AL-GI chip was used for the preparation of PLHNPs. PLHNPs were prepared by nanoprecipitation method in a rectangular channel using two different miscible solvents. For this, firstly, different solvents were selected for polymer and lipid. 1,4-Dioxane was chosen as the solvent for ATO 5 and DMF for PCL. The choice of solvent, which is one of the parameters affecting the formation of particles prepared on the basis of the nanoprecipitation, is important.

When it is known that the solvents used in microfluidic systems as well as the flow rate to be applied affect the properties of the particles to be formed, three different total flow rates were selected for the preparation of PLHNPs. In all flow rate conditions, the flow rate of the polymer phase was set to be 10% of the lipid phase. Considering the flow rates applied in the preparation of PLHMPs, the total flow rate used in the preparation of PLHNPs was adjusted to be at least 7.5 times. This information is given to indicate the differences in the formation mechanisms of hybrid micro- and nanoparticles prepared using microfluidic technology. Although both of these systems are droplet-based systems, the particle formation mechanisms are different from each other.

During the preparation of PLHNPs, no surfactant was used that could contribute to the formation process of the particles. Since miscible solvents are used in nanoprecipitation-based nanoparticle preparation, water phase was not used. However, the effect of surfactant presence on particle formation and stabilisation was investigated in studies

with PLHMPs. When nanoparticles were produced, particles were collected in a beaker filled with water phase containing PVA and SDS.

In nanoprecipitation based systems, polymer and lipid phases fed at high flow rates in the channel were obtained as particles with the help of microvortices formed in the channel. It is known that as the flow rate increases, the microvortices formed are also affected and there is an inverse relationship between flow rate and particle size [115]. Therefore, particles were obtained with a total flow rate of 110 $\mu\text{L}/\text{min}$, 1100 $\mu\text{L}/\text{min}$ and 2200 $\mu\text{L}/\text{min}$. In Table 4.7, particle size data of DLS and AFM analyzes of PLHNPs prepared with three different total flow rates are given together with PDI values. AFM images and DLS results of three different prepared particles are also given in Figure 4.25. The target size for these particles, which have the potential to be used as a drug delivery system, is approximately 200 nm. Therefore, different sizes were obtained by working at 3 different flow rates. When the analysis results of the particles at the lowest total flow rate of 110 $\mu\text{L}/\text{min}$ were examined, it was determined that the PDI value was 0.081 ± 0.02 , the average particle size obtained as a result of DLS was 268.34 ± 34.57 nm and the average particle size obtained as a result of AFM analysis was 171.30 ± 38.43 . At a total flow rate of 1100 $\mu\text{L}/\text{min}$, the PDI value was 0.058 ± 0.02 , the average particle size obtained by DLS was 192.48 ± 31.39 nm and the average particle size obtained by AFM analysis was 123.76 ± 24.65 nm. When the results of the analysis of the particles at the maximum total flow rate are examined, the PDI value is 0.068 ± 0.02 , the average particle size obtained as a result of DLS is 158.96 ± 29.22 nm and the average particle size obtained as a result of AFM analysis is 103.18 ± 18.19 nm. According to the characterization results obtained, it is possible to state that the structures can be prepared as monodisperse with a PDI value below 0.1 [116, 117]. Considering that the sizes measured by DLS at all three flow rate ratios belong to hydrodynamic radius, it was seen that the particle sizes analyzed by DLS and AFM confirmed each other. Considering the sizes of PLHNPs analyzed by AFM, it was seen that all of them could be prepared below 200 nm. At the same time, when the flow rate was 2200 ml/h, particle sizes were obtained around 100 nm. This shows that PLHNPs with a size of 100 nm can be obtained by optimising the flow rate ratios in the designed Al-Gl microfluidic system.

Table 4.7. The nanoparticle sizes with an increasing flow rate.

| Total flow rate($\mu\text{L}/\text{min}$) | Re | PDI | Size (nm) | |
|---|------|------------------|--------------------|--------------------|
| | | | DLS | AFM |
| 110 | 1.2 | 0.081 ± 0.02 | 268.34 ± 34.57 | 171.30 ± 38.43 |
| 1100 | 12.1 | 0.058 ± 0.02 | 192.48 ± 31.39 | 123.76 ± 24.65 |
| 2200 | 24.2 | 0.069 ± 0.02 | 158.96 ± 29.22 | 103.18 ± 18.19 |

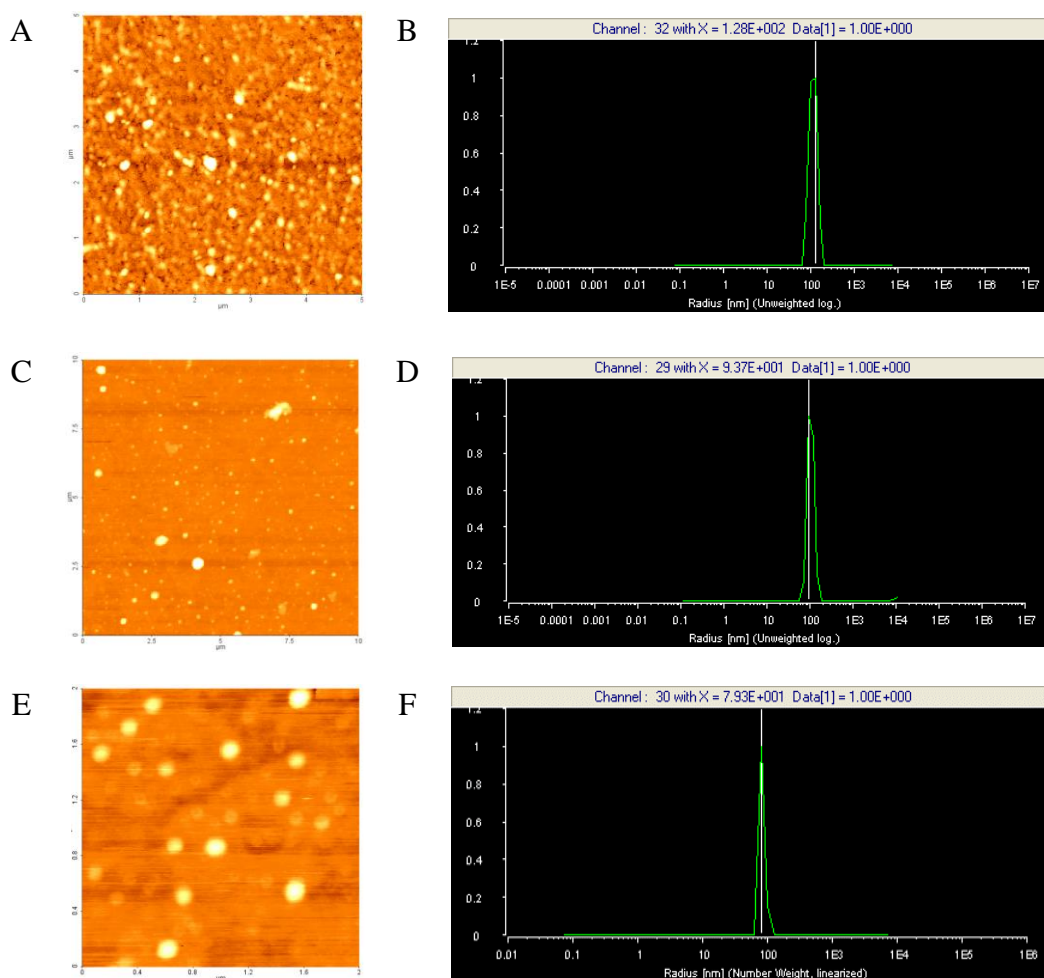


Figure 4.25. A) AFM images of PLHNPs at a total flow rate of $110 \mu\text{L}/\text{min}$, B) Particle size distribution of PLHNPs at a total flow rate of $110 \mu\text{L}/\text{min}$ determined by DLS, C) AFM images of PLHNPs at a total flow rate of $1100 \mu\text{L}/\text{min}$, D) Particle size distribution of PLHNPs at a total flow rate of $1100 \mu\text{L}/\text{min}$ determined by DLS, E) AFM images of PLHNPs at a total flow rate of $2200 \mu\text{L}/\text{min}$ determined by DLS, F) Particle size distribution of PLHNPs at a total flow rate of $2200 \mu\text{L}/\text{min}$ determined by DLS (Topography mode was used for the AFM images).

4.9. Investigation of Drug Encapsulation and Drug Release Properties of Different Drugs Loaded PLHMPs

PLHMPs have an important role in controlled drug release studies. Thanks to the hybrid structure, it is possible to load different drugs into the same particles. In particular, there are studies in the literature that both hydrophilic and hydrophobic drug active ingredients can be loaded into particles with Janus morphology [118]. In this part of the study, the drug active ingredient retention potential of PLHMPs prepared with microfluidic technology was investigated. At the same time, since the positioning of the active ingredients in the MP structure according to their physicochemical properties is among the determining features, drug encapsulation studies were carried out for PLHMPs with different polymer-lipid ratios.

It was examined in the last part of the study that the structures of PLHMPs prepared using Precirol ATO 5 are in Janus structure due to the positioning of polymer and lipid at the two opposite poles of the structure. When Janus particles are compared with other particles used in drug-active agent delivery systems, Janus particles have a very suitable structure for drug active ingredients with different physicochemical properties targeted to be transported, as mentioned before.

In this thesis, hydrophilic Rhodamine-B (RhB) and hydrophobic Resveratrol (RES) were used as model molecules and encapsulated separately in the polymer and lipid compartments of PLHMPs. At the solvent evaporation stage of PLHMPs, the polymer and lipid phases are separated into two separate compartments. Due to their hydrophilic and hydrophobic nature, the drug active ingredient and the polymer or lipid part, which have physicochemically different properties, do not mix during the phase separation process and it is evaluated that the hydrophilic molecule will be encapsulated into the lipid compartment, which is the more hydrophilic compartment, and the hydrophobic molecule will be encapsulated into the polymer compartment, which is the more hydrophobic compartment [119]. Thus, loading the model drug molecules individually into PCL-Precirol ATO 5 structure with 1:3 and 3:1 polymer-lipid ratio and investigating whether ROD and RES controlled release of the prepared PLHMPs will be performed will enable the investigation of the suitability of the use of PLHMPs as a candidate anticancer drug carrier system.

4.9.1. Investigation of Rhodamine-B Release from PLHMPs at Different Polymer-Lipid Ratios

At this part of the study, PCL-Precirol ATO 5 hybrid microparticles with Janus structure designed in the previous stages of the study were loaded with RhB and used as a drug delivery system. PCL-Precirol ATO 5 hybrid structures loaded with RhB with 1:3 and 3:1 polymer-lipid ratio were prepared with one nozzle system. During the preparation of PLHMPs, RhB was added 0.04% (w/w) directly with polymer and lipid and a dispersed phase was prepared

UV-Vis spectroscopy method was used to investigate the encapsulation efficiency and release profiles of PLHMPs with different polymer-lipid ratios. A calibration curve was prepared using RHB solutions at known concentrations. The calibration equation for RHB was established as $y=39.928x$ and this equation was used for all RHB releases to determine the encapsulation efficiencies and concentration values from the absorbance values of the samples at certain intervals from the release medium of PLHMPs under in vitro conditions.

When the encapsulation efficiencies of RhB into PLHMPs are examined (Table 4.8.), it is seen that RhB, which has hydrophilic properties, can be encapsulated 34.16% into PLHMPs with 3:1 polymer-lipid ratio, which has less lipid content. However, the encapsulation efficiency to PLHMPs with 1:3 polymer-lipid ratio, which has three times more lipid ratio, is 48.61%. The polymer and lipid areas of these two structures with different polymer-lipid ratios are shown in Table 4.8. Polymer and lipid compartments of these structures with different polymer to lipid ratios were calculated separately. The area calculations are the average area value calculated from the surface areas of 100 particles from the OM images of the particles. While the lipid area of the particle with a 1:3 polymer-lipid ratio was $7441 \mu\text{m}^2$, the polymer area of the particle with a 3:1 polymer-lipid ratio was calculated as $4349 \mu\text{m}^2$. When particles with 1:3 and 3:1 polymer-lipid ratios were compared, it was observed that the particle with 3:1 polymer-lipid ratio had 41.5% less area than 1:3. When this ratio is compared with the encapsulation efficiencies, it is seen that there is a linear relationship between the area and encapsulation efficiencies, considering that RhB is attached to the lipid part of PLHMPs.

When the release profiles of RhB encapsulated PLHMPs were compared with the literature, it was evaluated that the release of RHB from both particles was a sustained release [120]. Lower encapsulation efficiencies compared to hydrophobic drugs are due to particle preparation procedures. In the previous sections, it was stated that PLHMPs were kept in the water phase for approximately 24 hours after droplet formation. When the RhB release profiles of RhB encapsulated microparticles with different polymer-lipid ratios are examined, it is seen that they have similar release profiles (Figure 4.26.). However, the total RhB release of PLHMPs with 3:1 polymer-lipid ratio, which have lower encapsulation efficiency, reached 37.56% at the 4th hour, while the release of PLHMPs with 1:3 polymer-lipid ratio reached 67.08% at 6th hour. Considering that the release of RhB started during this period and when compared with the literature, it can be said that the release profile has an expected profile [121]. As a result, it was observed that RhB loaded PLHMPs with 1:3 and 3:1 polymer-lipid ratios could be suitable drug carriers for a hydrophilic drug. When the two particles were compared, it was seen that PLHMPs with 1:3 polymer-lipid ratio with higher encapsulation efficiency were more efficient as a hydrophilic drug carrier system than the other ratio.

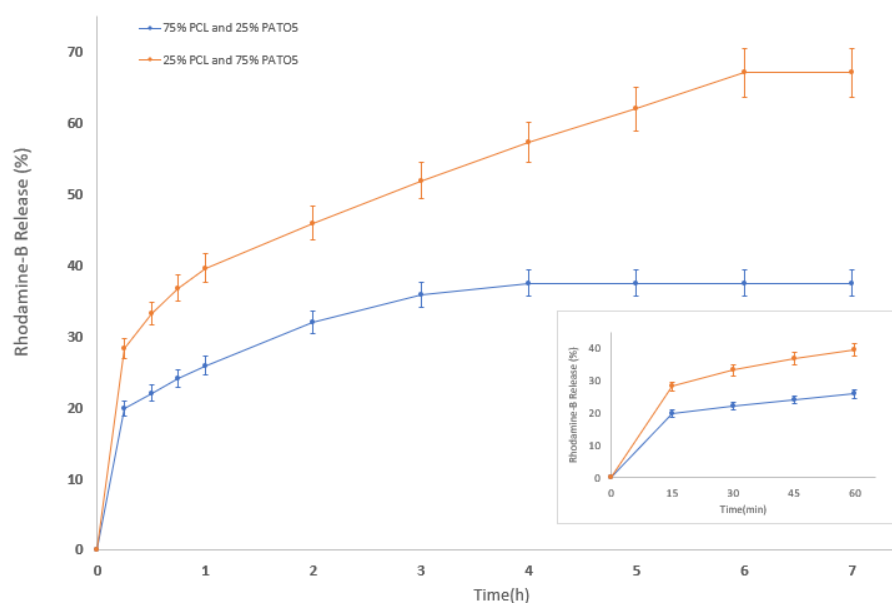


Figure 4.26. In vitro release profiles of Rhodamine-B from both PCL-ATO 5 MPs with different polymer-lipid ratios in PBS solution at 37 °C during 6 hours. Release medium: pH = 7.4. Inset shows Rhodamine-B release in 1 hour). [n=3]

4.9.2. Investigation of Resveratrol Release from PLHMPs with Different Polymer-Lipid Ratio

In this part of the study, the particles used for RhB release were loaded with RES and used as a drug carrier system. During the preparation of PLHMPs, 0.04% (w/w) RES was added to the dispersed phase. When the encapsulation efficiency of RES into PLHMPs was analyzed, it was observed that RES, which has hydrophobic properties, could be encapsulated 75.32% into PLHMPs with 1:3 polymer to lipid ratio. However, the encapsulation efficiency to PLHMPs with 3:1 polymer-lipid ratio, which has more polymer ratio, is 99.40%. The polymer and lipid areas of these two structures with different polymer-lipid ratios are given in Table 4.8. Area calculations are the average area value calculated from the surface areas of 100 particles from the OM images of the particles. While the polymer area of the particle with 1:3 polymer-lipid ratio was $1707 \mu\text{m}^2$, the polymer area of the particle with 3:1 polymer-lipid ratio was calculated as $3048 \mu\text{m}^2$. When particles with 1:3 and 3:1 polymer-lipid ratio were compared, it was observed that the particle with 3:1 polymer-lipid ratio had 43.99% more area than 1:3.

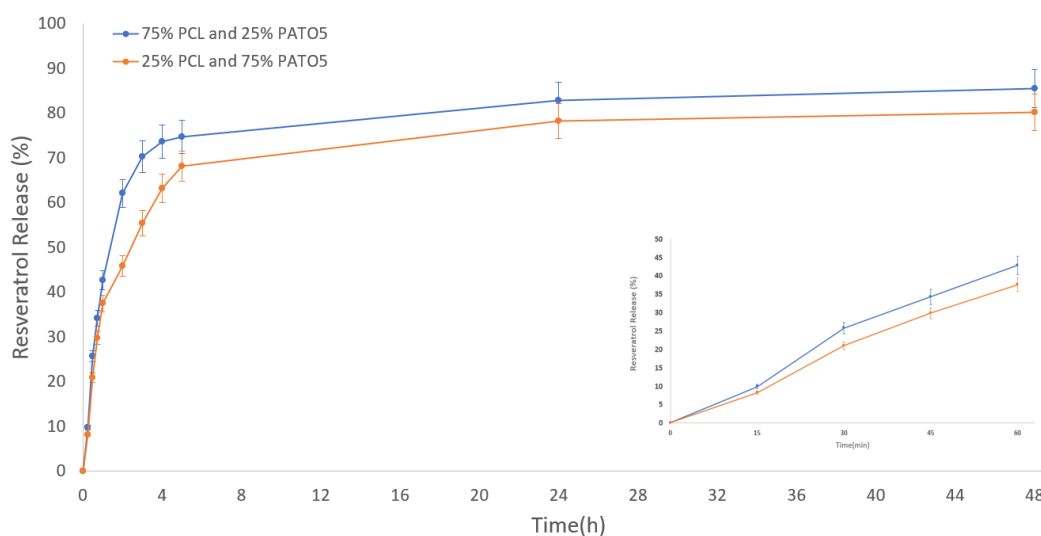


Figure 4.27. In vitro release profiles of Resveratrol from both PCL-ATO 5 MPs with different polymer-lipid ratio in PBS solution at 37 °C during 48 hours. Release medium: pH = 7.4, 0.1% Tween 20. Inset shows Resveratrol release in 1 hour). [n=3].

Table 4.8. The comparison of drug release profiles of PCL-Precirol ATO 5 microparticles with different polymer-lipit ratio



| P:L ratio | 3:1 | 1:3 |
|---|------------|------------|
| Area _{polymer} , µm ² | 3048 | 1707 |
| Area _{lipid} , µm ² | 4349 | 7441 |
| EE %, Rodamin B | 34.16 | 48.61 |
| Total Rhodamine-B Release % | 37.56 | 67.08 |
| EE %, Resveratrol | 99.40 | 75.32 |
| Total Resveratrol Release % | 86.35 | 81.34 |

The encapsulation efficiencies of these two structures are 99.40% for 3:1 and 75.32% for 1:3 polymer-lipid ratio. It is seen that the encapsulation efficiency of the structure with 3:1 polymer-lipid ratio is 31.97% higher than 1:3. Although the values do not match directly, since the area values calculated by OM analysis are two-dimensional analysis and there may be some differences with the volumetric calculation, it is seen that there is a connection between the areas of the polymer and lipid compartments of the structures and the encapsulation efficiencies. Considering that RES, a hydrophobic drug, is loaded into PCL, the hydrophobic component of PLHMPs, high encapsulation efficiencies can be achieved by controlling particle morphology. And one of the most important factors for this is the microfluidic technology employed in these particles. The microfluidic technology is a technology that provides high performance in the uniform preparation of drug delivery systems and ensures high encapsulation efficiencies.

In order to investigate the encapsulation efficiencies and release profiles of PLHMPs with different polymer-lipid ratios, the same procedure as for RHB release was applied. The calibration equation for RES was set as $y=88.989x$. The obtained RES release profiles are shown in Figure 4.27. The results show that both structures have similar release profiles and release percentages. PLHMPs with 1:3 polymer-lipid ratio reached 81.35% at the end of 48 hours of release, while structures with 3:1 ratio reached 86.35%. Although these

structures with different polymer-lipid ratios had different encapsulation efficiencies, thanks to their Janus structure, they were able to reach up to 80% by completing the release of the encapsulated drug in a controlled manner with similar profiles. When the release profiles of the particles encapsulated with Res alone were compared with the literature, the release of Res from both particles was found to be controlled and regular. Considering the time that the particles will reach the targeted region, it was determined that the Res release was slower and more controlled than the particle containing less lipid due to the lipid layer surrounding the polymer compartment containing RES. When the encapsulation efficiency of the particles and their unique two compartments are evaluated in terms of the encapsulation efficiency of the model molecules, the polymer compartment in PLHMPs enables high drug loading efficiency, while the lipid compartment acts as a buffer layer to ensure maximum drug retention in the polymer particle. In addition, the lipid compartment slows down the degradation of the polymer, increasing the in vivo stability of the hybrid particle and thus allowing the active substance concentration to be maintained at the desired level in the target region for a long time [117, 118]

5. CONCLUSION AND FUTURE RECOMMENDATIONS

In the first step of the study, PLHMPs with different lipids were prepared with one-nozzle microfluidic system and the prepared particles were characterized in terms of size, size distribution, morphology and optical properties. As the second step in the study, Al-GI microfluidic chip was designed and PLHNPs in the size range of 100-200 nm were prepared with the prepared chip.

The hydrophilic and hydrophobic model drug encapsulation efficiencies of hybrid particles with different polymer-lipid ratios were investigated and controlled release studies were carried out. The important results obtained during the study are given below:

- Within the scope of the thesis study, PLHMPs and PLHNPs were prepared by microfluidic technology, which has been popular in the literature in recent years.
- The polymer and lipid that will form the hybrid structure were first selected to prepare PLPHMPs. Then, a suitable solvent was selected, and the microfluidic device was designed with a chemically inert material to the solvent.
- First, a microfluidic device was designed for the preparation of PLHMPs. For this, a one-nozzle microfluidic system in co-flow geometry was prepared from chemically inert polyamide coated fused silica capillary. Since the desired microparticle size was below 100 μm , a fused silica capillary with an inner diameter of 40 μm was used in the system.
- Initially, different flow rates and regimes were investigated with a one-nozzle microfluidic system to prepare PLHMPs. Then, in the dripping regime region, the inner and outer phase flow rates were selected as 0.06 ml/h and 0.8 ml/h, respectively.
- Polymer and lipid MPs were prepared separately with selected flow rates and characterized by OM. PLHMPs were then prepared in a 1:1 polymer-lipid ratio with a one-nozzle microfluidic system.
- The size and size distribution, geometrical analysis of the prepared PLHMPs were performed by Optical Microscope and Scanning Electron Microscope, while Polarized Light Microscope was used to evaluate their optical properties.

- Surfactant concentration and type were firstly varied for the preparation of PLHMPs and PLHMPs with 1:1 polymer to lipid ratio were obtained with different morphologies. This was due to the interfacial tensions that changed with the change in the type of ionic surfactant used. In the presence of SDBS, polydisperse-tailed particles were formed, whereas in the presence of SDS, Janus particles with a high aspect ratio and high monodispersity were prepared.
- In order to further analyze the morphologies of PCL-ATO 5 (1:1) in the presence of ionic and non-ionic surfactants used, SDS was increased to 5% at constant PVA concentration and the particles changed from Janus morphology to spherical-like morphology with lower surface tension. PCL-ATO 5 (1:1) PLHMPs were then prepared using only PVA and Janus particles with lower aspect ratios were obtained. It was observed that the presence of non-ionic surfactants did not change the morphology, but ionic surfactants had an effect on particle morphology.
- The effects on the morphology of PCL-ATO 5 (1:1) particles were evaluated by performing the solvent evaporation step under three different conditions. As a result, it was found that the particles had Janus morphology in all cases, but the particles had higher aspect ratios in the case of slower solvent evaporation.
- In order to distinguish the compartments of PCL-ATO 5 (1:1) Janus microparticles, the particles were treated with acetone for 30 s, during which time the spherical structures retained their morphology, but the more heterogeneous part was destroyed. These results were followed by heating Janus MPs consisting of PCL and ATO 5 with different melting temperatures up to 60°C at certain temperature intervals, and it was observed that the lipid part with low melting temperature melted. With these two methods, it was proved that the morphology of PCL-ATO 5 (1:1) Janus microparticles is a hybrid structure, and the spherical part is the polymer part.
- The influence of the internal and external phase flow rate ratio used in the microfluidic system on the aspect ratio of the particles was investigated. As a result, it was observed that there is an inverse relationship between aspect ratio and flow rates. In the case of the same flow rate ratio values with different total flow rates, the particles were found to have similar aspect ratios.
- PCL-ATO 5 (1:1) Janus microparticles were prepared in polymer-lipid ratios of 1:1, 1:3 and 3:1, and in all cases, the lipid part occupied more area than the polymer part.

The ratios of lipid area to polymer area of the particles prepared with varying polymer-lipid ratios of 1:1, 1:3 and 3:1 were 3.80, 4.35 and 1.43, respectively. This showed that these particles, which can be used as drug delivery systems, were prepared with high aspect ratios and different volumes of polymer-lipid compartments.

- The stability test of the prepared PCL-ATO 5 (1:1) Janus microparticles was performed, and it was observed that they maintained their morphology for 23 days in the water phase at room temperature.
- After the PLHMPs were prepared with ATO 5, PLHMPs were also prepared using Softisan 100 and Stearic acid as lipids. For all lipid types, two different ionic surfactants were used, and it was observed that the presence of different ionic surfactants in the lipid type created different morphologies. The effect of different lipids on particle morphology showed that particles with ATO 5 produced Janus particles with a high aspect ratio, particles with stearic acid produced more spherical particles and SOFTISAN 100 produced spherical particles with a lower aspect ratio
- PLHMPs prepared with different lipids were then labelled with Rh-B to distinguish between polymer and lipid components. As a result, it was observed that SA and Softisan 100 PLHMPs were successfully labelled in a Janus structure in which the components could be distinguished.
- Considering the unclear surfaces of the two-component structures containing SA and their spherical structure, the amount of hydrophobic component in the structures was increased by adding Fluo to the structure. As a result of SEM characterization, it was observed that there were layers on the surfaces of the structures whose surfaces were not clearly visible in OM images. Especially the arrangement of layers on the surfaces of three-component PLHMPs containing Fluo was notable.
- The effect of surfactant type and concentration on the morphology of three-component structures containing SA was investigated. As a result of this study, it was observed that changing the concentration of SDS did not change the morphology of the structures, but replacing the ionic surfactant with SDBS resulted in the entrapment of small particles in the layers and particles on the surface of the structure. The type of ionic surfactant was found to change the morphology, and the results were similar to the previous study for PLHMPs with ATO 5.

- The change in morphology of PLHMPs containing three-component SA was investigated by varying the component amount. When the amount of SA was decreased, the layers around the structure disappeared and the structure was found to contain multiple particles around a spherical morphology. As a result of this study, the layers were suspected to be formed by SA.
- In order to examine in which component or components the layers on the surfaces of SA-containing structures are formed, the polymer was first removed from the 3-component structure and it was observed that the structure maintained the layers. Then, the 3-component structure was prepared without Fluo and the presence of layers was also observed in this case. However, when ATO 5 was used instead of SA in the 3-component structure, it was observed that the structures changed from a spherical structure with layers on the surface and formed an inhomogeneous morphology more similar to the morphology of PCL- ATO 5 PLHMPs. This indicated that the layers were formed due to the SA component.
- In order to use the three-component structures in different biomedical applications, the structures were made magnetic sensitive by loading MNP. It was observed that the MNP-loaded PLHMPs still retained the layers on the surface of the structures.
- The morphological changes in the structure of 3-component and MNP-loaded PLHMPs containing SA were investigated by changing the polymer and fluo ratios. While no morphological difference was observed in the 3-component structures, it was observed that the MNP-loaded particles changed their spherical structure to Janus structure at lower polymer concentration.
- The translational motions of the prepared MNP-loaded PLHMPs were investigated under magnetic field and the structures were found to have a translational velocity of $81.11 \pm 38.86 \mu\text{m/s}$.
- The presence of ordered layers on the surface of 3-component SA-containing PLHMPs was investigated by POM to determine whether the structures are light-responsive or not. It was found that 2-component, 3-component and MNP-loaded PLHMPs containing SA showed a birefringent property.
- The rotational motion of MNP-loaded PLHMPs under a magnetic field was observed. As a result of the study, it was observed that the particles have an angular

velocity of 0.05 rad/s. This shows that MNP-loaded PLHMPs have the potential to be used in biomedical applications as a micromotor capable of performing both rotational and translational motion.

- After the work with PLHMPs prepared in different morphologies with parameter studies, an Al-Gl microfluidic chip was designed to produce the structures in nano size. With this microfluidic system, three different PLHNPs were prepared using different flow rates and PLHNPs of different sizes were obtained with increasing total flow rate. With the prepared Al-Gl chip, monodisperse ($PDI < 0.1$) and hybrid structures with dimensions in the range of 100-200 nm were successfully prepared.

- The last part of the study was carried out with two model drug active substances Rh-B and Res in order to analyze the drug encapsulation efficiency and drug release profiles of the particles after the preparation of the particles of PLHMPs with ATO 5 with different polymer-lipid ratios with Janus geometry that may be suitable for drug delivery to the targeted site.

- The encapsulation efficiencies of Rh-B in 1:3 and 3:1 PLHMPs of the model molecules are 48.61% and 34.16%, respectively. When the polymer-lipid ratios of these PLHMPs are compared with the encapsulation efficiencies, it is seen that there is a linear relationship between the area of lipid components and encapsulation efficiencies, considering that RhB is attached to the lipid part of PLHMPs. According to the data obtained, it was determined that RH-B release from PLHMPs can be controlled.

- The encapsulation efficiencies of RES in 1:3 and 3:1 PLHMPs of the model molecules were 75.32% and 99.40%, respectively. According to the data obtained from PLHMPs with much higher encapsulation efficiency than the hydrophilic model drug, it was determined that RES release from PLHMPs can be realized in a controlled way.

- As a result of the study, multifunctional PLHMPs and PLHNPs with high aspect ratio, magnetic responsiveness, rotational and translational mobility, and birefringence, which can be used as drug delivery systems, were developed with microfluidic technology.

6. REFERENCES

- [1] J.J.F. Sleeboom, H.E. Amirabadi, P. Nair, C.M. Sahlgren, J.M.J. Den Toonder, DMM Disease Models and Mechanisms, Company of Biologists Ltd, **2018**.
- [2] S. Marre, K.F. Jensen, Chemical Society Reviews, 39 (**2010**) 1183-1202.
- [3] C.H. Yang, K.S. Huang, Y.S. Lin, K. Lu, C.C. Tzeng, E.C. Wang, C.H. Lin, W.Y. Hsu, J.Y. Chang, Lab on a Chip, 9 (**2009**) 961-965.
- [4] J. Ma, Y. Wang, J. Liu, Micromachines, 8 (**2017**) 255.
- [5] S. Damiani, U.B. Kompella, S.A. Damiani, R. Kodzius, Genes, 9 (**2018**) 103.
- [6] J.H. Kim, T.Y. Jeon, T.M. Choi, T.S. Shim, S.-H. Kim, S.-M. Yang, Langmuir, 30 (**2014**) 1473-1488.
- [7] G. Ballacchino, E. Weaver, E. Mathew, R. Dorati, I. Genta, B. Conti, D.A. Lamprou, International Journal of Molecular Sciences, 22 (**2021**) 8064.
- [8] S.I. Hamdallah, R. Zoqlam, P. Erfle, M. Blyth, A.M. Alkilany, A. Dietzel, S. Qi, International Journal of Pharmaceutics, 584 (**2020**) 119408.
- [9] M. Im, D.-H. Kim, J.-H. Lee, J.-B. Yoon, Y.-K. Choi, MRS Online Proceedings Library (OPL), 1222 (**2009**) 1222-DD1205-1203.
- [10] H. Zhang, C.H. Chon, X. Pan, D. Li, Microfluidics and nanofluidics, 7 (**2009**) 739-749.
- [11] V. Silverio, S. Guha, A. Keiser, R. Natu, D.R. Reyes, H. van Heeren, N. Verplanck, L.H. Herbertson, Frontiers in Bioengineering and Biotechnology, 10 (**2022**) 958582.
- [12] G.İ. Sakız, I. Bihi, I. Ziemecka, M. Briet, K.H. Hellemans, W. De Malsche, 25th National Symposium for Applied Biological Sciences (NSABS 2020), **2020**.
- [13] C.A. Griffiths, S. Bigot, E. Brousseau, M. Worgull, M. Hecke, J. Nestler, J. Auerswald, The International Journal of Advanced Manufacturing Technology, 47 (**2010**) 111-123.
- [14] C.-W. Tsao, Micromachines, 7 (**2016**) 225.
- [15] E. Gencturk, S. Mutlu, K.O. Ulgen, Biomicrofluidics, 11 (**2017**) 051502.
- [16] A.J. Kuehne, D.A. Weitz, Chemical Communications, 47 (**2011**) 12379-12381.
- [17] S. Krishnamurthy, R. Vaiyapuri, L. Zhang, J.M. Chan, Biomaterials Science, 3 (**2015**) 923-936.
- [18] C.-H. Weng, C.-C. Huang, C.-S. Yeh, G.-B. Lee, 2009 4th Ieee International Conference on Nano/Micro Engineered and Molecular Systems, IEEE, **2009**, pp. 219-222.

- [19] R.H. Fang, S. Aryal, C.-M.J. Hu, L. Zhang, *Langmuir*, 26 (2010) 16958-16962.
- [20] M.O. Oyewumi, A. Kumar, Z. Cui, *Expert Review of Vaccines*, 9 (2010) 1095-1107.
- [21] S. Zhao, C. Huang, X. Yue, X. Li, P. Zhou, A. Wu, C. Chen, Y. Qu, C. Zhang, *Materials & Design*, (2022) 110850.
- [22] A. Kiran, T.S. Kumar, R. Sanghavi, M. Doble, S. Ramakrishna, *Nanomaterials*, 8 (2018) 860.
- [23] N. Raina, R. Pahwa, J.K. Khosla, P.N. Gupta, M. Gupta, *Polymer Bulletin*, 79 (2022) 7041-7063.
- [24] A. Rai, S. Senapati, S.K. Saraf, P. Maiti, *Journal of Materials Chemistry B*, 4 (2016) 5151-5160.
- [25] A. Sosnik, K.P. Seremeta, *Advances in Colloid and Interface Science*, Elsevier B.V., 2015, pp. 40-54.
- [26] P. Joyce, C.P. Whitby, C.A. Prestidge, *ACS Applied Materials and Interfaces*, 7 (2015) 17460-17470.
- [27] Y. Wang, K. Kho, W.S. Cheow, K. Hadinoto, *International Journal of Pharmaceutics*, 424 (2012) 98-106.
- [28] C.Y. Lee, C.L. Chang, Y.N. Wang, L.M. Fu, *International Journal of Molecular Sciences*, 2011, pp. 3263-3287.
- [29] E.K. Sackmann, A.L. Fulton, D.J. Beebe, *Nature*, 507 (2014) 181-189.
- [30] Y. Zhang, L. Kang, H. Huang, J. Deng, (2020).
- [31] S. Akbari, T. Pirbodaghi, R.D. Kamm, P.T. Hammond, *Lab on a Chip*, 17 (2017) 2067-2075.
- [32] C.-H. Chen, R.K. Shah, A.R. Abate, D.A. Weitz, *Langmuir*, 25 (2009) 4320-4323.
- [33] D. Yin, N.R. Jiang, Z.Y. Chen, Y.F. Liu, Y.G. Bi, X.L. Zhang, J. Feng, H.B. Sun, *Advanced Optical Materials*, 8 (2020) 1901525.
- [34] A. Forigua, A. Dalili, R. Kirsch, S.M. Willerth, K.S. Elvira, *ACS Applied Polymer Materials*, 4 (2022) 7004-7013.
- [35] H.J. Kwon, S. Kim, S. Kim, J.H. Kim, G. Lim, *BioChip Journal*, 11 (2017) 214-218.
- [36] C.A. Serra, Z. Chang, *Chemical Engineering & Technology: Industrial Chemistry-Plant Equipment-Process Engineering-Biotechnology*, 31 (2008) 1099-1115.
- [37] J.H. Kim, T.Y. Jeon, T.M. Choi, T.S. Shim, S.H. Kim, S.M. Yang, *Langmuir*, 30 (2014) 1473-1488.

- [38] F. Ejeta, Drug Design, Development and Therapy, (2021) 3881-3891.
- [39] L. Zhang, Q. Chen, Y. Ma, J. Sun, ACS Applied Bio Materials, 3 (2019) 107-120.
- [40] T. Yang, J. Peng, Z. Shu, P.K. Sekar, S. Li, D. Gao, Micromachines, 10 (2019) 832.
- [41] P.N. Nge, C.I. Rogers, A.T. Woolley, Chemical reviews, 113 (2013) 2550-2583.
- [42] G.T. Vladislavljević, R. Al Nuumani, S.A. Nabavi, Micromachines, MDPI AG, 2017.
- [43] X.-T. Sun, R. Guo, D.-N. Wang, Y.-Y. Wei, C.-G. Yang, Z.-R. Xu, Journal of Colloid and Interface Science, 553 (2019) 631-638.
- [44] A. Rai, S. Senapati, S.K. Saraf, P. Maiti, J Mater Chem B, 4 (2016) 5151-5160.
- [45] J. Ahn, J. Ko, S. Lee, J. Yu, Y.T. Kim, N.L. Jeon, Advanced Drug Delivery Reviews, Elsevier B.V., 2018, pp. 29-53.
- [46] H. Xie, Z.G. She, S. Wang, G. Sharma, J.W. Smith, Langmuir, 28 (2012) 4459-4463.
- [47] A.J. Mieszawska, Y. Kim, A. Gianella, I. Van Rooy, B. Priem, M.P. Labarre, C. Ozcan, D.P. Cormode, A. Petrov, R. Langer, O.C. Farokhzad, Z.A. Fayad, W.J.M. Mulder, Bioconjugate Chemistry, 24 (2013) 1429-1434.
- [48] C.-S. Lee, C.-H. Choi, J.-H. Jung, 2010 IEEE 5th International Conference on Nano/Micro Engineered and Molecular Systems, IEEE, 2010, pp. 902-905.
- [49] B. Karagoz, L. Esser, H.T. Duong, J.S. Basuki, C. Boyer, T.P. Davis, Polymer Chemistry, 5 (2014) 350-355.
- [50] N. Kapate, J.R. Clegg, S. Mitragotri, Advanced Drug Delivery Reviews, 177 (2021) 113807.
- [51] X. Lu, L. Miao, W. Gao, Z. Chen, K.J. McHugh, Y. Sun, Z. Tochka, S. Tomasic, K. Sadtler, A. Hyacinthe, Science translational medicine, 12 (2020) eaaz6606.
- [52] S.T. Koshy, D.K. Zhang, J.M. Grolman, A.G. Stafford, D.J. Mooney, Acta biomaterialia, 65 (2018) 36-43.
- [53] R. Kuai, L.J. Ochyl, K.S. Bahjat, A. Schwendeman, J.J. Moon, Nature materials, 16 (2017) 489-496.
- [54] X. Huang, X. Teng, D. Chen, F. Tang, J. He, Biomaterials, 31 (2010) 438-448.
- [55] Z.Y. Feng, T.T. Liu, Z.T. Sang, Z.S. Lin, X. Su, X.T. Sun, H.Z. Yang, T. Wang, S. Guo, Frontiers in Bioengineering and Biotechnology, 9 (2021).
- [56] Y.L. Fan, C.H. Tan, Y. Lui, D. Zudhistira, S.C.J. Loo, RSC Advances, 8 (2018) 16032-16042.

- [57] O.E. Puspita, F. Widodo, M.A. Putri, I. Rossariza, A. Fadhillah, N.P.J. Sari, *International Journal of Applied Pharmaceutics*, (2021) 150-153.
- [58] Z. Wang, Z. Wu, J. Liu, W. Zhang, *Expert opinion on drug delivery*, 15 (2018) 379-395.
- [59] S. Ranjan, K.K. Zeming, R. Jureen, D. Fisher, Y. Zhang, *Lab on a Chip*, 14 (2014) 4250-4262.
- [60] S. Torza, S. Mason, *Journal of colloid and interface science*, 33 (1970) 67-83.
- [61] C. Ding, L. Ge, H. Jin, Q. Bian, R. Guo, *Colloids and Surfaces A: Physicochemical and Engineering Aspects*, 583 (2019) 123947.
- [62] O. Sarheed, M. Dibi, K.V. Ramesh, *Pharmaceutics*, 12 (2020) 1223.
- [63] N. Saito, R. Takekoh, R. Nakatsuru, M. Okubo, *Langmuir*, 23 (2007) 5978-5983.
- [64] M. Okubo, H. Kobayashi, T. Matoba, Y. Oshima, *Langmuir*, 22 (2006) 8727-8731.
- [65] M. Okubo, N. Saito, T. Fujibayashi, *Colloid and Polymer Science*, 283 (2005) 691-698.
- [66] M.R.S.A. Janjua, S. Jamil, N. Jahan, S.R. Khan, S. Mirza, *Chemistry Central Journal*, 11 (2017) 1-14.
- [67] X. Cao, W. Li, T. Ma, H. Dong, *RSC Advances*, 5 (2015) 79969-79975.
- [68] J.S. Winkler, Rutgers The State University of New Jersey, School of Graduate Studies (2016).
- [69] N.V.V. Linh, H. Dai Phu, *VNUHCM Journal of Natural Sciences*, 1 (2017) 130-137.
- [70] E. Gounari, A. Komnenou, E. Kofidou, S. Nanaki, D. Bikiaris, S. Almpnidou, K. Kouzi, V. Karampatakis, G. Koliakos, *Stem cells international*, 2022 (2022).
- [71] M.W. Tibbitt, J.E. Dahlman, R. Langer, *J Am Chem Soc*, 138 (2016) 704-717.
- [72] U. Arif, S. Haider, A. Haider, N. Khan, A.A. Alghyamah, N. Jamila, M.I. Khan, W.A. Almasry, I.-K. Kang, *Current pharmaceutical design*, 25 (2019) 3608-3619.
- [73] K. Nagase, M. Hasegawa, E. Ayano, Y. Maitani, H. Kanazawa, *International journal of molecular sciences*, 20 (2019) 430.
- [74] T. Date, V. Nimbalkar, J. Kamat, A. Mittal, R.I. Mahato, D. Chitkara, *Journal of controlled release*, 271 (2018) 60-73.
- [75] S. Bochicchio, G. Lamberti, A.A. Barba, *Pharmaceutics*, 13 (2021) 198-198.
- [76] K. Maeda, H. Onoe, M. Takinoue, S. Takeuchi, *Adv Mater*, 24 (2012) 1340-1346.

- [77] Y. Zhang, K. Huang, J. Lin, P. Huang, *Biomaterials science*, 7 (2019) 1262-1275.
- [78] Z.-Q. Feng, K. Yan, J. Li, X. Xu, T. Yuan, T. Wang, J. Zheng, *Materials Science and Engineering: C*, 104 (2019) 110001.
- [79] J. Yang, C. Zhang, X. Wang, W. Wang, N. Xi, L. Liu, *Science China Technological Sciences*, 62 (2019) 1-20.
- [80] Q. Zhang, R. Dong, X. Chang, B. Ren, Z. Tong, *ACS Applied Materials & Interfaces*, 7 (2015) 24585-24591.
- [81] W. Chen, R. Jiang, X. Sun, S. Chen, X. Liu, M. Fu, X. Yan, X. Ma, *Chemistry of Materials*, 34 (2022) 7543-7552.
- [82] X. Zhang, C. Liu, Y. Lyu, N. Xing, J. Li, K. Song, X. Yan, *Journal of Colloid and Interface Science*, (2023).
- [83] Y. Xiao, Z. Wu, Q. Yao, J. Xie, *Aggregate*, 2 (2021) 114-132.
- [84] Y. Jiao, M.E. Kandel, X. Liu, W. Lu, G. Popescu, *Optics Express*, 28 (2020) 34190-34200.
- [85] M. Marjanovic, J. Wang, Y. Xu, E.J. Chaney, D.R. Spillman, A.M. Higham, N.N. Luckey, K.A. Cradock, G.Z. Liu, S.A. Boppart, *Cancer Research*, 78 (2018) 3038-3038.
- [86] S. Chang, J. Handwerker, G.A. Giannico, S.S. Chang, A.K. Bowden, *Journal of Biomedical Optics*, 27 (2022) 074711-074711.
- [87] S.P. Foy, R.L. Manthe, S.T. Foy, S. Dimitrijevic, N. Krishnamurthy, V. Labhasetwar, *ACS nano*, 4 (2010) 5217-5224.
- [88] A. Mittal, I. Roy, S. Gandhi, *Magnetochemistry*, MDPI, 2022.
- [89] Y. Qiu, F. Wang, Y.M. Liu, W. Wang, L.Y. Chu, H.L. Wang, *Scientific Reports*, 5 (2015).
- [90] J. Chomoucka, J. Drbohlavova, D. Huska, V. Adam, R. Kizek, J. Hubalek, *Pharmacological Research*, 2010, pp. 144-149.
- [91] A.K. Gupta, R.R. Naregalkar, V.D. Vaidya, M. Gupta, *Nanomedicine*, 2007, pp. 23-39.
- [92] J.V. Frangioni, *Journal of Clinical Oncology*, 2008, pp. 4012-4021.
- [93] J. Li, B.E.F.D. Ávila, W. Gao, L. Zhang, J. Wang, *Science Robotics*, American Association for the Advancement of Science, 2017.
- [94] S. Atay, K. Pişkin, F. Yilmaz, C. Çakir, H. Yavuz, A. Denizli, *Analytical Methods*, 8 (2016) 153-161.

- [95] X. Yu, Y. Li, J. Wu, H. Ju, *Analytical Chemistry*, 86 (2014) 4501-4507.
- [96] A. Boujakhrou, E. Sánchez, P. Díez, A. Sánchez, P. Martínez-Ruiz, C. Parrado, J.M. Pingarrón, R. Villalonga, *ChemElectroChem*, 2 (2015) 1735-1741.
- [97] M. Wu, H. Wei, H. van der Mei, J. de Vries, H. Busscher, Y. Ren.
- [98] H.-Y. Hsieh, T.-W. Huang, J.-L. Xiao, C.-S. Yang, C.-C. Chang, C.-C. Chu, L.-W. Lo, S.-H. Wang, P.-C. Wang, C.-C. Chieng, *Journal of Materials Chemistry*, 22 (2012) 20918-20928.
- [99] S. Freitag, B. Baumgartner, S. Radel, A. Schwaighofer, A. Varriale, A. Pennacchio, S. D'Auria, B. Lendl, *Lab on a Chip*, 21 (2021) 1811-1819.
- [100] J. Lim, S.P. Yeap, H.X. Che, S.C. Low, *Nanoscale Research Letters*, 8 (2013) 1-14.
- [101] Y. Bai, Q.Q. Mao, J. Qin, X.Y. Zheng, Y.B. Wang, K. Yang, H.F. Shen, L.P. Xie, *Cancer science*, 101 (2010) 488-493.
- [102] C.K. Singh, M.A. Ndiaye, N. Ahmad, *Biochimica et Biophysica Acta (BBA)-Molecular Basis of Disease*, 1852 (2015) 1178-1185.
- [103] K. Robinson, C. Mock, D. Liang, *Drug development and industrial pharmacy*, 41 (2015) 1464-1469.
- [104] L. Mei, Y. Zhang, Y. Zheng, G. Tian, C. Song, D. Yang, H. Chen, H. Sun, Y. Tian, K. Liu, Z. Li, L. Huang, *Nanoscale Research Letters*, 4 (2009) 1530-1539.
- [105] L.-L. Zhen, T.-H. Ma, J.-H. Tang, T.-F. Xia, J. Ge, W.-J. Yuan, L. Chen, R. Wan, J.-X. Cheng, Z.-K. Chen, Z.-H. Cheng, W. Song, *Oncotarget*, 0 (2017).
- [106] X. Gao, Li, Luo, F. Wang, T. Ye, B. Shao, W. Nie, X. Deng, Shi, C.-Y. Gong, N. Huang, Wei, *International Journal of Nanomedicine*, (2013) 2453.
- [107] A. Khames, M.A. Khaleel, M.F. El-Badawy, A.O. El-Nezhawy, *International journal of nanomedicine*, 14 (2019) 2515.
- [108] P. Kolhar, A.C. Anselmo, V. Gupta, K. Pant, B. Prabhakarandian, E. Ruoslahti, S. Mitragotri, *Proceedings of the National Academy of Sciences of the United States of America*, 110 (2013) 10753-10758.
- [109] S.A. Ali, *IOP Conference Series: Materials Science and Engineering*, IOP Publishing, 2016, pp. 012035.
- [110] S.A. Nabavi, G.T. Vladisavljević, S. Gu, E.E. Ekanem, *Chemical Engineering Science*, 130 (2015) 183-196.
- [111] K. Horiuchi, *SN Applied Sciences*, 2 (2020).

- [112] G.D. Kalaycioglu, N. Aydogan, Colloids and Surfaces a-Physicochemical and Engineering Aspects, 510 (2016) 77-86.
- [113] A.W.H. Lee, B.D. Gates, Langmuir, 32 (2016) 13030-13039.
- [114] C.E. Okuyucu, Hacettepe University, 2023, pp. 186.
- [115] Q. Feng, L. Zhang, C. Liu, X. Li, G. Hu, J. Sun, X. Jiang, Biomicrofluidics, 9 (2015) 052604.
- [116] L. Silvestro, A.S. Ruviano, G.T.d.S. Lima, P.R.d. Matos, E. Rodríguez, P.J.P. Gleize, Revista IBRACON de Estruturas e Materiais, 16 (2023).
- [117] S. Sutriyo, R. Iswandana, F.M. Ivariani, International Journal of Applied Pharmaceutics, 12 (2020) 237-241.
- [118] O.B. Garbuzenko, J. Winkler, M.S. Tomassone, T. Minko, Langmuir, 30 (2014) 12941-12949.
- [119] J.S. Winkler, M. Barai, M.S. Tomassone, Exp Biol Med (Maywood), 244 (2019) 1162-1177.
- [120] F. Márquez, G.M. Herrera, T. Campo, M. Cotto, J. Ducongé, J.M. Sanz, E. Elizalde, Ó. Perales, C. Morant, Nanoscale Research Letters, 7 (2012).
- [121] C. Berkland, K. Kim, D.W. Pack, 2003.